NTERSCIENCE TRACTS ON PHYSICS AND ASTRONOMY

Edited by R. E. MARSHAK
University of Rochester

---

1. **D. J. Hughes**

   NEUTRON OPTICS

2. **M. S. Livingston**

   HIGH-ENERGY ACCELERATORS

Additional volumes in preparation

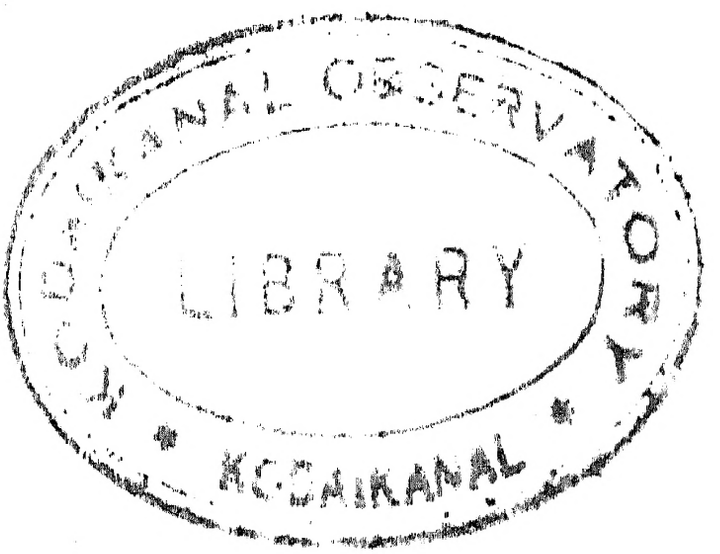

HIGH-ENERGY ACCELERATORS

STANLEY LIVINGSTON
Massachusetts Institute of Technology, Cambridge, Massachusetts

NTERSCIENCE PUBLISHERS, INC., NEW YORK
nterscience Publishers Ltd., London 1954

Library of Congress Catalog Card Number 54-11776

INTERSCIENCE PUBLISHERS, INC.
250 Fifth Avenue, New York 1, N. Y.

For Great Britain and Northern Ireland:
INTERSCIENCE PUBLISHERS LTD.
88/90 Chancery Lane, London W. C. 2

PRINTED IN THE UNITED STATES OF AMERICA

PREFACE

The history of accelerator development has not yet been written. Almost the entire literature on the subject is published in research journals or in laboratory reports. Except for relatively brief survey articles, there are no publications in which a scientist, an engineer or a student can find a description of the physical principles of particle acceleration, or of the successful designs and techniques of the several types of accelerators. The need for such a compilation and study is clear. Many a student wants to know more about the field to guide his further studies. Nuclear physicists must understand accelerators to evaluate experimental evidence. Scientists or engineers in borderline areas are curious about the machines which are the sources of nuclear data, and occasionally the director of an expanding laboratory must acquire an appreciation of the relative merits of the several machines as a basis for future plans.

This monograph is an attempt to present one part of the story of accelerators—that associated with the newest, largest, and highest-energy machines, which have become so important in the rapidly developing field of nuclear forces and high-energy particles. The early development of the field, covering the direct voltage machines of the 1930's, electrostatic generators, cyclotrons, and the like, cannot be included in this brief volume. This may leave a big, although unavoidable, gap for some readers. However, the story of the high-energy accelerators is almost a complete story in itself.

The emphasis is on the physical principles of operation, the properties of particle orbits, and the design principles of the

basic components. No attempt has been made at a complete coverage of all installations, but certain ones are chosen as typical and are described in some detail to demonstrate a particularly effective and coordinated set of components. It has also been the urge of the writer to show the similarities in principle of the several machines, especially in the way they depend on the basic equations of motion of particles in electric and magnetic fields. To emphasize the similarities, the mathematical analysis of particle motion, as applied to most of the accelerators, is presented in a separate chapter where the common features of acceleration, focusing, and stability are derived from the equations of motion.

Accelerators are undergoing continuous development, especially those designed for the highest energies. The most exciting recent developments are not yet finalized into a working machine. As a result the last chapter is openly speculative, and it is to be expected that some of the concepts and designs presented will be changed as these new machines evolve. However, such a preview into the early stages of development of a new type of accelerator is the best possible illustration of the accelerator art. It shows, more clearly than a factual description of a working machine, how new concepts develop, how new problems arise and how the application of ingenuity and technology can solve the problems, to achieve a new voltage record and a new tool for nuclear research.

M. Stanley Livingston

Cambridge, Massachusetts
May 18, 1954

CONTENTS

CHAPTER 1

High-Energy Accelerators as Tools for Nuclear Research

1.1 Introduction

Particle accelerators are among the most useful tools in nuclear science. The high-speed particles which they produce can penetrate the force fields of nuclei, where they supply the energy necessary to disintegrate the nucleus, or serve as probes to study the properties of nuclear forces. Atomic nuclei are composed of protons and neutrons bound together by short-range forces, with an approximately constant nuclear density. The nuclear radius can be expressed as $r = r_0 A^{1/3}$, where A is the number of nucleons. The radius of a single nucleon, $r_0 \sim 1.4 \times 10^{-13}$ cm, can be taken as a measure of the range of nuclear forces.

When positively charged particles are used to bombard a nucleus, they are repelled by the Coulomb force. The potential energy of a singly charged particle at the radius r (the potential barrier) associated with nuclei of $1 < A < 200$ is between 1 and 10 Mev. Particles must have kinetic energies of this magnitude to approach to the "surface" of a nucleus, where they have a high probability of initiating a nuclear reaction. At lower energies the nuclear processes observed are understood in terms of the wave-mechanical probability of penetration of the barrier.

Energies of several million electron volts have been available for many years from the early accelerators such as voltage multipliers, the electrostatic generator, and the cyclotron. Experiments at such energies have served to explore the gross structure of the nucleus, to measure disintegration thresholds

and low-lying excitation levels in nuclei. The conditions of stability in nuclei have been investigated, and many measurements have been made on the properties of the unstable, radioactive nuclides. Angular distributions of the products in disintegration and scattering processes show the noncentral character of nuclear forces. At somewhat higher energies (greater than 10 Mev) disintegration processes become more complex; the multi-particle character of most nuclei is revealed in the many competing reactions, often resulting in multi-particle emission.

At much higher energies the characteristics of the phenomena change, and we enter the field of the properties of fundamental particles. Processes resolve themselves into interactions between elementary nucleons and give direct evidence of the properties of the nuclear force at extremely short range. This change in character of the interactions is expressed in wave-mechanical terminology by the wavelength of the bombarding particle becoming short relative to nuclear dimensions. In the billion-volt region particle wavelength is small even compared to the dimensions of a single nucleon. The wavelength associated with a proton of one billion electron volts (1 Bev = 1000 Mev), for example, is given by: $\lambda = 1 \times 10^{-14}$ cm. A proton of this energy (or higher) is visualized as having a reaction with one (or at the most a few) of the individual nucleons in traversing a nucleus. The multi-particle character of heavy nuclei is significant primarily in that it represents a greater density of nuclear matter and so increases the probability of interaction.

The fundamental nuclear force, between pairs of nucleons, is now believed to involve the production and absorption of mesons. Theoretical interpretation is by no means complete, but many experiments show that mesons are produced when targets are bombarded by sufficiently high-energy particles or radiations. Mesons were discovered in cosmic ray observations, and a large fraction of present evidence on the properties of mesons has been obtained by using the high, but uncontrollable, energies of

cosmic rays. Furthermore, the most significant recent evidence for still heavier unstable particles has come from exposure of photographic emulsions to the primary cosmic rays at high altitudes, attained in balloon flights, and from cloud chamber photographs taken in mountain laboratories.

1.2 Unstable Particles and Threshold Energies

Many of the elementary particles, and perhaps all, can be created through materialization of energy. Electron-pair production by gamma rays is now a relatively well-understood phenomenon: $\gamma \rightarrow e^+ + e^-$. This process occurs in the presence of the electric field of a nucleus or electron, and the minimum gamma-ray energy required is equal to the sum of the rest energies of the electron and positron (1.02 Mev). Above this threshold the cross section for absorption of gamma radiation through pair production rises rapidly until it is the dominating process at very high energies.

The inverse process, of annihilation of a positron with a negative electron, results in the release of two quanta of gamma radiation, each of 0.51 Mev energy, following the reaction: $e^+ + e^- \rightarrow \gamma + \gamma$. Or, occasionally, in special circumstances three quanta are produced or a single gamma ray of 1.02 Mev results. Annihilation occurs most efficiently after the positrons have been slowed down to thermal energies by scattering and ionization in the surrounding medium.

These processes of electron-pair production and annihilation give us basic information about the interaction between light elementary particles and the electromagnetic field. Equally important insight into the properties of the heavy elementary particles is anticipated from studies of the creation and absorption of mesons.

A brief survey of the known unstable particles is appropriate, to show the threshold energies required for their production and the significance of accelerators as tools to study the properties of such particles. Space does not permit a complete survey of the high-energy particle field, nor is the author sufficiently versed

in this field to present and interpret the rapidly accumulating new evidence. The discussion to follow is restricted to those particles which are most well established; readers should go elsewhere[1] for a more complete and documented analysis of high-energy physics.*

μ-Mesons. The original mesons discovered in cosmic ray experiments are now known as μ-mesons. Both positively and negatively charged μ-mesons are observed in cloud chambers, on which a magnetic field is superimposed, by the different directions of curvature of the tracks. Whenever the μ^+-meson is seen to stop in the cloud chamber a single electron of the same sign of charge is observed as a product. The electron tracks usually make sharp angles with the meson tracks and show a continuous energy distribution extending up to about 50 Mev, indicating a 3-particle process in which two nonionizing radiations are also emitted. These neutral particles are presumed to be neutrinos:

$$\mu^+ \rightarrow e^+ + 2\nu$$
$$\mu^- \rightarrow e^- + 2\nu \qquad (1\text{-}1)$$

Electronic experiments show that the half-life for decay into electrons is about 2.1×10^{-6} sec. The relatively long life and the fact that most μ-mesons survive to be slowed down before decaying show that they do not react strongly with nuclei. This small nuclear interaction cross section is incompatible with the large cross section for production of mesons in nuclear interactions and led to the prediction and discovery of another type of meson, the π-meson, which is responsible for the large production cross section.

Observation of the characteristic 2.1×10^{-6} sec decay period with electronic time-delay apparatus can be used to identify the μ-mesons. The delayed 0.51-Mev positron annihilation radiation is also useful in identifying the positive

* Superior numbers refer to the Bibliography at the end of the book.

μ-meson. The mass of the μ-meson is $(209.6 \pm 2.4)\, m_e$, where m_e is the mass of an electron at rest.[1]

π-Mesons. The mesons produced and absorbed in nuclear interactions are called π-mesons. In the absence of other processes they decay into μ-mesons with a characteristic mean life of 2.65×10^{-8} sec. following the reactions:

$$\pi^+ \rightarrow \mu^+ + \nu$$
$$\pi^- \rightarrow \mu^- + \nu \qquad (1\text{-}2)$$

Observation of this decay period is evidence for the presence of π-mesons. Neutral π-mesons at rest disintegrate into two gamma rays of 68 Mev each:

$$\pi^0 \rightarrow \gamma + \gamma \qquad (1\text{-}3)$$

with a very short mean life estimated as 10^{-14} sec. The resulting γ-rays can be detected through their electron-pair production.

π-mesons are produced by accelerators through a wide variety of reactions, resulting in both charged and neutral mesons. The simplest, conceptually, is photo-production, in which the bombarding radiation is a photon which acts directly on a single nucleon. Evidence has been obtained for the following reactions:

$$\gamma + p \rightarrow n + \pi^+$$
$$\gamma + p \rightarrow p + \pi^0$$
$$\gamma + n \rightarrow p + \pi^-$$
$$\gamma + n \rightarrow n + \pi^0 \qquad (1\text{-}4)$$

Nucleon-nucleon reactions are in even greater variety, of the types:

$$p + p \rightarrow p + n + \pi^+$$
$$p + p \rightarrow p + p + \pi^0$$
$$p + n \rightarrow p + p + \pi^-$$

$$p + n \rightarrow n + n + \pi^+$$
$$p + n \rightarrow p + n + \pi^0$$
$$n + n \rightarrow n + p + \pi^-$$
$$n + n \rightarrow n + n + \pi^0 \qquad (1\text{-}5)$$

plus others in which more than one π-meson is produced, if sufficient energy is available. The primary use of accelerators in the 200- to 500-Mev range has been for the production of π-mesons, and a large share of the research using such accelerators has been on the properties of π-mesons and in measurements of interaction cross sections of the secondary reactions where mesons act as the bombarding agents.

In any reaction in which a new particle is produced, energy equivalent to the rest energy of the particle must be supplied. Present experimental evidence indicates rest energies for charged and neutral π-mesons of[1]:

$$m_{\pi^+} = (276.1 \pm 2.3)m_e = 141 \text{ Mev}$$
$$m_{\pi^-} = (276.1 \pm 1.3)m_e = 141 \text{ Mev}$$
$$m_{\pi^0} = (264.6 \pm 3.2)m_e = 135 \text{ Mev}$$

Threshold energy for meson production is given by the condition that the product particles have zero relative kinetic energy. This means that the products move off together with the center-of-mass velocity. Momentum must also be conserved in the collision. In the gamma-ray reactions (Eqs. 1-4) the incident momentum is small, so the threshold gamma ray energy is only slightly larger than the rest energy, or about 151 Mev. In heavy particle collisions the incident particle must also supply the kinetic energy of the moving center-of-mass. Threshold energy is given by[1]:

$$E_0 = 2m_\pi c^2 \left(1 + \frac{m_\pi}{4M}\right) \qquad (1\text{-}6)$$

where m_π is the π-meson mass and M is the mass of the nucleon.

When it is evaluated for the proton-nucleon reactions (Eqs. 1-5), this threshold energy is 293 Mev for production of $\pi^{\pm}$-mesons or 280 Mev for π^0-mesons.

Bombarding particle energy must be well above the threshold to produce a reasonable intensity of mesons. The excitation function for the process shows a rapid increase in cross section with energy above the threshold. Furthermore, the bombarding particles lose energy by ionization in the material of the target, so the effective target thickness depends on the excess energy above the threshold, and the total yield of mesons is an even steeper function of energy. To illustrate this point the total meson flux for equivalent beam currents at the University of Chicago synchrocyclotron (450-Mev protons) is about 50 times that at the University of Rochester machine (240-Mev protons). Experiments become simpler, and precision improves with higher meson intensities. Furthermore, the residual kinetic energy of the meson formed also depends on the energy excess above threshold, and it is clear that a wide range in meson energy is desirable for a thorough understanding of meson properties. In planning accelerators it is well to recognize this requirement for particle energies well above threshold limits of the reactions to be studied.

When either the target nuclei or the bombarding particles consist of more than single nucleons, the threshold energy is lower than that computed from Eq. 1-6. This can be understood in terms of the internal Fermi energy T_F of a nucleus consisting of several particles and the average potential energy of a nucleon in such a nucleus, V. Threshold energy for meson production is given approximately by[1]: $T_0 = m_\pi c^2 + T_F + V$. For nuclei heavier than helium, π-mesons can be produced by incident nucleons having energies as low as 180 Mev. Studies of reaction thresholds in such complex nuclei reveal more about the nucleon-nucleon forces within the nucleus than about the π-meson process. Most large accelerators are now arranged to accelerate protons in order to simplify the interpretations, and in so far as is practical hydrogen targets are being developed to reduce complexity in studying target interactions.

Heavy Mesons. In high-energy cosmic ray processes, several other particles have been observed by using the technique of exposing photographic emulsions to the primary cosmic rays at high altitudes. At the start these were classified according to their different mechanisms of interaction with nuclei and were called by the names V, K, κ, τ, etc. They each seemed to be distinctly heavier than the π-meson and would require higher bombarding energies to produce. Some are observed only in processes involving extremely high-energy primary particles, inferred from the number of prongs and the angle of the forward "jet" in the "stars" in which they are formed. Present estimates suggest and preliminary experimental results show that a primary energy of several Bev will be required to form some of these "strange" particles in sufficient intensity to be observable in the presence of the more common π-mesons.

The neutral "V-particle" has for its defining property an inverted V-track in the emulsion or cloud chamber, of which one prong has the dense ionization and small scattering associated with the proton, and the other has the characteristics of a π-meson. The nonionizing, neutral particle which decays into such products must have a rest energy significantly greater than that of a neutron. More detailed evidence from cloud chamber tracks has confirmed the identification of the proton and negative π-meson products in several instances.

However, in some early cosmic ray observations an analysis of the prongs of a V-track showed them both to be of less than nucleonic mass; so sub-classes were recognized, described as V_1, V_2, V_4, etc. Furthermore, some charged particle tracks making a sharp change in direction and track density were interpreted as leading to one charged and one neutral prong; the primary radiation in this case was called a "charged V-particle." The original type then became known as a $V_1{}^0$-particle.

In the revised terminology proposed at the Bagnères Conference in July, 1953, the heavier-than-nucleon particles (hyperons) are called Λ-particles, the intermediate mass particles

are called K-mesons and the light mesons μ and π retain their former designations.

Accelerators can also be used to produce and study the heavy unstable particles. A single example will be cited in illustration. Recent photographic evidence obtained using a hydrogen-filled cloud chamber in the π-meson beam of the Brookhaven cosmotron (see Chap. 6) suggests that two kinds of neutral V-particles can be created in pairs. The few photographs obtained and analyzed to date indicate the strong possibility of a process of the following type:

$$\begin{aligned} &\pi^- + p \rightarrow \Lambda^0 + \theta^0 \\ &\Lambda^0 \rightarrow \pi^- + p + (27 \pm 11)\ \text{Mev} \\ &\theta^0 \rightarrow \pi^- + \pi^+ + (258 \pm 35)\ \text{Mev} \end{aligned} \qquad (1\text{-}7)$$

Figure 1-1 is a sketch made from a photograph obtained by Fowler, Shutt, Thorndike, and Whittemore[2] in late 1953. The termination of the original π-meson track (1.5 Bev) indicates the point where the primary reaction occurred. Of the two V-tracks resulting, one consists of a proton and a negative meson, the other of two mesons, described by the secondary equations (1-7). Measurements of the angles and of the momenta of the tracks obtained from their radii of curvature in the magnetic field give the Q-values indicated, and lead to mass estimates of the two neutral particles of: $m(\Lambda^0) = (1100 \pm 12)$ Mev and $m(\theta^0) = (538 \pm 40)$ Mev. Thus the Λ^0 is heavier than nucleonic mass, and the θ^0 is in the intermediate range between π-mesons and nucleons. An estimate of the energy threshold of the incident protons required to produce this reaction is about 1.0 Bev. Considerably higher energy is needed to obtain adequate intensity and to study the process in detail.

Graphical Summary. Our present understanding of the relations between some of the better known nuclear particles and radiations is summarized in Fig. 1-2, in which the particles are displayed on a mass or rest-energy diagram in Bev units. Each particle is indicated by a horizontal line and an identify-

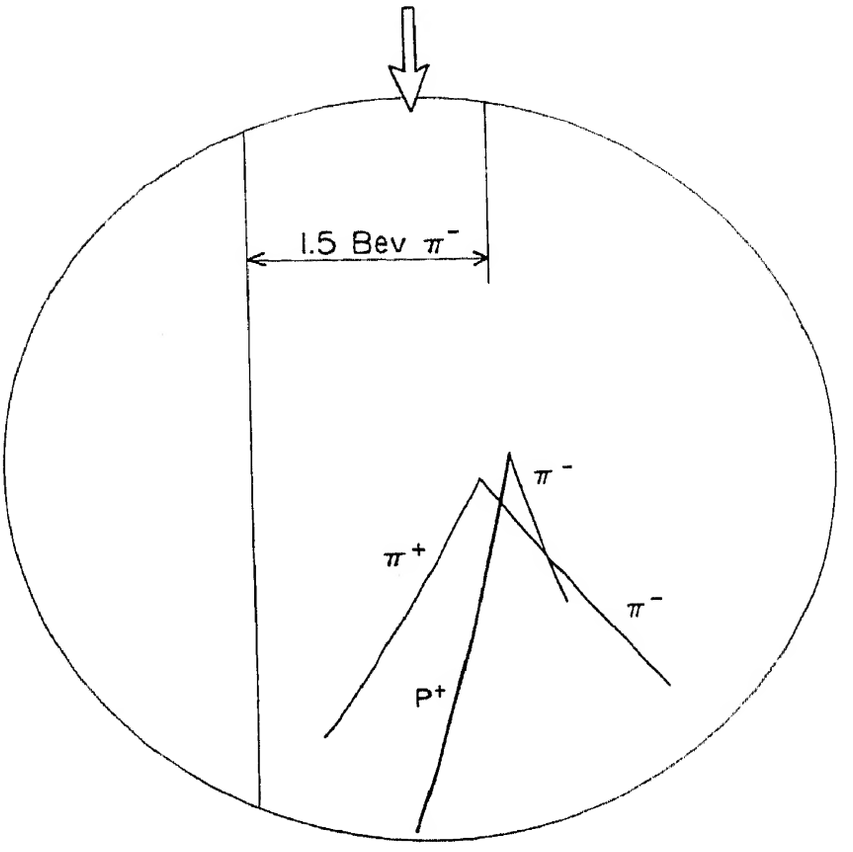

FIG. 1-1. Sketch from photograph of double V-event in a hydrogen filled pressure cloud chamber irradiated by 1.5-Bev mesons from the Brookhaven cosmotron. Two neutral particles are produced, one decaying into a p^+ and a π^--meson, and the other into two π-mesons. (Courtesy of Fowler, Shutt, Thorndike, and Whittemore, Brookhaven National Laboratory, September, 1953.)

ing symbol, with superscripts indicating the charge. Only two of the states indicated have an infinite life, those for the proton p^+ and the electron e^-. All others are unstable in the free state. Known decay half-lives are listed; a few well identified decay processes are illustrated by arrows leading to the product particles. Where a nonionizing zero-mass radiation accompanies the decay, it is indicated by the symbol γ or ν beside the arrows; the energy released (the Q-value) is also given in brackets. Other particles observed in cosmic rays (τ, K, κ) are not located specifically. The τ-meson mass is very close to that of the θ^0 particle, and for the others the mass values are believed to be in the same region. It is possible that some of these "strange" particles are related to the θ^0-particle. Similarly

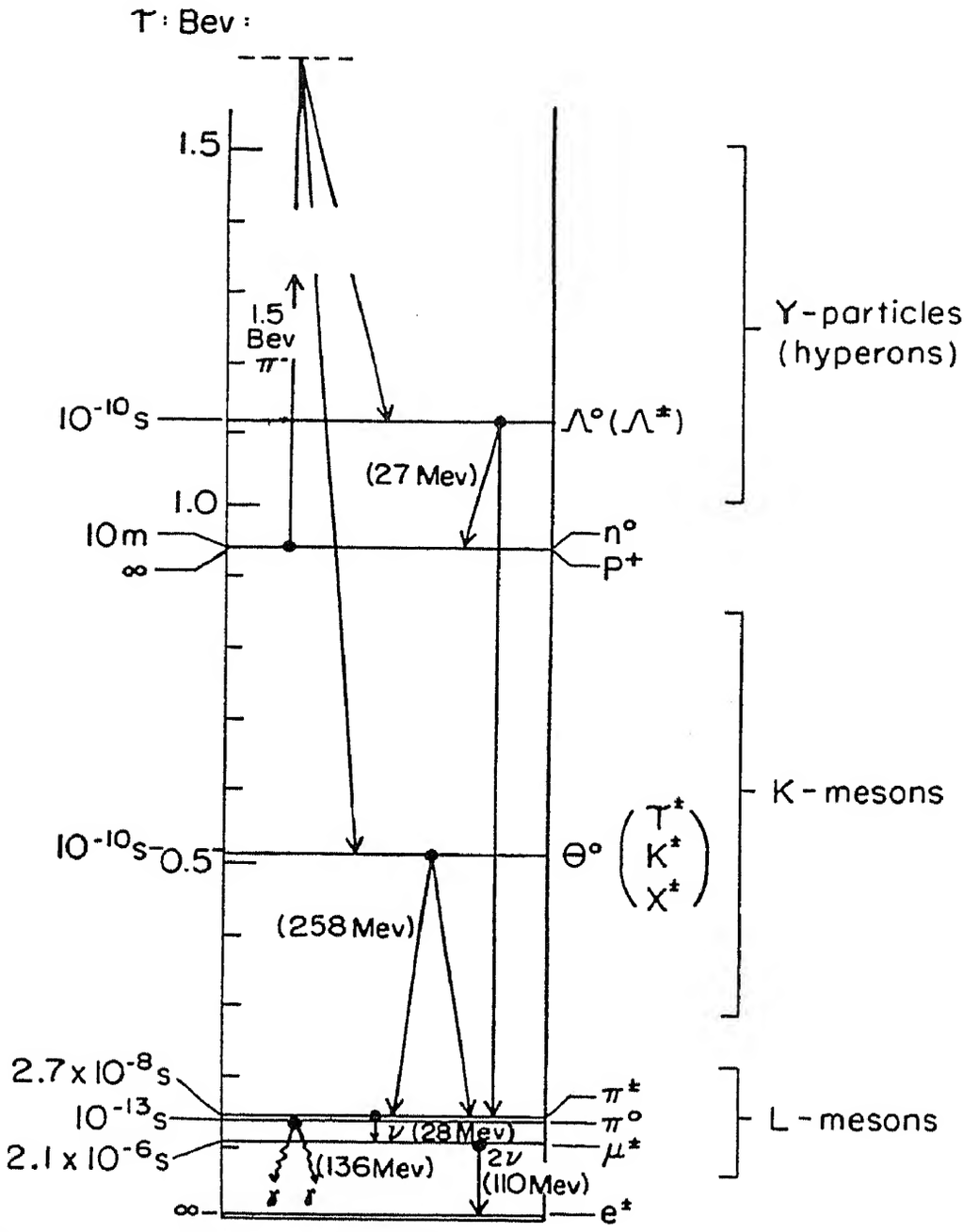

FIG. 1-2. Mass-energy diagram of some of the better known particles. Each particle is represented by a line at the appropriate value of rest energy in Bev units and identified by symbols and the decay half-life. Arrows show the decay processes and products. The Brookhaven double V-event reaction is also indicated.

the charged Λ-particles are included in brackets opposite the Λ^0-particle, although their exact mass values and even their existence are still uncertain.

Figure 1-2 serves the useful purpose of identifying the new particle terminology on a mass scale and shows the three

classes of unstable particles: the L-mesons (light), the K-mesons (intermediate) and the Y-particles or hyperons. One production reaction is illustrated in the figure, the one observed at Brookhaven and given in Eq. 1-7. This particular process is of special interest in the present context, showing how such high-energy accelerators can provide the means of studying essentially all the known nuclear particles and radiations.

If a single particle of nucleonic mass is to be created directly through materialization of energy, the threshold energy of the incident proton obtained from Eq. 1-6 is 2.34 Bev. If nucleons can be produced only in pairs, in analogy to electron-pair production, the threshold kinetic energy in a nucleon-nucleon reaction would be 5.6 Bev. If heavy particles are to be formed in an excitation state of higher rest energy than a stable nucleon, believed to be true for the $\Lambda^{\pm}$ particles, the threshold energies would be correspondingly higher. In any case the energy required to produce the phenomenon with sufficient intensity to be observable would be well above the threshold energy for the protons.

Proof of the production of a "negative proton," either by nucleon-pair production or from some other process, would be of considerable theoretical significance. Reasoning from the charge symmetry exhibited by other elementary particles would suggest a place in nature for such a negatively charged nucleon. In reactions involving the annihilation of a negative proton with a positive proton the total energy release in the center-of-mass system of corrdinates would be 1,876 Mev. A variety of competing reactions can be anticipated, yielding mesons in various numbers and types.[1] The search for new particles is one of the more stimulating features of research in high-energy particle physics.

For all the processes described above high energies are desirable, and for some of them the energies required may be greater than those available from any existing accelerator. High beam intensities are equally important to obtain statistically significant results. The high intensities available from accelerators make them more suitable than naturally occurring

cosmic rays for some research problems. Beam density, in particles per square cm per second, is 10^6 to 10^8 times higher than the cosmic ray flux, even at the top of the atmosphere. This is not to say that accelerators are likely to take over the entire cosmic ray field. The top end of the cosmic ray energy spectrum ($>10^{17}$ electron volts) exceeds by many orders of magnitude the most optimistic energy estimates by accelerator designers and, of course, studies of the origin and properties of the cosmic rays offer a continuing challenge for the cosmic ray physicist.

1.3 Meson-Producing Accelerators

The several accelerators already in service in the 200- to 500-Mev energy range have added greatly to our knowledge of elementary particle processes. Protons from synchrocyclotrons produce large intensities of positive and negative π-mesons, and the production of neutral π-mesons with the University of California 184-in. machine resulted in the first precise measurement of the properties of this new particle. Electron synchrotrons and linear accelerators produce mesons through photonuclear processes (Eqs. 1-4) and offer a hope for the future of very high-intensity meson beams.

Meson production efficiency (excitation functions) and meson properties such as mass and mean lifetime have been quite accurately determined. Cross sections for interaction of positive and negative mesons with protons and other nuclei have been obtained for meson energies up to 200 Mev. Angular distributions observed in the scattering of mesons by nucleons can be interpreted to show the range and other properties of the meson-nucleon force. Scores of other experiments have confirmed and extended the precision of cosmic ray observations.

The Brookhaven cosmotron, a proton synchrotron capable of producing 3 Bev protons, has been in operation since 1952 at 2.3 Bev, and has recently reached its designed maximum energy. At Berkeley the Bevatron is approaching completion; it is capable of reaching still higher energies, of up to 6 Bev.

Experimental research with the cosmotron is underway on

many fronts. Cloud chamber photographs in high-pressure hydrogen gas have shown evidence for Λ^0-particles, multiple meson production, many-pronged stars and other phenomena. Electronic scintillation crystal counters in coincidence circuits have been used to observe charged mesons and to study the interaction cross sections of mesons with nuclei up to 1.5 Bev. Nuclear emulsions show a variety of phenomena, including multiple-pronged stars, meson production, and some evidence for some of the rare heavy mesons.

1.4 Multi-Bev Accelerators

The role of high-energy accelerators is the study of elementary particle processes and of the short range properties of the force between such particles. The nuclear force, which binds nuclei together and leads to the concentration of energy released in fission and in thermonuclear processes, is only very imperfectly understood. Information coming from the disintegration of nuclei and scattering of particles at lower energies has been necessary and valuable, but itself appears to be inconclusive. There is a growing conviction among theoretical physicists that a complete description of nuclear forces will involve meson fields in the nucleus. To study meson properties high-energy accelerators are essential, and scientists are attacking this problem with a considerable number of 200- to 500-Mev accelerators. It is also probable that the "strange" unstable particles must be studied intensively in order to understand meson properties. Energies required for further progress in the unstable particle field are in the range above 1 Bev, where few of the present machines can go.

The real hope for exploring the multi-billion-volt range seems to lie in utilizing the principle of "alternating gradient focusing" or "strong-focusing," in the proton synchrotron, which makes accelerators of 10 or more Bev economically practical. This development, initiated at the Brookhaven National Laboratory in the summer of 1952, offers a practical method of reducing cost at this high-energy range.

The several accelerators mentioned above will be described in the chapters to follow, including the present stage of design of the strong focusing synchrotron. But first it seems advisable to discuss some general principles of motion of particles which apply to all high-energy accelerators. These can be described in terms of the equations of motion and include the properties of ion and electron orbits in magnetic and electric fields, the focusing forces resulting from certain configurations of these fields, and the several principles of resonance and synchronous stability which can be called on to accelerate the particles. We start, then, with a brief analysis of the equations of motion to define the problems and to anticipate the principles of design of high-energy accelerators.

CHAPTER 2

Principles of Acceleration to High Energies

Charged particles are accelerated only by electric fields, and in the direction of the field (for positively charged particles). Magnetic fields exert forces at right angles to the direction of particle motion and cannot change the energy, except through time variations. Both electric and magnetic fields are quantities that vary in direction and magnitude as a function of position or of time. Electric fields are established by arrays of electrodes on which suitable potentials are impressed. Magnetic fields, in accelerators, are usually developed between the pole faces of an iron magnetic circuit which is powered by current-carrying coils. One purpose of the magnetic field is to produce circular orbits of the otherwise extremely long particle paths, so as to confine particle motions within a circular, evacuated chamber which contains the accelerating electrodes. Another function is to provide restoring forces that restrict particle motions to a region close to the desired circular orbit.

The general motion of a charged particle acted upon both by electric and magnetic fields, which may vary in direction, in magnitude or in time, can be extremely complicated. The particle obeys the laws of electrodynamics, in accordance with the equations of motion. In principle, if the fields are known at every point in the path, the complete trajectory of the particle from source to target can be computed. However, exact point-by-point calculations of particle motion would be an impossibly tedious task. It is necessary to simplify the application of the equations of motion.

In all practical accelerators simplification of the motion results from symmetry of the fields. Whenever electric and

magnetic fields are used together, their major components are crossed at right angles to one another. The resulting magnetic force is in the same plane as the electric accelerating force, and particle orbits are confined to this plane. Field components in other directions are smaller in magnitude and arranged to be symmetrical about the orbit plane so as to provide restoring forces for particles which deviate from this plane. Such symmetry results in a considerable simplification in solving the equations of motion. The orbital motion of particles in the central plane can be considered separately, and the additional motions due to the minor components of the fields can be treated as small perturbations.

Another simplification results from the repetitive nature of acceleration in high-energy accelerators. In the circular magnetic accelerators the particles make many revolutions over almost identical orbits. The relatively slow variations in energy or orbit radius can be treated as smoothly varying, adiabatic changes, by allowing certain parameters in the equations of motion to vary slowly. Such variations can then be superimposed on the equations of orbital motion without serious error.

2.1 Relativistic Equations of Motion

Most of the modern high-energy accelerators, such as the cyclotron, the synchrocyclotron, the betatron, the electron synchrotron, and the proton (or frequency-modulated) synchrotron, use magnetic fields to produce motion in circular orbits. The equations of motion are fundamentally the same. Cylindrical coordinates give the simplest formulation of the equations of motion in an axially symmetric magnetic field where the accelerating electric fields are applied tangentially and act as torques about the axis of symmetry. We will use r for orbit radius, θ for angular position, and z for displacement from a median plane, as illustrated in Fig. 2-1.

Radial motion can be described in terms of the central force on the moving particle provided by the axial magnetic

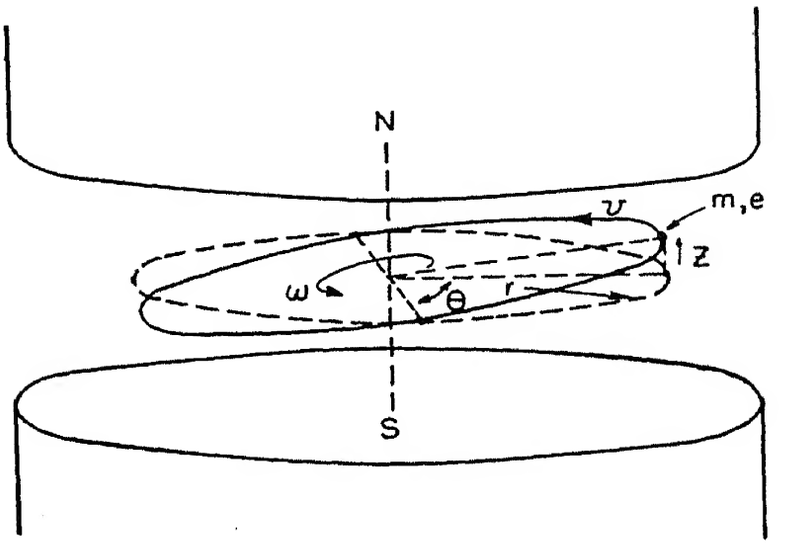

FIG. 2-1. Cylindrical coordinates of motion, r, θ, z. A particle orbit (solid line) is shown relative to the median plane (dotted line) in a uniform magnetic field.

field: $F_r = mv^2/r = evB_z$, where m, e, and v are the mass, charge, and velocity of a particle moving in a circular orbit r in a field having an axial component B_z. We need to study the change in the radial motion due to variations in v, B, etc., the deviations from an ideal circular orbit, in which case the equation of motion can be written:

$$m\frac{d^2r}{dt^2} = m\frac{v^2}{r} - evB_z$$

We use $\dot{\theta} = \omega = v/r$ for angular velocity, $m\dot{r} = m\,dr/dt$ for radial momentum and treat the mass m as a variable to allow for relativistic changes. The time rate of change of radial momentum becomes:

$$\frac{d}{dt}(m\dot{r}) = mr\dot{\theta}^2 - er\dot{\theta}B_z \qquad (2\text{-}1)$$

Angular motion is described in terms of the time rate of change of angular momentum $(d/dt)(mr^2\dot{\theta})$ and the torques acting to change this momentum. The torque due to the applied electric field can be expressed as $dw/d\theta$, the work dw done on the particle in an angular displacement $d\theta$. The decelerating torque $dL/d\theta$ is the energy lost by radiation due to

the radial acceleration of the charged particle in its circular orbit. A third torque is due to the induced electromotive force caused by any time variation of the magnetic flux threading the orbit, and the energy involved is $e\ (d\Phi/dt)$ per turn or $(e/2\pi)$ $(d\Phi/dt)$ per radian, where Φ is the flux through the orbit. The general equation for angular motion is given by:

$$\frac{d}{dt}\left(mr^2\dot{\theta} - \frac{e\Phi}{2\pi}\right) = \frac{dw}{d\theta} - \frac{dL}{d\theta} \tag{2-2}$$

Axial momentum is affected only by axial forces due to a radial component of magnetic field B_r, and is described as:

$$\frac{d}{dt}(m\dot{z}) = er\dot{\theta}B_r \tag{2-3}$$

In the three equations of motion above (Eqs. 2-1, 2-2, 2-3) rationalized mks units are used. The algebraic signs apply for electrons; they can be adapted to positively charged particles by changing the sign of the charge e. All the intentionally applied variations in the experimental parameters are included for all the circular accelerators. No terms have been included, however, to represent physical imperfections in the experimental apparatus. It is assumed, for example, that the magnetic field is symmetrical with angle, so no term is included associated with an azimuthal component of field, B_θ. It is also assumed that the field is symmetrical about the median plane ($z = 0$). Furthermore, the equations will not show the limitations to particle orbits due to the physical walls of the vacuum chamber or to the finite extent of the magnetic field.

Completely general solutions to these equations of motion would be unnecessarily complicated and of questionable value. We shall analyze the equations first with regard to the separable components of motion and shall derive the simple relations applicable to individual machines.

Consider first the orbital motion described by Eq. 2-1. The simplest case, that for an orbit of constant radius, comes

by letting $\dot{r} = 0$, and we have:

$$m\dot{\theta} = m\omega = eB_z \tag{2-4}$$

This is the fundamental relation for motion in a circular orbit, more commonly expressed in terms of the velocity in the form:

$$mv = eB_z r \tag{2-5}$$

Another form of this equation involving the frequency of revolution of the particles in the orbit, $f = \omega/2\pi$, is the cyclotron resonance relation:

$$f_0 = \frac{eB_z}{2\pi m} \tag{2-6}$$

The frequency of revolution will be a constant in a uniform and steady magnetic field if the mass of the particle remains constant; this is true only for nonrelativistic velocities.

For high energies we must use the relativistic expression for momentum:

$$mv = \frac{(E^2 - E_0^2)^{1/2}}{c} = \frac{[T(T + 2E_0)]^{1/2}}{c}$$

Here $E = mc^2$ is the total energy, $E_0 = m_0c^2$ is the particle rest energy, and T is the kinetic energy, following the definition, $E = E_0 + T$.

Using this relation we can express Eq. 2-5 in terms of the orbit radius:

$$r = \frac{[T(T + 2E_0)]^{1/2}}{ceB_z} \tag{2-7}$$

When E_0 and T are expressed in Mev units and B_z is in webers per square meter (units of 10,000 gauss) this becomes:

$$r = \frac{[T(T + 2E_0)]^{1/2}}{300B_z} \text{ meters} \tag{2-7a}$$

Values of rest energy, $E_0 = m_0c^2$, in Mev units, are given below for the particles used in accelerators:

Particle	*Rest Energy E_0, Mev*
Electron	0.51
Proton	938.
Deuteron	1877.
Hydrogen molecular ion	1876.
Doubly ionized helium	3733.

By rearrangement of Eq. 2-7 the kinetic energy is given by:

$$T^2 + 2TE_0 = c^2e^2B_z^2r^2 \tag{2-8}$$

In the relativistic limit where the kinetic energy T is very large relative to rest energy E_0, this reduces to:

$$T \sim ceB_zr \tag{2-8a}$$

This shows the proportionality between kinetic energy and momentum, B_zr, at very high energies.

In Table 2-1 a few typical values of orbit radius computed from Eq. 2-7 are listed to show the dimensional requirements of accelerators. (In using Eq. 2-7 for alpha particles the charge e must be doubled.) Note the approach to a linear relationship for electrons at quite low energies. Note also the converging dimensions for electron and heavy-ion orbits at high energies.

The relativistic expression for orbital frequency comes

Table 2-1. Orbit radius (meters) in a magnetic field of 1 weber/m².

T, Mev	Electrons	Protons	Deuterons	He^{++} ions
1	0.00473	0.144	0.204	0.144
10	0.0349	0.457	0.646	0.454
100	0.334	1.48	2.06	1.45
1000	3.33	5.64	7.25	4.85
10000	33.3	36.3	39.0	22.0

from Eq. 2-6 by inserting the energy equivalent of the mass:

$$f = \frac{eB_z}{2\pi} \frac{c^2}{(E_0 + T)} = \frac{eB_z}{2\pi m_0} \left(\frac{1}{1 + T/E_0} \right)$$

$$= f_0 \left(\frac{1}{1 + T/E_0} \right) \qquad (2\text{-}9)$$

Here f_0 is the nonrelativistic cyclotron frequency, which can be considered a constant of the motion. Equation 2-9 shows the change in applied frequency necessary to maintain resonance in the uniform field of a synchrocyclotron with increasing particle energy.

Orbital frequency can also be expressed in terms of orbit radius by using the relativistic relation for velocity:

$$f = \frac{v}{2\pi r} = \frac{c\beta}{2\pi r} = \frac{c}{2\pi r} \left[1 - \left(\frac{E_0}{E_0 + T} \right)^2 \right]^{1/2} \qquad (2\text{-}10)$$

The numerical constant is readily evaluated. As long as T and E_0 are expressed in the same units, and r is in meters, we have:

$$f = \frac{47.8}{r} \left[1 - \left(\frac{E_0}{E_0 + T} \right)^2 \right]^{1/2} \text{Mc/sec} \qquad (2\text{-}10a)$$

As an example, consider a high-energy electron in an orbit of 1 m radius in a synchrotron (the magnetic field must have the proper value). For energies above a few Mev the second term involving the energies becomes negligible, and the frequency approaches a constant value of 47.8 Mc/sec.

Table 2-2. Orbital frequency (Mc/sec) at 1 weber/m².

T, Mev	Electrons	Protons	Deuterons	He^{++} ions
1	9,500.	15.2	7.60	7.61
10	1,635.	15.2	7.60	7.61
100	143.	13.8	7.34	7.40
1000	14.3	7.46	5.00	6.05
10000	1.43	1.32	1.22	2.11

In Table 2-2 a few typical values of ion rotation frequency are listed for the several particles. The magnetic field is 1 weber/m^2, and the orbit radii are those given in Table 2-1. Note the converging values of frequency for all particles at very high energies. The rotation frequencies for different magnetic fields are inversely proportional to the flux density.

2.2 Orbital Stability

An additional requirement for accelerators is that they provide restoring forces for particles that deviate from the central orbit. Focusing forces are essential to prevent loss of the beam against the chamber walls while the particles are traversing their thousands of revolutions. In an absolutely uniform magnetic field a particle making a small angle with the plane of the orbit would traverse a helical spiral, and the axial displacement would increase linearly with the number of revolutions. Furthermore, radial displacements of the actual orbit may occur which would cause the particle to be lost against the sides of the vacuum chamber. It is essential that the applied electric and magnetic fields provide suitable restoring forces to focus the particles about the central orbit.

Such restoring forces will exist in a *magnetic field which decreases in magnitude with increasing radius.* In this field the lines of magnetic flux are concave inward. This concave shape is the natural shape of the magnetic field near the periphery between cylindrical poles with flat faces and is called "fringing." In other regions this shape can be achieved by contouring the pole faces so that gap length increases, and flux density decreases, with increasing radius. Figure 2-2 is a diagram of a magnetic field between cyclotron pole faces commonly used to illustrate this concave field and shows the direction of the forces on charged particles moving in orbits above or below the median plane.

The direction of the magnetic force on the moving particle is normal to the local direction of the magnetic flux. For particles above the median plane it will have a downward compo-

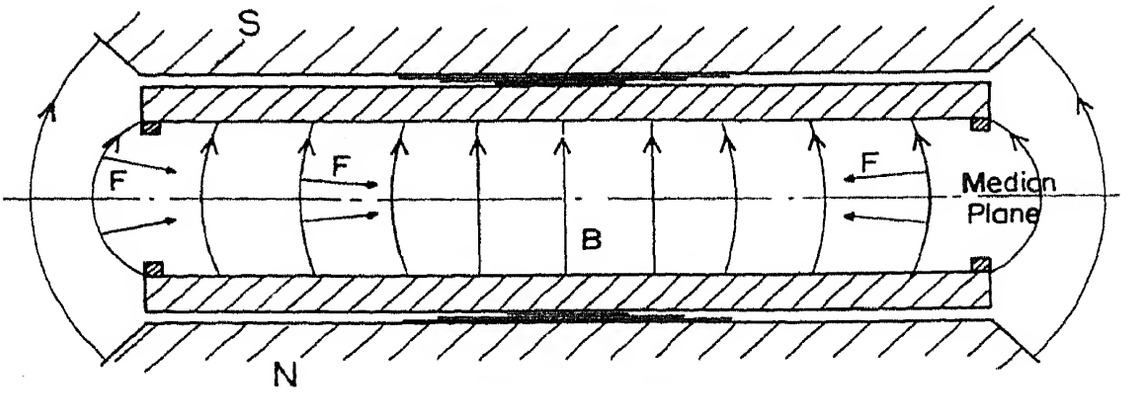

FIG. 2-2. Restoring forces for particles in orbits above or below the median plane in the radially decreasing magnetic field of a cyclotron. The flat pyramid shims shown in the shimming gaps are arranged to provide a small radial decrease in field in the center of the gap between poles. Ring shims at the periphery increase the region of useful field.

nent, owing to the radial component of the flux B_r ; conversely, an upward force is exerted on particles below the median plane. The radial component of field is zero on the median plane, but for all other locations two components exist, B_z and B_r . The magnitude of the radial component needed to provide adequate restoring forces is small, and the concave flux lines have large radii of curvature relative to displacements from the median plane; hence the shape of the flux lines near the median plane will approximate arcs of circles, and the radial component B_r will be proportional to the displacement z. This proportionality will be evaluated below in terms of the "slope" or radial decrease of the field.

A radially decreasing field can be specified in terms of an index n which is the exponent of the radial variation:

$$B_z = B_{z0}(r_0/r)^n \tag{2-11}$$

Here B_{z0} is the field on the median plane at the orbit r_0 , and B_z the field at a nearby radius r. The index n, which defines the rate of decrease, can be obtained by differentiation, as:

$$n = -\frac{r_0}{B_{z0}}\frac{dB_z}{dr} \tag{2-12}$$

Any positive value of n will produce the vertical restoring forces

described above; a value of $n = 0$ represents a uniform field, with no radial variation; a value of $n = 1$ is a field which varies inversely with the first power of the radius.

We are considering magnetic fields similar to those in free space and are neglecting time-varying electric or magnetic potentials. For such magneto-static or "conservative" fields curl $B = 0$, and we have for the relation between components:

$$\frac{dB_r}{dz} = \frac{dB_z}{dr} \tag{2-13}$$

By integrating and using Eq. 2-12, we find for the radial component at a displacement z from the median plane:

$$B_r = -\frac{nB_z z}{r} \tag{2-14}$$

The restoring component of force F_z is given by:

$$F_z = evB_r = -ne\omega_0 B_z z = -\kappa_z z \tag{2-15}$$

It is clear that the vertical restoring force is proportional to the displacement, leading to oscillatory motion about the median plane.

Radial restoring forces also exist in this radially decreasing field. The radius of the true, theoretical orbit is given by Eq. 2-7, and in a cylindrically symmetrical magnetic field the orbit will be located with its center concentric with the isomagnetic circles. We will call this the "equilibrium" orbit and label its radius r_0. A particle that deviates from this orbit and is temporarily at a larger radius r will be in a reduced magnetic field B_z; hence the magnetic force producing motion in a circle will be less. The converse is true for a particle of the same energy which is physically displaced to a location of smaller radius r. If the motion is to be stable, there must be restoring forces that will return the deviant particle to the equilibrium radius r_0.

Under certain conditions the centripetal force producing motion in a circle will be sufficient to cause the orbit to return

to its equilibrium radius. The limiting value of decrease of field with radius for which there will be a restoring action is that for which the field B_z allows the particle to continue rotating in a true circle having the displaced radius r. At this limit, since particle energy is the same for both orbits, we have the relation:

$$B_z r = B_{z0} r_0 \quad \text{or} \quad B_z = B_{z0}(r_0/r) \tag{2-16}$$

This limit represents a field for which the field index $n = 1$. Any field in which the decrease is slower, i.e., varying with an exponent less than unity, will result in a centripetal force sufficient to restore the orbit to its equilibrium position.

Another method of visualizing this radial stability is to consider temporarily a coordinate system located on the moving particle. In this system the magnetic force, $F_m = eB_z v$, is directed toward the center of the orbit, and the D'Alembertian "centrifugal" force, $F_c = mv^2/r$, is radially outward. These forces will be in equilibrium at the equilibrium orbit. Now if the magnetic field decreases with increasing radius, the magnetic force will be weaker than the centrifugal force for $r < r_0$ and stronger for $r > r_0$. In either case there will be a net restoring force to return the deviant particle to the equilibrium orbit.

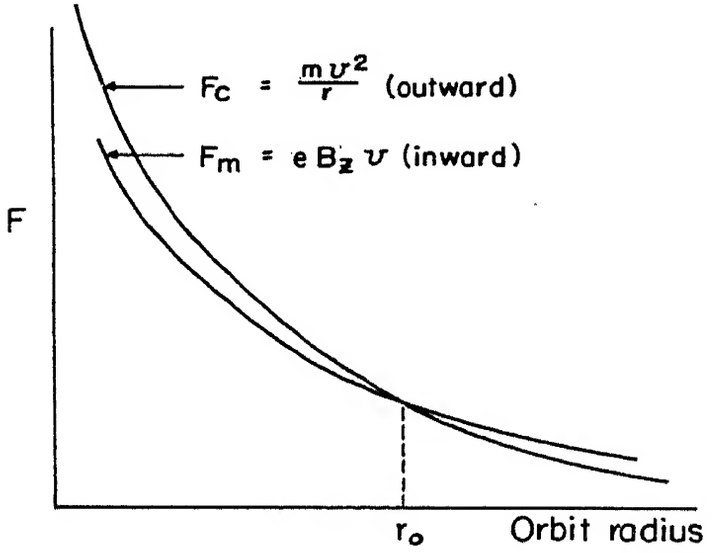

FIG. 2-3. D'Alembertian forces acting on a particle in a radially decreasing field B_z. The net force is directed toward the equilibrium orbit r_0 for particles in both larger and smaller orbits.

This argument is illustrated qualitatively in Fig. 2-3, in which F_c decreases inversely with radius and F_m decreases at a slower rate. For stability the magnetic field must not decrease more rapidly than with $1/r$, for which $n = 1$, the same conclusion as was reached above. The restoring force, which is the difference between F_m and F_c, is to a good approximation proportional to the displacement from the equilibrium orbit. The proportionality constant cannot be obtained in as simple a manner as was possible for the vertical restoring forces, but can be derived from the equations of motion.[3] From the qualitative argument above, however, it is clear that the net radial restoring force is proportional to the radial displacement from the equilibrium orbit:

$$F_r = -\kappa_r \rho \tag{2-17}$$

where $\rho = r - r_0$ is the radial displacement.

The conclusion from this argument is that restoring forces exist in a radially decreasing magnetic field for particles displaced vertically from the median plane for values of n greater than zero, and for radial displacements from the equilibrium orbit for values of n less than unity.

2.3 Free Oscillations

Motion of any system under a restoring force which is proportional to the displacement is oscillatory in nature. For the radial and vertical displacements and restoring forces described in the last section, the oscillatory motion can be described by the differential equations:

$$\frac{d^2\rho}{dt^2} + \omega_r^2 \rho = 0 \tag{2-18a}$$

$$\frac{d^2z}{dt^2} + \omega_z^2 z = 0 \tag{2-18b}$$

Here ω_r and ω_z are the angular frequencies of the two oscillations. These are the "betatron" or free oscillations of a particle in a radially decreasing field, in which the rate of decrease is

between the limits given by:

$$0 < n < 1 \qquad (2\text{-}19)$$

The derivation of these oscillation frequencies from the equations of motion (Eqs. 2-1 and 2-3) has been given by several writers, especially by Kerst and Serber[3] in their theoretical analysis of the betatron. The results are:

$$\omega_r = (1 - n)^{1/2}\omega_0 , \quad \text{or} \quad f_r = (1 - n)^{1/2}f_0 \qquad (2\text{-}20a)$$

$$\omega_z = n^{1/2}\omega_0 , \quad \text{or} \quad f_z = n^{1/2}f_0 \qquad (2\text{-}20b)$$

Here f_0 is the orbital frequency of ion revolution given by Eq. 2-6, sometimes known as the cyclotron frequency. The results show that these free oscillation frequencies are in both cases smaller than the orbital frequency; for the special case of $n = 0.5$, they are equal and are given by:

$$f_r = f_z = 0.707f_0 \quad (\text{for } n = 0.5) \qquad (2\text{-}21)$$

In general the particles traverse more than one revolution before completing a full oscillation cycle in either the radial or the vertical coordinate.

Such free oscillations in vertical and radial position occur for particles displaced from the equilibrium orbit in any magnetic accelerator. As long as amplitudes are small enough, the results can be superimposed on the orbital motion without serious error. It can be shown, for example, that ions in the cyclotron perform such radial and vertical oscillations, and that these oscillations in fact set limits to ion beam intensity. Similarly, such betatron oscillations occur in synchrotrons and in the synchrocyclotron, superimposed on the much longer period phase oscillations to be described in a following section.

The properties of the free oscillations can be visualized by considering the limiting cases. In a uniform magnetic field, for which $n = 0$, a particle displaced radially from its original circular orbit will still describe a circular path of the same radius, crossing the original orbit twice per revolution; this can be described as a radial oscillation of frequency f_0. In this

same uniform field a particle displaced by a distance z from its original plane will rotate in a parallel orbit; this is a vertical oscillation of frequency $f_z = 0$. At the other limit of $n = 1$, the field varies inversely with radius, so the product $B_z r$ is constant. A particle of momentum $mv = eB_z r$ will traverse concentric circular orbits of any radius, which means that the radial oscillation frequency is zero. Finally, since Eq. 2-14 shows that the radial component of field B_z varies directly with z for a fixed radius at $n = 1$, the vertical oscillation frequency will be identical with the angular frequency f_0.

Oscillation amplitudes are harmonic functions which are solutions of the equations of motion (Eq. 2-18);

$$\rho = P \cos \omega_r t \tag{2-22a}$$

$$z = Z \cos \omega_z t \tag{2-22b}$$

The maximum amplitudes, P and Z, are associated with the transverse energy in the oscillations. At low energies we can express this energy as:

$$\tfrac{1}{2} m v_r^2 = \tfrac{1}{2} K_r P^2 \tag{2-23a}$$

$$\tfrac{1}{2} m v_z^2 = \tfrac{1}{2} K_z Z^2 \tag{2-23b}$$

where K_r and K_z are the oscillation force constants given by:

$$K_r = (1 - n)\, \omega_0^2/m \tag{2-24a}$$

$$K_z = n\, \omega_0^2/m \tag{2-24b}$$

From Eqs. 2-23 and 2-24 we find:

$$P = \frac{mv_r}{\omega_0} \frac{1}{(1 - n)^{1/2}} \tag{2-25a}$$

$$Z = \frac{mv_z}{\omega_0} \frac{1}{n^{1/2}} \tag{2-25b}$$

The energy in these transverse oscillations arises from errors in direction of the beam of particles coming from the source at the start of acceleration or from asymmetries in the

magnetic or electric fields. In most accelerators the aperture available to the particle beam determines the initial amplitude and energy. Careful design to produce symmetrical and uniform fields will avoid further increase in oscillation energy during acceleration. However, as the particle moves into a region of higher n (as in the cyclotron), the radial amplitude increases, and the vertical amplitude decreases in accordance with Eqs. 2-25. Both these changes are advantageous in the cyclotron in that they simplify the problem of deflecting an emergent beam.

Amplitudes also vary with increasing magnetic field (as in the synchrotron), following the linear variation of orbital frequency with field given by Eq. 2-4. If the field B_z increases with time during acceleration, ω_0 increases and also the frequencies of the radial and vertical oscillations; the amplitudes decrease correspondingly. A useful way of describing this effect is in terms of the fractional variation in the variable. If we substitute expressions for ω_0 and n which show their dependence on magnetic field (Eqs. 2-4 and 2-12) in Eq. 2-25, and integrate, we obtain:

$$dP/P = \tfrac{1}{2}dB_z/B_z\,; \quad P/P_0 = (B_{z0}/B_z)^{1/2} \tag{2-26a}$$

$$dZ/Z = \tfrac{1}{2}dB_z/B_z\,; \quad Z/Z_0 = (B_{z0}/B_z)^{1/2} \tag{2-26b}$$

Thus we see that both transverse oscillations are damped to smaller amplitude with increasing magnetic field, varying with $B_z^{-1/2}$. This is the explanation of the very small transverse cross section of the high-energy particle beams in betatrons and synchrotrons.

2.4 Particle Energy

The second of the equations of motion (Eq. 2-2) describes the torques acting to change the kinetic energy of the particle in its orbit. This equation can be rewritten:

$$\frac{d}{dt}\left(mr^2\omega - \frac{e}{2\pi}\Phi\right) = \frac{dw}{d\theta} - \frac{dL}{d\theta} \tag{2-27}$$

The significance of this equation can be made more obvious, for nonrelativistic velocities, by expressing it in terms of the change in particle energy. To see this we multiply the equation by ω which is $d\theta/dt$:

$$\frac{d}{dt}(mv^2) = \frac{e\omega}{2\pi}\frac{d\Phi}{dt} + \frac{dw}{dt} - \frac{dL}{dt} \qquad (2\text{-}28)$$

The term in $d\Phi/dt$ involves the time rate of change of flux linking the orbit, which determines the induced voltage experienced by the particles. This is the principle of the transformer and is responsible for the acceleration of electrons in the betatron. By neglecting momentarily the two terms on the right of Eq. 2-27, we have:

$$\frac{d\Phi}{dt} = \frac{d}{dt}\left(2\pi\frac{m}{e}\omega r^2\right) \qquad (2\text{-}29)$$

Substituting the general expression for ω of Eq. 2-4, we find:

$$\frac{d\Phi}{dt} = 2(\pi r^2)\frac{dB_z}{dt} \qquad (2\text{-}30)$$

This is the relation between rate of change of flux linking the orbit and rate of change of flux density at the orbit, for acceleration *at constant radius.* It can be integrated over a cycle starting with $B_z = 0$ and $\Phi = 0$ at $t = 0$ to give:

$$\Phi = 2(\pi r^2)B_z \qquad (2\text{-}30a)$$

For acceleration at constant radius with these initial conditions, the *total flux* linking the orbit must be at all times *twice* that obtaining if the field inside the orbit were uniform and equal to the *field at the orbit.* This is the betatron "2 to 1" rule.

The induced voltage is zero for any accelerator in which B_z is constant with time, such as the cyclotron. It must be included in those accelerators, such as synchrotrons, in which B_z increases with time. The sign of the term depends on magnet geometry; it can be decelerating if the net flux through the orbit is opposite in direction to the flux at the orbit.

The second energy term comes from the first term on the right in Eq. 2-27, which is the electrical torque, here expressed as a generalized force $dw/d\theta$, where dw is the work done during a displacement $d\theta$. This torque is usually applied by means of one or more accelerating gaps between high-frequency electrodes. There are two accelerations per turn between the D's of a cyclotron, or one in the single accelerating cavity of a synchrotron. However, the number of particle revolutions is generally so large in synchronous accelerators (10^4 to 10^6 for synchrotrons) and the fractional increase in energy per revolution so small, that we can treat the acceleration process adiabatically and describe it in terms of an azimuthally uniform accelerating torque which varies slowly with time. The value of the torque can be expressed in terms of the energy acquired in traversing a voltage drop V in each revolution:

$$\frac{dw}{d\theta} = \frac{Ve}{2\pi} \tag{2-31}$$

Such an externally applied electrical field must be oscillatory and must be phased to be in resonance with the charged particles, which will become bunched in phase with respect to the field and so also bunched in azimuthal location in the orbit. To study this bunching we introduce the phase at which particles cross the accelerating gap, as:

$$\frac{dw}{d\theta} = \frac{Ve}{2\pi} \sin \phi \tag{2-32}$$

Here ϕ is the phase angle of the field when the particle crosses the gap and V is now the peak rf voltage across the gap. Choice of the sine function is equivalent (for electron acceleration) to defining zero phase as the instant when the field is zero and becoming positive, or when it is changing from accelerating to decelerating.

The third torque term, $dL/d\theta$, describes the radiation loss due to the radial acceleration of the particle in its orbital motion. The magnitude of this effect can be derived from

the classical theory of the electromagnetic field. Several writers[4] have shown that the magnitude is given (in mks units) by:

$$\frac{dL}{d\theta} = \frac{2}{3}\frac{e^2}{4\pi\epsilon_0 R}\left(\frac{E}{E_0}\right)^4 \tag{2-33}$$

The radiation loss increases with the fourth power of the ratio of energy to rest energy for constant radius. However, when the linear relation between energy and orbit radius at a fixed maximum value of magnetic field is included, we find that the radiation loss increases approximately with the cube of particle energy, or as $(E/E_0)^3$. When evaluated for the radial dimensions required for an electron synchrotron (Table 2-1), Eq. 2-33 shows a loss of roughly 30 kv per turn at 1 Bev energy, or 240 kv at 2 Bev. Existing electron synchrotrons use a single rf accelerating gap, and this last figure is close to the maximum practical acceleration per turn, restricting maximum energy to about 2 Bev. However, heavy particles such as protons have so large a rest energy that the energy loss by radiation is negligible for all energies considered to date.

We see that particles can be accelerated in a circular magnetic accelerator either by betatron induction or by rf electric fields applied to suitable electrodes. Energy can be lost by radiation from electrons at high energy. Otherwise the only significant energy loss is caused by particles striking residual gas molecules in the chamber, or by hitting the walls.

2.5 Phase Stability in Circular Motion

Resonance accelerators operate on the principle of providing successive small accelerations synchronized with the motion of the particles. The problem in high-energy machines is to keep synchronization for an extremely large number of accelerations. This requires control of the phasing between the electric fields applied to the electrodes and the bunch of particles revolving in the orbit. The mechanism which makes this possible is a stable oscillation in the phase at which the particle crosses

the accelerating gap, about a mean value which is just adequate to provide the desired volts per turn to keep the particles in resonance with the applied frequency. This is called the principle of "phase stability." It was proposed independently in 1945 by McMillan[5] and Veksler[6] as a method of maintaining resonance indefinitely in a cyclotron-like accelerator. It has led to two classes of accelerators: the synchrotron, for the acceleration of electrons, and the synchrocyclotron, for the acceleration of light positive ions.

Phase oscillations can be described qualitatively by using simple physical concepts. Let us consider first the "stationary" orbits of a charged particle rotating in a steady magnetic field, shaped to give orbital stability ($0 < n < 1$) as described earlier. Let us provide at one point in the orbit a gap between electrodes across which a high-frequency electric potential can be impressed, and let us apply to these electrodes a frequency identical with the natural rotational frequency of the ions given by Eq. 2-9.

The phase relations between the ions and the electric field are illustrated in Fig. 2-4, in which the paths of the particles are considered as unrolled into a straight line along the time axis. A particle which crosses the gap at zero phase, ϕ_0, when the electric field is crossing zero in the direction of changing from accelerating to decelerating, is indicated by the points labeled 0, 2π, 4π, etc. This particle will neither gain nor lose energy, will remain in precise resonance, and will continue to rotate at constant frequency and in the same orbit.

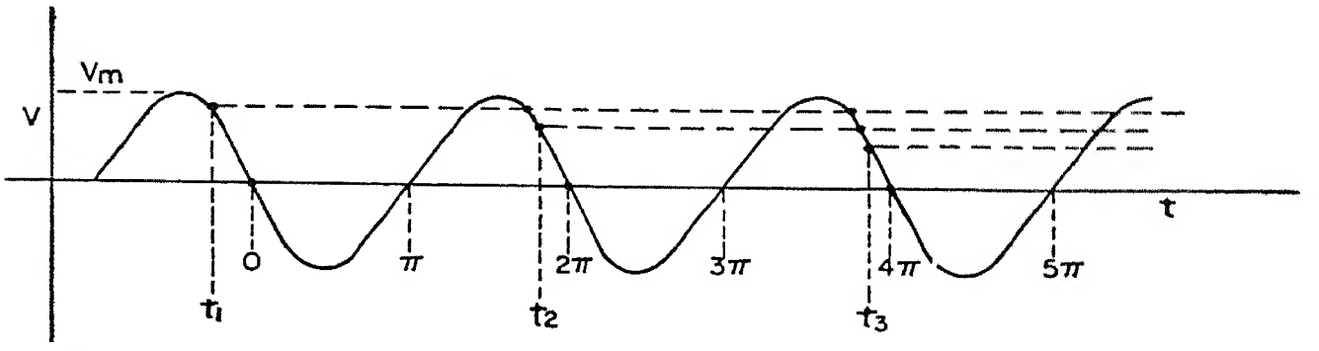

FIG. 2-4. Variation of accelerating potential with time showing origin of phase oscillations.

Now to see that this orbit is stable, consider a particle crossing the gap at an earlier phase, such as t_1 in Fig. 2-4. In its first traversals this particle will gain energy, and its frequency will decrease as shown by Eq. 2-9. (We shall neglect temporarily the small variation of magnetic field B_z with radius.) The reduced frequency will cause the particle to be delayed slightly in subsequent traversals of the gap, illustrated by points t_2, t_3, etc., in Fig. 2-4. It will continue this migration in phase until it crosses the gap at zero phase. However, it will have an accumulated excess of energy, so it will continue the phase shift into the decelerating part of the cycle. Now the situation is reversed, and it loses energy; its frequency increases, and it is again returned to the zero phase position.

This motion represents an oscillation in phase about the phase of the undisturbed orbit for which the frequencies are in exact resonance. It also represents an oscillation in energy about the equilibrium value. Furthermore, since orbit radius varies with energy as shown by Eq. 2-7, it results in a radial oscillation. As long as the energy exceeds the equilibrium energy, the particle will travel in orbits of larger radii; conversely, it will have smaller orbits at lower energy.

The principle of phase stability is based on the existence of phase oscillations as described above, centered about the equilibrium values of phase, of energy and of radius. For an assumed steady magnetic field the particles will be spread around the entire circuit, over a phase bracket extending from $\phi_1 = \pi$ to $\phi_2 = -\pi$. Each particle migrates slowly forward or back along the length of the bunch, requiring many hundreds or thousands of revolutions to complete a phase cycle. This type of oscillating orbit with fixed average energy can be called stationary.

Note that particles crossing the gap at the alternate zero voltage positions of $\phi = \pi, 3\pi$, etc., are in a condition of unstable equilibrium. If slightly disturbed, such a particle would either gain or lose energy and would fall into large amplitude oscillations about the stable phase.

Let us now consider how the energy in such a stationary orbit can be increased in a particle accelerator. We need to consider two cases: constant particle velocity (i.e., high energy electrons with $v \simeq c$) and increasing particle velocity (protons or other positive ions with $v < c$).

In the first case, if magnetic field is increased by a small amount, the electron frequency will increase proportionately, as shown by Eq. 2-9. This will be accompanied by a temporary decrease in orbit radius. The electron will cross the gap at earlier phases, acquiring more energy each time, until it reaches that energy for which it is again in resonance with the applied electric field, and the orbit radius is back to the original value. Furthermore, *if magnetic field is increased* slowly and continuously, *the electrons* will follow this change and *gain energy at a steady rate determined by the time rate of increase of magnetic field.* This is the principle of the synchrotron.

For the other case, where particle velocity increases with energy, consider the effect of a small decrease in frequency of the applied electric field, with magnetic field held constant. This lengthening of the time cycle, while particle frequency remains fixed, also causes the particle to cross the gap at earlier phases, acquiring energy until it reaches the energy which is in resonance at the new frequency, following Eq. 2-9. Increased energy in the nearly uniform magnetic field means that the final orbit radius is larger. Now, *if frequency is decreased* slowly and continuously, *the particles* will follow this change, will *gain in energy*, and will increase in orbit radius *at a steady rate determined by the rate of frequency modulation.* This is the principle of the synchrocyclotron.

Under either of the conditions described above there will be an equilibrium phase ϕ_e about which the phase oscillations are centered. This is illustrated in Fig. 2-5 in which the range of phase oscillations is indicated as extending between arbitrary limits ϕ_1 and ϕ_2. For a particle having such a phase oscillation, and making several hundred revolutions to complete the phase cycle, as we will see later, there will be an average energy gain

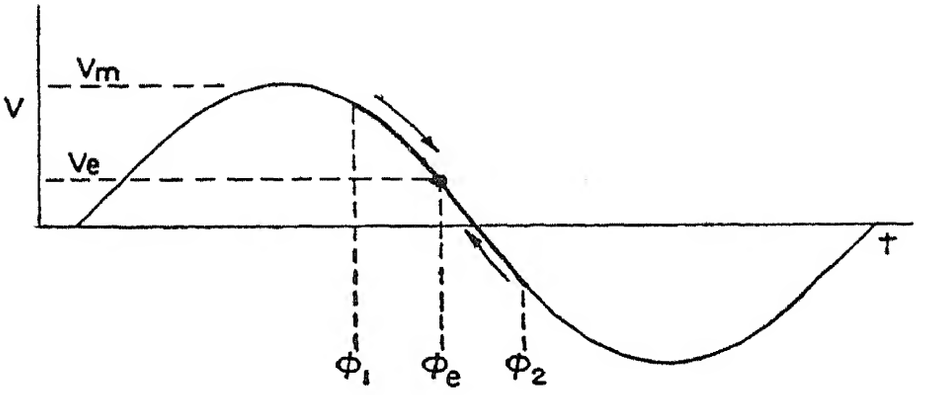

FIG. 2-5. Phase oscillation about equilibrium phase ϕ_e between arbitrary limits ϕ_1 and ϕ_2.

per turn, $V_e e$, given by the value of the potential difference across the gap at equilibrium phase. The particle migrates up and down along the phase curve, at one extreme acquiring excess energy and at the other having a deficit.

Another visualization of phase oscillations is illustrated in Fig. 2-6. Here the oscillations in energy of a particle are portrayed as a function of time, with the equilibrium energy increasing slowly. This figure can be interpreted as a potential energy diagram with stable potential valleys in which particles are trapped. The dots represent consecutive positions of a particle which is oscillating within this potential valley. As the magnetic field increases, and the oscillations progress, the

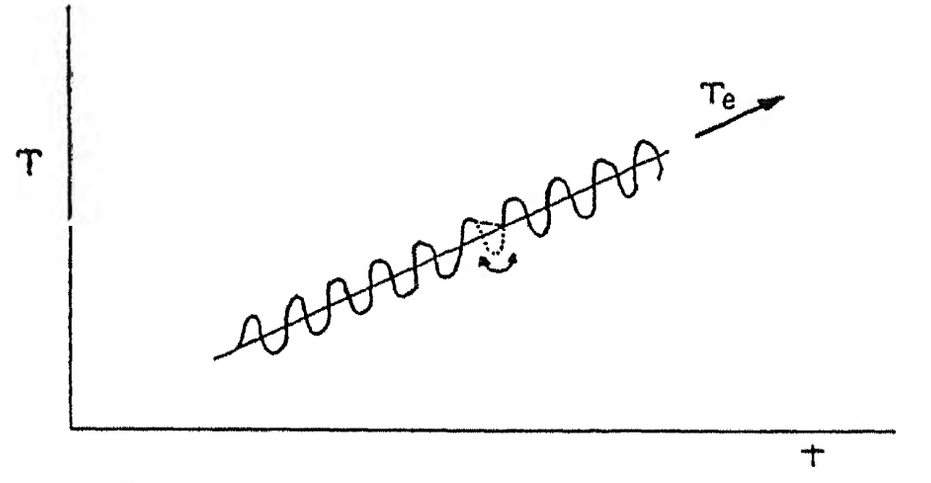

FIG. 2-6. Energy oscillations in phase stable acceleration. Particles are trapped in a potential valley and are carried to high energy by modulation of magnetic field (synchrotron) or frequency (synchrocyclotron).

pattern will move upward and to the right along a line which represents the average energy increase, carrying the trapped particles to higher energies. The solid curve in Fig. 2-6 represents the variation in energy of a particle at the extreme limit of phase oscillation. Other particles will have smaller amplitude variations. The limit of stability appears here as the peak of a potential hill. If a particle crosses over the rim of one trough, it will be lost from synchronism.

Several writers have pointed out that the phase oscillations described above are analogous to the motion of a pendulum to which is applied a constant torque. A physical model can be constructed as a simple pendulum mounted on a good bearing and with a cord carrying a weight wrapped around the hub. Such a pendulum is illustrated in Fig. 2-7. When at rest, the pendulum has an angular displacement θ_e ; when set into motion it oscillates about this equilibrium position. The limit of stable oscillation is for $\theta_1 = \pi - \theta_e$. If the amplitude exceeds this limit, the pendulum will cease to oscillate and will spin continuously in one direction.

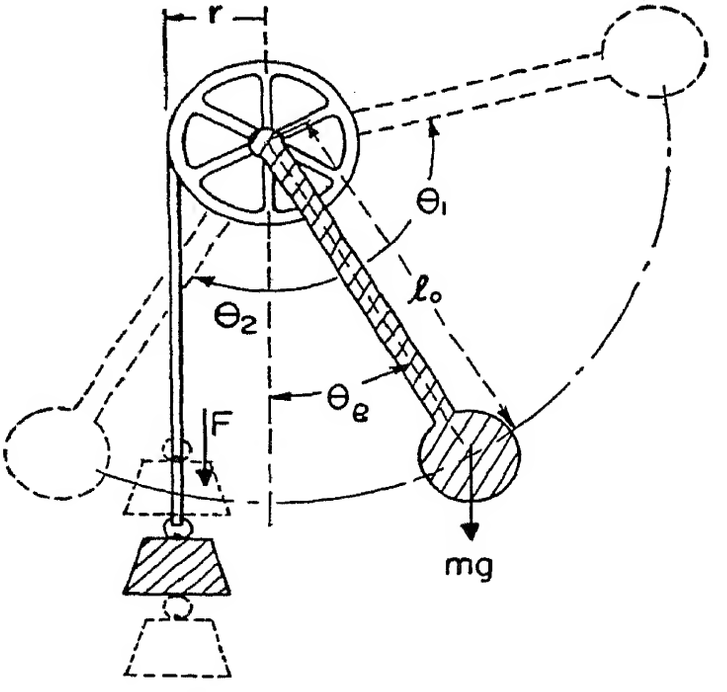

FIG. 2-7. Pendulum analogue of phase oscillations. A constant torque Fr results in an equilibrium angle θ_e about which oscillations are centered.

The equation of motion for the pendulum is of the form:

$$\frac{d^2\theta}{dt^2} + \frac{mgl_0}{I} (\sin \theta - \sin \theta_e) = 0 \qquad (2\text{-}34)$$

where the term $mgl_0 \sin \theta_e$ represents the constant perturbing torque, I is the moment of inertia, and oscillations occur about the equilibrium angle θ_e. If the perturbation is small relative to the maximum displacement, the angular frequency of oscillation is given, to a high degree of approximation, by:

$$\omega = \left(\frac{mgl_0}{I}\right)^{1/2} \qquad (2\text{-}35)$$

The equation for phase oscillation is similar, with the phase angle in particle motion substituting for the angular displacement of the pendulum, the average accelerating energy per turn taking the place of the perturbing torque due to the weight, and the equilibrium phase substituting for equilibrium angle. To complete the analogy, however, the mass and length of the pendulum (its moment of inertia) should vary slowly to be equivalent to the increasing mass and energy of the particles.

Derivation of the equations of phase oscillation from the equations of motion goes beyond the scope of this monograph. However, the method will be described briefly, and the results given. The first two of the equations of motion are used, Eqs. 2-1 and 2-2. It is assumed that the phase oscillations are so slow and the amplitude of the associated radial oscillations so small, that we can neglect the radial acceleration term in Eq. 2-1. This is the basic assumption used by all writers utilizing the quasi-stationary theory; it is accomplished by letting $dr/dt = 0$ in Eq. 2-1. We also neglect the radiation loss term $dL/d\theta$, which is significant only for electrons at very high energy. The betatron induction term $d\Phi/dt$ is retained because it affects the oscillation energy associated with the changing orbit radius.

With these simplifications, when the two equations of

motion are combined, they take the form:

$$\frac{d}{dt}\left(r^2 B_z - \frac{\Phi}{2\pi}\right) + \frac{V}{2\pi}\sin\phi = 0 \qquad (2\text{-}36)$$

However, this equation cannot be solved directly to obtain the phase oscillations.

The method of small variations is used, in which r and $\dot{\theta}$ are assumed to have the form: $r = r_0 + \rho$ and $\dot{\theta} = \omega_0 + \dot{\phi}$. The two equations of motion are first expanded as a function of the quantity ϕ alone, and are then combined in the form of an equation of oscillation. The result is[7]:

$$\frac{d^2\phi}{dt^2} + \frac{V\omega_0}{2\pi r_0^2 B_{z0}(1 - n)}(\sin\phi - \sin\phi_e) = 0 \qquad (2\text{-}37)$$

By analogy with the pendulum equation we see that the angular frequency of this phase oscillation is given by:

$$\omega = \left(\frac{V}{2\pi r_0^2 B_{z0}(1 - n)\omega_0}\right)^{1/2}\omega_0 \quad \text{(rel.)} \qquad (2\text{-}38)$$

The equation above is valid for the relativistic case represented by high-energy electrons. At lower velocities, such as for protons in the synchrocyclotron, different approximations are required in the solution. In this case the frequency of phase oscillation is:

$$\omega = \left(\frac{Vn}{2\pi r_0^2 B_{z0}(1 - n)\omega_0}\right)^{1/2}\omega_0 \quad \text{(nonrel.)} \qquad (2\text{-}39)$$

The difference between frequencies calculated from the two equations is small when n is of the order of unity (0.5 to 0.8). In the most extreme case, for protons in the synchrocyclotron where $n \simeq 0.05$, Eq. 2-39 gives frequencies smaller by about a factor of 5. Evaluation of the frequency of phase oscillation for practical cases shows it to be 200 to 2000 times smaller than the orbital frequency ω_0, so the particle makes this many turns around the orbit to complete a phase cycle. This justifies the assumptions made in the derivation and in the use of the quasi-stationary approximation.

Phase amplitude is damped slightly due to the increasing magnetic field (in synchrotrons) varying approximately with $B_z^{-1/4}$. So the azimuthal spread in the bunch of particles is decreased to about half the initial amplitude during acceleration. In a practical case this might reduce an initial 180° azimuthal spread to about 90°. The radial amplitude of phase oscillations decreases in the increasing magnetic field, however, so the bundle of particles becomes very much smaller in cross section.

2.6 Coupling between Oscillations

Coupling can occur between the several types of particle oscillations when the frequencies are integral multiples. This is the familiar phenomenon of beats. A simple analogy is the coupled pendulum. As is well known, two such pendulums which are in resonance will feed energy from one to the other and back again, the more rapidly the tighter is the coupling and the closer the resonance. It is also known that there is no significant transfer of energy if the oscillation frequencies are not in resonance.

Energy can be transferred between the several modes of oscillation in synchronous accelerators because of the irregularities and nonlinearities in the electric and magnetic fields. These were neglected in the simple approximations used for solving the equations of motion. However, second order terms do exist, and the fields are not so smooth and regular as assumed. The coupling can be studied by including second order terms in the small quantities ρ, $\dot{\phi}$, and z, and analyzing the coupling terms in the solutions.

The most common type of coupling is between the two transverse modes of the free oscillations, the radial and the vertical. Equations 2-20 give the frequencies as a function of the index n. When $n = 0.5$, the two frequencies are identical, and amplitudes can alternate between the radial and vertical mode. At $n = 0.2$ there is a first harmonic resonance between the two modes. Energy in radial oscillations can transfer to the vertical mode at this value of n, observed in the synchrocyclotron as

the radial position at which the beam "blows up" into large vertical oscillations, and is lost against the D.

Detailed study has led to a list of certain critical or partially forbidden values of n for circular synchronous accelerators. The most significant are for $n = 0, 0.2, 0.25, 0.5, 0.75, 0.80, 1.0$. Some of these n-values are not absolutely forbidden, since amplitudes may be too small for the energy transfer to be serious, or they may occur over such a narrow band of pole face that particles can cross through the critical region in only a few revolutions, and the time may be too short for significant energy exchange to occur. Nevertheless, they represent possible difficulties and are usually avoided in design. A typical value of n for synchrotrons is 0.6, and it is assumed that regions of the field in which n is less than 0.5 or greater than 0.75 are outside the useful aperture.

Still other resonances have been recognized and are avoided in design where possible, such as between the phase oscillation frequency and harmonics of the 60-cycle ripple usually impressed on the magnet if an alternating-current power supply is used.

2.7 Description of Particle Motions

The results of the preceding discussion can be summed up by describing the physical characteristics of the bunch of particles in an accelerator. Let us first consider the synchrotron, in which the particles move in a doughnut-shaped vacuum chamber around an orbit of fixed radius. The phase oscillations represent a variation in time of crossing the accelerating gap. Particles will be distributed initially around a large angle in azimuth, approaching 360° for the limiting case of very slow acceleration and about 180° in practical cases. This spread in angle will be reduced by damping to about 90° by the end of the acceleration interval. Individual particles will be migrating slowly through the bunch from front to back and return, taking several hundred revolutions about the orbit to complete a phase cycle. Radial phase oscillations will be associated with the energy os-

cillations, so the bundle will have a certain radial width. Superimposed on these slow synchronous radial oscillations are the higher frequency free oscillations in both transverse coordinates, owing to spatial deviations from the smoother synchronous orbits. The bunch of ions is thus enclosed within an envelope shaped like a long, thin sausage, bent around the orbit. The center of this bunch revolves at the resonant frequency f_0 about the circle. Figure 2-8 is a schematic illustration of the bunch of ions, with a rather imaginative treatment of the several oscillations. During acceleration the transverse dimensions of the envelope become very small on account of damping, of the order of a few millimeters in electron synchrotrons.

In the synchrocyclotron, positive ions are released from an ion source at the center of a large flat chamber between flat

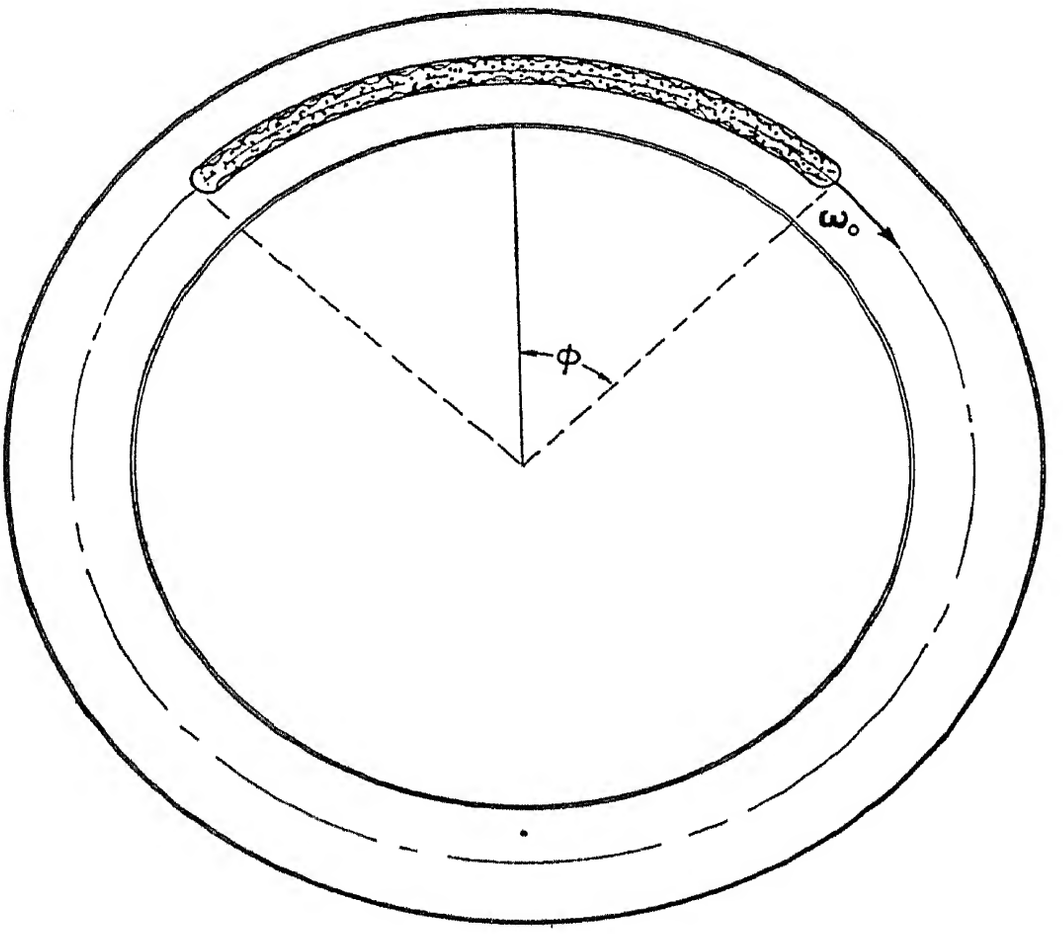

FIG. 2-8. Schematic view of "bunch" of phase-focused particles in a synchrotron, showing the spread due to phase oscillation and suggesting the superimposed free oscillations.

pole faces. The magnetic field is very nearly uniform, decreasing slightly with radius to provide focusing forces. The bunch of synchronous ions has much the same properties and the elongated sausage shape described for the synchrotron, except that the equilibrium orbit expands slowly and steadily in radius as frequency is changed. The several oscillations occur about this expanding equilibrium orbit and are slightly modified by the changing n-value of the magnetic field. For example, as the n-value grows larger near the periphery, the vertical oscillations are decreased in amplitude, while the radial amplitudes increase. Synchronous oscillations cause a "breathing" motion of the instantaneous particle orbits as the equilibrium orbit slowly expands.

In either type of accelerator a single pulse of particles is swept to high energy in each sweep of the magnetic field or of the applied frequency. The machines are operated cyclically, repeating the sweep at regular intervals. So the final output is a sequence of pulses of high-energy particles at the cyclic repetition rate.

CHAPTER 3

The Electron Synchrotron

3.1 Early Development

Very-high-energy accelerators—in the billion-volt range—utilize the principle of resonance acceleration with phase stability first demonstrated with electrons in the synchrotron at much lower energies. Although additional features are required to exceed one billion volts, such as the use of protons rather than electrons and the development of variable frequency acceleration techniques, the basic principle is still that of phase-stable synchronous acceleration.

The principle of phase-stable acceleration described in Chap. 2 was proposed independently and almost concurrently by McMillan[5] at the University of California and by Veksler[6] in the U.S.S.R. McMillan described an electron accelerator utilizing this principle and named it the synchrotron. His first designs were for a machine to operate at 300 Mev, which was completed in 1947. Unlike previous accelerators, most of which required slow and tedious development starting with small models, the synchrotron was conceived in its full stature as a high-energy accelerator, and most of the early installations were designed for the 300- to 400-Mev energy range, at which the electrons and x-rays are capable of producing mesons. By 1950 there were 6 synchrotrons of over 300 Mev energy built or under construction in the United States and several others abroad. More recently, a synchrotron capable of reaching 1 Bev has passed its preliminary tests at 0.5 Bev at the California Institute of Technology, and others in the 1-Bev range are contemplated. A listing of the larger machines is given in Table 3-1.

Table 3-1. List of the larger electron synchrotrons.

Location	Energy, Mev	Status in 1954
University of California, Berkeley, California	322	Operation
Cornell University, Ithaca, New York	300 (1000)	Operation Testing
Massachusetts Institute of Technology, Cambridge, Massachusetts	330	Operation
University of Michigan, Ann Arbor, Michigan	300	Operation
General Electric Company, Schenectady, New York	300	Operation
Purdue University, Lafayette, Indiana	300	Operation
National Bureau of Standards, Washington, D. C.	180	Construction
Glasgow University, Glasgow, Scotland	300	Testing
Oxford University, Oxford, England	140	Construction
California Institute of Technology, Pasadena, California	500 (1000)	Operation (Eventual)
Nobel Institute, Upsala, Sweden	(600)	Design
Professor Salvini, Rome	(600)	Design
Betatron, University of Illinois, Urbana, Illinois	250	Operation

Meanwhile, and before any of the larger synchrotrons could be finished, Goward and Barnes[8] in England were able to demonstrate the principle with a much smaller machine (8 Mev) built from an old betatron magnet. The next to succeed was a group at the General Electric Company Research Laboratory,[9] where there had been previous experience in betatron design, with a 70-Mev synchrotron. A series of experiments with these early machines demonstrated the range of validity of the stability principle, worked out the necessary conditions for injecting electrons so they would be captured in synchronous orbits and explored some of the properties of the high-energy beam of x-rays. The larger machines, in the 300- to 400-Mev region, were in general put to immediate use for research experiments.

The theory of synchronous oscillations has been extended beyond that reported in the original articles by McMillan and by Veksler. Dennison and Berlin[10] analyzed the stability of the synchronous orbits and found that the amplitude of synchronous oscillations decreases with increasing particle energy. Bohm and Foldy[11] obtained the same results on orbit stability and also showed how betatron operation could be used at the start to avoid the difficulties of frequency modulation. Frank[12] examined in detail the process of transition from betatron to synchrotron action. All these studies are in basic agreement, varying only in the type of approximations used in the calculations and in the emphasis placed on the several aspects of the motion. Theoretical understanding of the synchrotron seems to be adequate.

Seldom has an accelerator been brought to such a high state of development in such a short time. The concept was simple, the first design studies were essentially complete, and all observers recognized the virtues of the new proposal and accepted its success as assured. The simplicity of the concept is reflected in the relatively few competing techniques which have been reported and in the comparatively small number of publications. All the basic properties were recognized from the start, and most designers have used similar techniques with relatively little variation. In a few instances special and new concepts have been developed, but seldom in more than one laboratory. Thus, the "race track" orbit, the "frequency-modulated" start, and the "air-cored" magnetic field have had proponents, but have not been found essential for the 300- to 500-Mev range.

The electron synchrotron has to a large extent replaced the betatron as a source of very-high-energy electrons. It has two important advantages. First, the magnet structure is much lighter, consisting essentially of a ring magnet to provide a guide field across the doughnut-shaped vacuum chamber; the large and heavy laminated core needed in the betatron for induction to produce the accelerating electric field is replaced by

a compact cavity resonator which supplies the rf field in the synchrotron. Also, the correction for radiative losses is applied automatically in the synchrotron by phase shifts which supply additional accelerating potential. The complicated compensating devices necessary in the betatron are not required.

3.2 Principle of Operation

The synchrotron accelerates electrons in an orbit of essentially constant radius by means of a rf electric field applied across a gap at one point in the orbit. The electrons are constrained to move in their circular path by a magnetic field which increases with time, from a low field which is just adequate to deflect low energy electrons at injection, to the maximum value permitted by the permeability of iron. A ring-shaped magnet provides the magnetic field over the doughnut-shaped vacuum chamber which encloses the electron orbits. The pole faces are accurately shaped to provide a field which decreases slightly with increasing radius with a value of n of about 0.6 so as to supply focusing forces for the electrons. The magnetic field is pulsed on and off at the repetition rate provided by the magnet power supply. Pulsed operation would result in eddy currents which would distort the carefully shaped magnetic field if the magnet core were of solid iron, so the core is laminated as in a transformer. The cyclic operation results in a sequence of pulses of high-energy electrons at the pulse repetition rate.

Electrons are emitted from an "electron gun" source at a point on the outer side of the vacuum chamber, accelerated by a direct-current potential difference of between 50 and 100 kv. At this energy the electrons have not yet attained relativistic velocities. They are usually accelerated for a short time by induction, as in the betatron, until they reach an energy of 2 to 4 Mev, at which their velocity is essentially equal to that of light. This requires a time rate-of-change of flux linking the orbit given by Eq. 2-30:

$$\frac{d\Phi}{dt} = 2(\pi r_0^2)\frac{dB_z}{dt} \tag{3-1}$$

The linkage flux Φ is provided by "flux bars" on the inside of the orbit, which are of negligible size compared with the heavy central core required in the betatron to provide acceleration to top energy.

When the electrons reach relativistic velocities, the radio-frequency system is turned on and applies an accelerating potential across the gap which continues the process of acceleration to high energies, matching the increasing magnetic field. During this process synchronous oscillations are set up which bunch the electrons in phase and provide the phase stability characteristic of the synchrotron. The frequency of the applied electric field is the constant value of rotation frequency reached by the electrons in their orbit of radius r_0 at the velocity of light. It is given by:

$$f = \frac{c}{2\pi r_0} = \frac{47.8 \times 10^6}{r_0} \text{ cycles/sec} \qquad (3\text{-}2)$$

where r_0 is in meters. This applied rf voltage is developed in a resonant cavity circuit built into the vacuum chamber, driven by vacuum tubes at the resonant frequency.

Maximum energy of the electrons depends on orbit radius and on the maximum value of the magnetic field, following Eq. 2-8 of Chap. 2, and illustrated in Table 2-1. For our purposes the equation can be presented as:

$$T = ceBr_0 = 300Br_0 \text{ Mev} \qquad (3\text{-}3)$$

The constant on the right applies when B is in units of webers per square meters and r_0 is in meters. For example, a magnetic field of 1 weber/m^2 and an orbit radius of 1 m will retain an electron energy of 300 Mev.

The available aperture inside the vacuum chamber extends over a considerable radial width, of the order of $\pm 5\%$ of r_0. This will accommodate an energy spread of nearly $\pm 5\%$ or will allow the frequency to differ by the same amount. Too high a frequency will produce resonance at a smaller orbit radius, and will result in lower-energy electrons. Conversely, the orbit

can be expanded by applying a lower frequency at the end of the acceleration interval to push the beam out against a target at the periphery (often the shield surrounding the electron gun), and the electron energy will also be increased by about 5% above the nominal energy at the central orbit.

The aperture width described above is required at the start to accommodate the radial betatron oscillations established at injection due to angular and energy variations. A somewhat smaller vertical aperture is required for the associated vertical oscillations. These oscillations, and also the damping of amplitudes with increasing magnetic field, proportional to $B^{-1/2}$, have been described and analyzed in Chap. 2. The free oscillations are ultimately reduced to very small amplitudes, such that the final dimension of the beam of electrons is the order of a few square millimeters.

3.3 Magnet

The first synchrotrons used H-type magnet frames similar in structure to those used for betatrons, but without the large central laminated core. Modern design, however, uses a ring of C-type magnets, each providing the field over a short sector of the orbit. This arrangement reduces the quantity of iron significantly and simplifies the structure. For small orbits the flux-return path of the C-magnets must be outside the orbit. For larger machines the flux return can be inside the orbit which makes the chamber more readily accessible. Figure 3-1 is a schematic drawing of the assembly of the M.I.T. synchrotron with outside flux-return circuits.

Remanent fields and eddy currents in the iron may result in time distortions of the magnetic field in different portions of the gap. Symmetrical design and high precision in assembly will reduce these effects. If necessary, correcting coils can be wound about the pole tips in appropriate locations, and time-phased currents can be empirically determined which will correct the distortions. For example, circular windings distributed across the pole face surfaces can be used to vary the value of the field gradient index n. Other windings about individual sectors

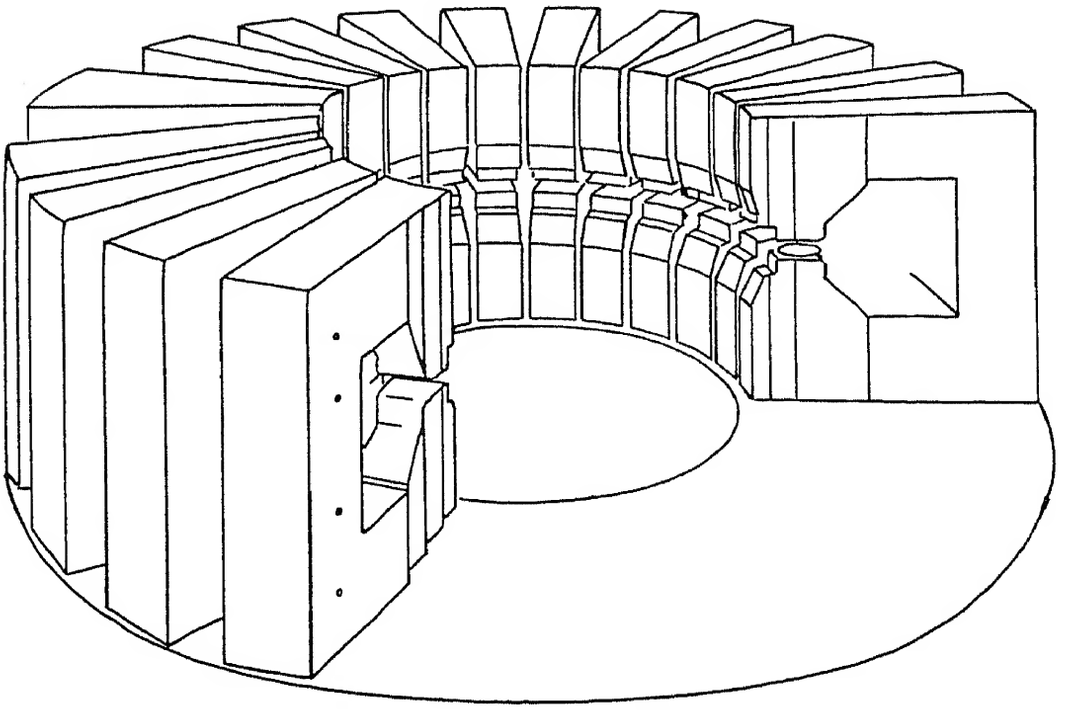

FIG. 3-1. Sketch of the Massachusetts Institute of Technology synchrotron showing the C-magnet assembly and the location of the vacuum chamber doughnut between poles.

of the pole can be used to correct for azimuthal variations in the field.

One synchrotron has been constructed without iron poles, by using heavy currents in four bar conductors properly arranged around the orbit region, by Lawson[13] at the General Electric Company. The chief disadvantage is the large mechanical force on the conductors, which requires rigid clamping of the conductor bars to prevent distortion of the field. The ironless synchrotron is probably most suited to small orbits, high magnetic fields and relatively low electron energies.

The cyclic operation of the magnet requires either alternating or pulsed current. Continuous ac excitation requires a great deal of power and results in heat losses. Magnets must be designed with large copper windings and with provision for cooling. Pulsed excitation can be used to reduce power requirements by keeping the duty factor small, but of course the x-ray output is also reduced.

Capacitors are used to store energy for the magnets either

for pulsed or ac operation. With ac excitation the capacitor is made to resonate with the inductance of the magnet at the chosen frequency, usually 60 or 180 cycles per second. It must store energy equal to the peak stored energy of the magnetic field, which determines the kva rating. In such a resonant system the energy alternates between the magnet and the capacitor bank, and the power line merely supplies the losses in the system.

In pulsed operation the capacitor is charged from a dc source and is then discharged through the magnet. Pulse rise time is determined by the inductance and capacitance of the system, and can be made quite short to reduce power losses. Ignitrons or other suitable control tubes are used to initiate the pulse, and to stop it after one oscillation when the energy has been returned to the capacitor. The dc source supplies the system losses between pulses. Electrical problems arise chiefly from the transient voltage surges occurring during the switching, which can be controlled by appropriate damping circuits.

3.4 Injection

Electrons of 50 to 100 thousand ev energy are obtained from an "electron gun," consisting of a thermionic cathode inside a grounded shield, with the cathode at high negative potential. Figure 3-2 is a sketch of a source typical of synchrotron usage. Electrons are focused crudely by a reflector cup (or sometimes by a grid structure to which potential can be applied) so as to emerge from a slit in the grounded shield, aimed in the direction of acceleration. Only a small fraction of the many milliamperes of current available from such a gun is directed within the narrow cone which can be accepted into stable orbits. The remainder of the electrons emitted strike the walls of the vacuum chamber within the first half revolution. Internal walls of the vacuum chamber must be made sufficiently conducting to prevent the accumulation of charge due to the electron spray. Otherwise the resulting electrostatic fields would deflect and destroy the resonant beam.

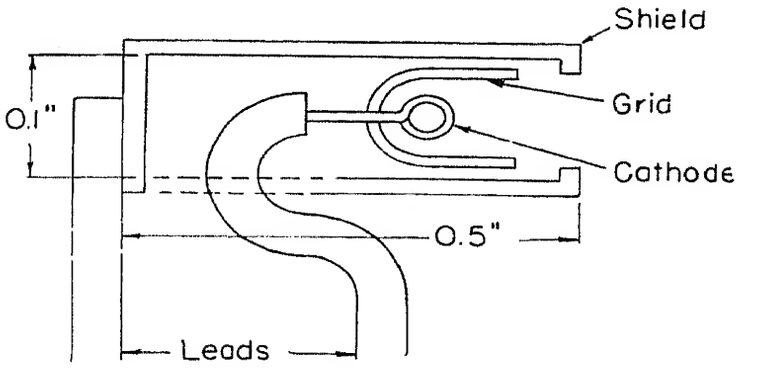

FIG. 3-2. Typical electron gun source used in the synchrotron.

The gun is usually located just inside the outer chamber wall, and the radial thickness of the shield is made as small as possible. Betatron oscillations about the equilibrium orbit (for electrons having the injection energy) will cause the individual orbits to miss the back of the injector gun on the second, third, etc. circuits, but in principle the orbits should return to the original phase after a small number of revolutions. Some decrease in amplitude is expected from damping due to the increasing magnetic field during this time. However, most theoretical calculations of orbits indicate that a large fraction of the injected beam must be lost by striking the back of the gun after a few turns. The observation, originally noted in betatron operations, that a significant fraction of the injected electrons do miss the gun and survive to be accelerated, is one of the pleasant accidents of accelerator history. Several attempts have been made to explain this favorable capture efficiency, with only partial success. It is still not certain what phenomenon is responsible for the observed high efficiencies.

Betatron operation is commonly used to accelerate the electrons from their initial energy of 50 to 100 kv to the order of 2 Mev at which they have a velocity of 0.98 c and so travel in an orbit of radius not significantly smaller than the geometrical central orbit. The flux required for acceleration by induction to this energy is supplied by flux bars attached to the inside of the poles of the guide field magnet. These bars are significant only during the early part of the cycle, after which

they become saturated and have no further effect. The air gap between the tips of the flux bars is made short, and the flux density in the bars is much greater than that of the guide field during the early stages. So it is possible to use relatively small flux bars made of a high permeability material and yet retain the betatron stability condition. Care must be taken to obtain the correct rate of rise of flux density in the bars, involving the effects of eddy currents, remanent fields and saturation in the flux bars as well as in the main magnet. Back biasing the main field by special windings has proved to be a useful method of applying such corrections.

Crane,[14] at the University of Michigan, has chosen to avoid some of the difficulties of the betatron start by injecting electrons at about 400 kev and frequency-modulating the rf cavity until the electrons reach relativistic velocities. The method is sound in principle, but has introduced other difficulties of equivalent magnitude in the frequency modulation. Another feature pioneered by Crane is the "race-track" magnet, in which two semicircular sectors are spaced by two straight sections. Dennison and Berlin[15] have shown that such an arrangement results in equivalently stable orbits, and their predictions are justified experimentally.

3.5 Radiofrequency Acceleration

The gap across which the rf voltage is applied for acceleration is usually the open end of a quarter-wave resonant cavity, driven at its resonant frequency by a vacuum tube oscillator circuit. In the most efficient design the quarter-wave cavity forms a sector of the glass or ceramic vacuum chamber by having the inner and outer surfaces coated with conducting material. The desired resonant frequency is determined in advance from the orbit radius, following Eq. 3-2. Such a resonator can have a relatively high Q, so the necessary voltage can be obtained with a small power input to the cavity. The simplicity and low power requirements of the rf accelerator for the synchrotron constitute one of its primary advantages.

The peak voltage developed across the gap should be about $\sqrt{2}$ times the average volts-per-turn requirements, in order that the equilibrium phase angle be about 45°, which is adequate for synchronous oscillations. This required volts-per-turn V is obtained from the rate of rise of magnetic field, being given by:

$$V = 2\pi r_0^2 \, dB/dt \tag{3-4}$$

Evaluating for a system in which the magnetic cycle has a rise rate determined by a basic 60-cycle frequency and a 10-kilogauss peak field, and an equilibrium orbit radius of 1 m, the voltage needed per turn for resonant acceleration is 3.0 kv. Variation of the phase angle is sometimes used to provide damping of phase oscillations following injection. This can be accomplished by applying a rising voltage to the gap, equivalent to decreasing the phase angle.

The quarter-wave resonant cavity can be made physically shorter than the 90° in arc associated with fundamental resonance with velocity-of-light particles by loading it with material of a high dielectric constant. The practical method of accomplishing this result is to form the resonator of a high dielectric ceramic and make it a section of the vacuum chamber, with plated electrodes inside and outside the sector to form the conducting walls of the cavity, and an insulated gap at one end across which the rf voltage is developed. Ceramics having dielectric constants of up to 80 are available for this purpose. The plated walls are scribed longitudinally with scratches to insulate against eddy currents which otherwise would be developed in the conducting surfaces. Figure 3-3 is a sketch of such a resonator developed for the 330-Mev synchrotron at the Massachusetts Institute of Technology. The 50-Mc oscillator is coupled to the resonator by capacitative coupling near the rf node of the quarter-wave cavity. Potentials of 3 to 4 kv peak are developed across the open end of the resonant cavity with an input power to the oscillator of about 10 kw.

An alternate resonator—the half-wave drift tube or C electrode—was developed at the University of California, but

of 350 Mev. Total energy lost by radiation increases with the fourth power of the electron energy (expressed in terms of the ratio of total energy to rest energy) if orbit radius is constant, as described in Chap. 2.

The loss of energy by radiation is about 100 ev per turn at 300 Mev energy and is compensated automatically by the phased rf accelerating electric field. Any loss of energy results in a temporary reduction in orbit radius and in orbital frequency of the electrons. This causes a shift in phase of crossing the gap so the electron acquires more energy per turn, just sufficient to maintain synchronous acceleration.

The radiation from a target is also a continuous distribution of x-rays extending up to the maximum energy of the electrons. The low-energy radiation in the visible and ultraviolet is absorbed in the target and the wall of the vacuum chamber, so the shape of the energy distribution emerging from the machine is distorted to favor the higher-energy radiations. This beam of high-energy x-rays occurs as a sharp pulse in time, of a duration depending on the time required for the electrons to spiral into and hit the target, and modulated at the particle-bunch rotation frequency of about 50 Mc. When a short pulse is desired, a rapid ejection scheme is used, and pulses as short as 1 microsecond have been obtained. On the other hand, some types of measurement using electronic instrumentation are most satisfactory when the pulse length is spread out in time, and under best conditions pulse lengths of 2500 microseconds have been obtained.

Measurements of output intensity are difficult, because of the wide range in frequency of the emitted radiation and the relatively narrow range of sensitivity of the several available detection devices. Calorimetric absorption of the entire beam is limited by the penetration of the high-energy x-rays and by the necessity of applying corrections for absorption in the target and window. Total ionization measurements are similarly limited by the physical requirements of an ionization chamber. Electron-pair production is a quite effective measure of intensity

at the high-energy end of the spectrum, but it cannot extend the measurements below the threshold at 1 Mev energy. Thin-walled ionization chambers are normally used to obtain a measure from which total beam intensity can be calculated. When converted into the familiar roentgen unit of x-rays, the output at 300 Mev is found to be about 1 r/pulse at a distance of 1 m inside ⅛ in. of lead and at the center of the conical beam. Depending on pulse repetition rate, the various machines operating at 300 to 350 Mev give x-ray beams of the order of 1000 r/min at 1 m.

CHAPTER 4

The Synchrocyclotron*

4.1 Early Development

The relativistic limitation on energy for fixed-frequency cyclotrons has restricted the size of magnets to the order of 60-in.-diameter pole face and the proton or deuteron energy to about 25 Mev. This limit is set by the relativistic increase in mass of the ions, which causes the ion rotation frequency to decrease, so that the ions drop out of resonance with the fixed frequency applied electric field.

This maximum energy limitation can be removed and the ions accelerated indefinitely if the applied frequency is varied to match exactly the ion rotation frequency. In Chap. 2 it was shown that particles in phase-stable orbits in a cyclotron will follow a slow change in applied frequency. The phase of crossing the accelerating gap oscillates about a mean value which allows just sufficient energy increase per turn to maintain resonance with the changing frequency.

When frequency is varied cyclically, a short bunch of ions will be accelerated to high energy in each frequency sweep, resulting in a sequence of such bursts occurring at the modulation frequency. The reduced effective duty cycle results in a much lower average ion output than in the conventional cyclotron (about 1%), but it avoids the resonance limitation due to a fixed frequency and allows acceleration to much higher energies.

The use of frequency modulation as a remedy for the relativistic limitations of the cyclotron was suggested by McMillan, of the University of California, and independently by Veksler,

* Also known as the frequency-modulated, or f-m cyclotron.

of the U.S.S.R. in 1945. The 184-in. magnet at the University of California had originally been conceived as a giant standard cyclotron by Professor E. O. Lawrence and his co-workers. It was assembled and used for experimental purposes in the Manhattan District during World War II but was not completed as a cyclotron. At the end of the war when McMillan proposed the use of frequency modulation, it became obvious that this method would result in higher energies, and plans were made to convert the magnet into a synchrocyclotron.

The first test of the principle, at Berkeley, was made on the older 37-in. cyclotron magnet by an ingenious method of simulating the expected relativistic mass change with an exaggerated radial decrease in the magnetic field. Ion rotation frequency will decrease at very high energies owing to the relativistic increase in mass. It can also be made to decrease with increasing energy in a small cyclotron if the magnetic field at large radii is reduced below the central field. The test was modeled on the anticipated operation of the 184-in. cyclotron. Deuterons of 200 Mev would experience an 11 % increase in mass during acceleration. The associated change in frequency, plus an additional 2 % for the radial decrease in field required for focusing, would require a total frequency change of 13 % during acceleration. To duplicate this frequency change the field of the 37-in. magnet was equipped with radially tapered pole faces, requiring a 13 % modulation in frequency to maintain resonance with the low-energy (7-Mev) deuterons produced. With this arrangement the techniques of frequency modulation could be studied, and the principle of phase-stable synchronous acceleration could be tested.

The results of the 37-in. model test were completely successful. The deuterons remained in resonance for many thousands of revolutions, validating the theory and giving valuable data for the conversion of the 184-in. magnet to the synchrocyclotron principle.

The 184-in. cyclotron was brought into operation in November, 1946, accelerating deuterons to 190 Mev or He^{++}

ions to 380 Mev. The development was notable for its speedy success, illustrating the soundness of the principle of phase stability and the simplicity of the techniques. Several years later the radiofrequency system was rebuilt to allow tuning to higher frequencies for proton acceleration, and it was eventually tuned up to produce protons of 350 Mev energy.

The immediate success of the Berkeley laboratory led others to build similar accelerators. Table 4-1 shows a listing of the larger synchrocyclotrons, giving pole diameter, maximum magnetic field, and particle energy. The highest energy reached to date is 450-Mev protons with the University of Chicago machine. The 184-in. magnet at Berkeley is now being rebuilt with higher power and higher magnetic fields to produce protons of 730 Mev. The largest new machine planned is being designed for the CERN (Western European) Laboratory in Geneva, which will be capable of producing protons of 600 Mev energy.

4.2 Principle of Operation

In the cyclotron an approximately uniform magnetic field is used to constrain the ions in circular orbits, so they pass many times through the rf electric field of a large, semicircular, hollow electrode called a D. The frequency applied to the electrode is identical with the ion rotation frequency, so that the particles experience an acceleration on each traversal of the accelerating gap. Particles cross the gap, between the diametral face of the D and a dummy D at ground potential, twice during each revolution. The magnitude of the acceleration at each crossing depends on the instantaneous rf voltage, and so on the phase of crossing the gap relative to the rf wave. As the ions gain in energy on each traversal of the gap, they travel in circles of larger radii, ultimately reaching the maximum practical radius. The problem is to keep the ions in precise resonance with the applied rf field for a very large number of revolutions.

Resonance is maintained automatically in the synchrocyclotron through the principle of phase stability. Oscillations occur in the phase at which ions cross the gap, about an average phase which produces just sufficient voltage per turn to keep the

Table 4-1. List of the larger synchrocyclotrons.

	Pole diameter, inches	Magnetic field, gauss	Proton energy, Mev	Status, 1954
University of California, Berkeley, California	184	15.0 (23.0)	350 (730)	Operation (conversion)
University of Rochester, Rochester, New York	130	17.0	240	Operation
Columbia University, New York, New York	164	17.4	385	Operation
Atom Energy Research Establishment, Harwell, England	110	16.8	175	Operation
University of Chicago, Chicago, Illinois	170	18.6	450	Operation
Carnegie Institute of Technology, Pittsburgh, Pennsylvania	142	20.0	435	Operation
University of Liverpool, Liverpool, England	156	18.0	400	Testing
CERN Laboratory, Geneva, Switzerland	196	20.5	(600)	Design
Harvard University, Cambridge, Massachusetts	95	16.5	110	Operation
McGill University, Montreal, Canada	82	16.4	100	Operation
Nobel Institute, Upsala, Sweden	90	22.0	200	Operation
University of Amsterdam, Amsterdam, Holland	71	13.7	28 (deuterons)	Operation

particles in resonance. The mechanism has been explained in some detail in Chap. 2.

The relation governing ion rotation frequency has been presented in Chap. 2 as:

$$f = \frac{c^2 eB_z}{2\pi(E_0 + T)} = f_0 \frac{1}{1 + T/E_0} \qquad (4$$

Here f_0 is the low-energy cyclotron frequency set by the magn field and the charge-to-mass ratio of the ions e/m_0. The quency f must be decreased below f_0 when kinetic energy becomes significant relative to rest energy E_0. For proton kinetic energy T in Mev units, in a field B in webers per sq meter (units of 10,000 gauss), the frequency is given by:

$$f = \frac{14{,}300B}{938 + T} \text{ mc/sec} \qquad (4$$

Figure 4-1 is a plot of the relative change of frequency in te of f/f_0 as a function of energy, valid for any uniform valu magnetic field B. The total frequency swing must also incl the effect of the designed decrease in field B with increa radius required for focusing. As an example, if the field d by 5% and the frequency decrease associated with 400-M protons (computed from Eq. 4-1a) is 30%, the total freque swing required will be 35%.

For continuous operation the frequency is modula cyclically by a rotating capacitor in the resonant D circ

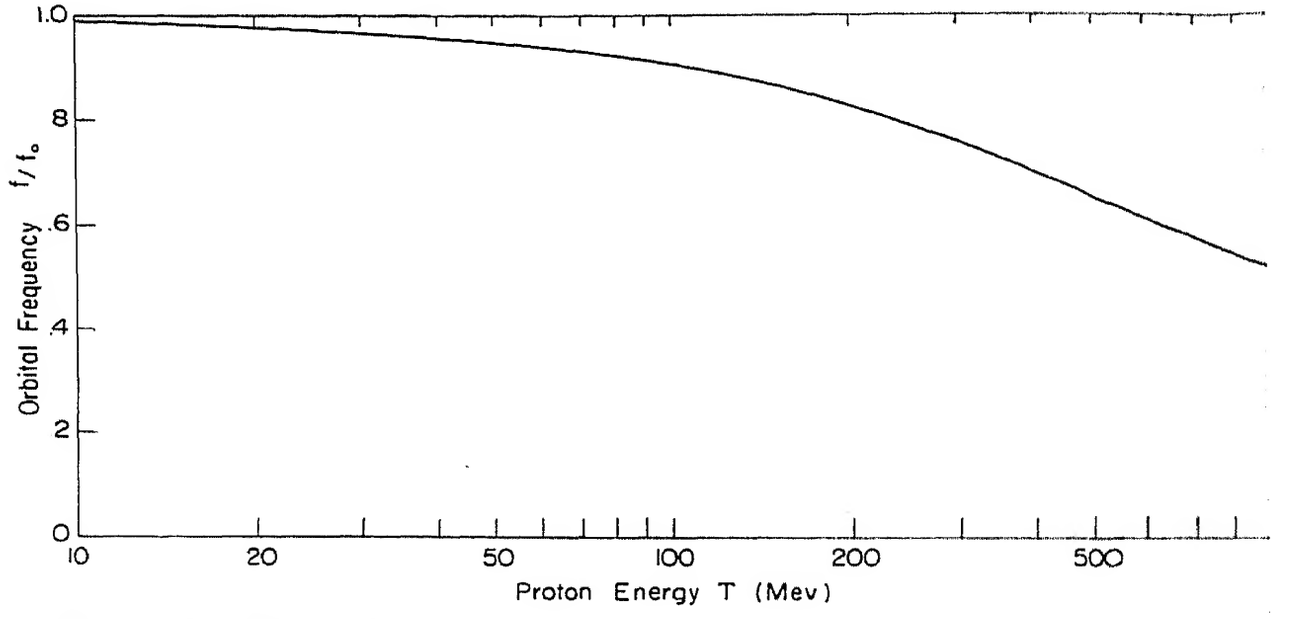

FIG. 4-1. Variation of orbital frequency f/f_0 for protons in a uni form magnetic field as a function of proton kinetic energy.

The frequency change as a function of time for a typical circuit with such a rotating capacitor is illustrated in Fig. 4-2. During each sweep a bunch of ions is accelerated to high energy, so the output consists of pulses at the cyclic frequency.

The process of the phase oscillations can be visualized with the aid of Fig. 4-3, which is a plot of the voltage across the gap as a function of time. Particles which cross at the equilibrium phase t_e will receive exactly the right acceleration, $V_e e$, to remain in resonance, and will cross at the same phase on subsequent traversals of the gap. A particle crossing at phase t_1 will gain too much energy, and its frequency will decrease as shown by

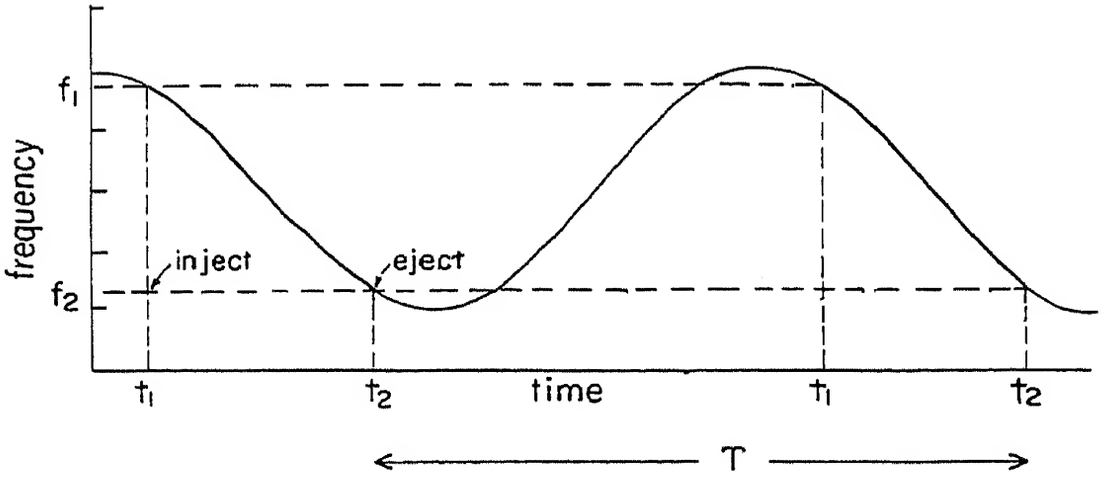

FIG. 4-2. Frequency modulation of a rf circuit utilizing a rotating capacitor between initial frequency f_1 and final frequency f_2. Particles are accelerated during the intervals $t_1 - t_2$, resulting in bursts of high-energy particles at the cyclic period T.

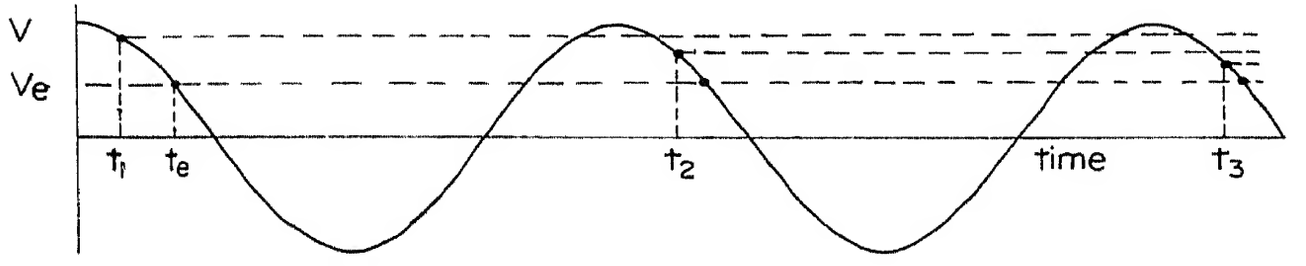

FIG. 4-3. Origin of phase oscillations. Particles which cross the accelerating gap at time t_1 acquire excess energy, rotate at reduced frequency and are delayed in subsequent crossings, illustrated by points t_2 and t_3. Continuation of this motion leads to oscillations in phase about the equilibrium phase t_e.

Eq. 4-1; the reduced frequency will cause the particle to be delayed in subsequent traversals of the gap, illustrated by points t_2, t_3, etc. This represents a migration of phase toward the equilibrium phase. The inverse situation, in which the particle crosses at a time when it receives too small (or even negative) acceleration, will also result in restoring the phase toward the equilibrium phase t_e. So the particles oscillate in phase of crossing the gap, gaining an average amount of energy just sufficient to maintain resonance. The details of the phase oscillations and methods of computing the frequency and amplitude of the oscillations in energy and in radial location are given in Chap. 2.

4.3 The Magnetic Field

Particle energy attained in a synchrocyclotron is determined by the magnetic field at the maximum orbit radius R. The quadratic relation given in Chap. 2 is:

$$T^2 + 2TE_0 = c^2e^2B_z{}^2R^2 \tag{4-2}$$

Numerical values obtained from this relation for protons, deuterons, and He^{++} ions that illustrate the dimensional requirements of the accelerator are also presented in Chap. 2. Maximum magnetic field is severely restricted by the permeability limits of iron, at about 18 to 20 kilogauss. The field at the maximum orbit radius is still further reduced by the requirements for focusing. Maximum orbit radius must be inside the region of stability for free oscillations, which is well within the physical edge of the pole faces. Careful contouring of the pole face surfaces will produce a field in which this point is inside the pole edges about one-half the gap length. So magnet pole face diameter must be a minimum of twice the orbit radius required for the desired energy plus one pole gap length.

Magnet weight increases roughly with the cube of pole diameter. In the low-energy, nonrelativistic range, particle energy varies with the square of orbit radius. Thus magnet weight for small cyclotrons is roughly proportional to the $\frac{3}{2}$

power of the energy: $wt \sim T^{3/2}$. But for higher energies, particle energy approaches a linear proportionality with radius, and the magnet weight increases more rapidly, approaching the relation $wt \sim T^3$. This rapid increase in weight and cost is the chief limitation on the practical maximum energy for synchrocyclotrons.

The magnetic circuit is of a basically simple structure, utilizing the H type frame with dual return circuits commonly employed for smaller cyclotrons. The frame consists of six elements; two poles, two yokes, and two uprights. The poles are cylinders, machined to a good finish, sometimes tapered to smaller diameter at the gap, and terminating in pole face disks which are contoured to give the radially decreasing field required for focusing. The yokes and uprights are rectangular machined forgings arranged to carry the load of the structure and to have a magnetic flux path as short as is practical. In the larger machines each of these six elements must be built up of several separate slabs, to keep the unit weight within limits required for handling and assembly. The precision required in flatness and parallelness of the gap is of the order of 0.01 in., a severe requirement on machining such large structures. Figure 4-4 is an illustration of the Chicago magnet, showing the assembly.

Exciting windings are stacks of flat, layer-wound coils around the two poles divided into two identical coils symmetrically spaced from the gap. The chief variation in design is in the method of cooling the conductors. Examples exist of air-blast cooling, oil-bath cooling, and internal water or oil flow through channels in the conductors.

The contouring of the pole faces to give a small radial decrease in field is illustrated in Fig. 4-5, taken from the Chicago design study report. Such contouring gives a correctly shaped field for only a narrow range of values of the field, due to the effects of saturation of iron. The numerical value of n in the region of acceleration varies smoothly from zero at the center to about 0.05 at large radii. Then as the field falls off rapidly near the pole edge, because of fringing effects, the value

of n rises sharply. A plot of n-value as a function of radius is also shown in Fig. 4-5. The sudden rise in n starts at about 75 in. radius for the Chicago machine, and it reaches $n = 0.2$ at 76.5 in., and the limit of stability ($n = 1.0$) at 78 in.

The $n = 0.20$ point represents the maximum limit for acceleration and defines the maximum energy. At this value of n a harmonic resonance occurs between the radial and vertical oscillations, and the radial frequency is just twice the vertical frequency. The beam "blows up" into vertical oscillations and is lost against the top and bottom surfaces of the D. Probe targets are located inside this radius, and deflection systems for

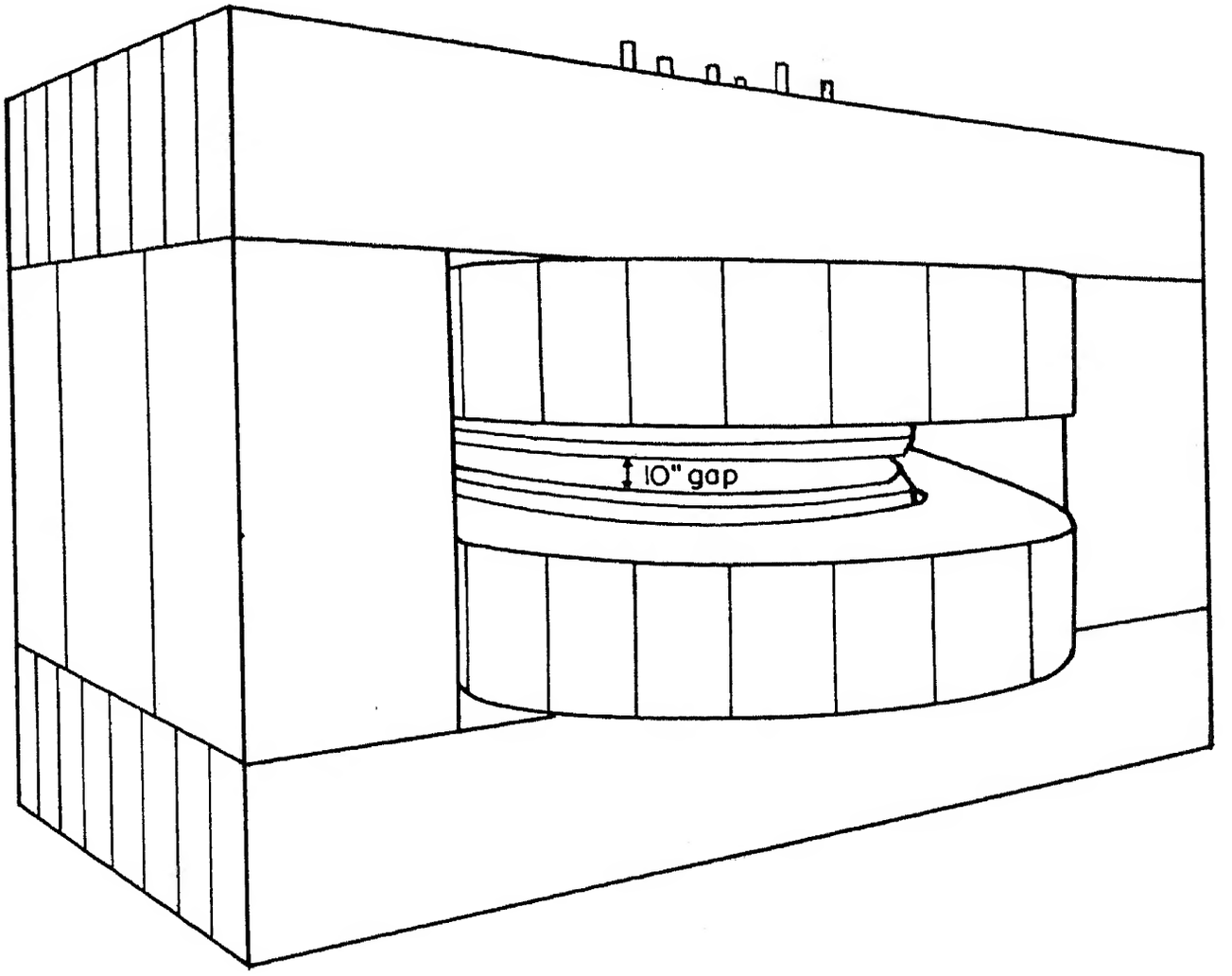

FIG. 4-4. Schematic diagram of the Chicago 170-in. diameter synchrocyclotron magnet, showing the assembly of slabs and disks. The magnet is excited by two current carrying coils located symmetrically about the gap.

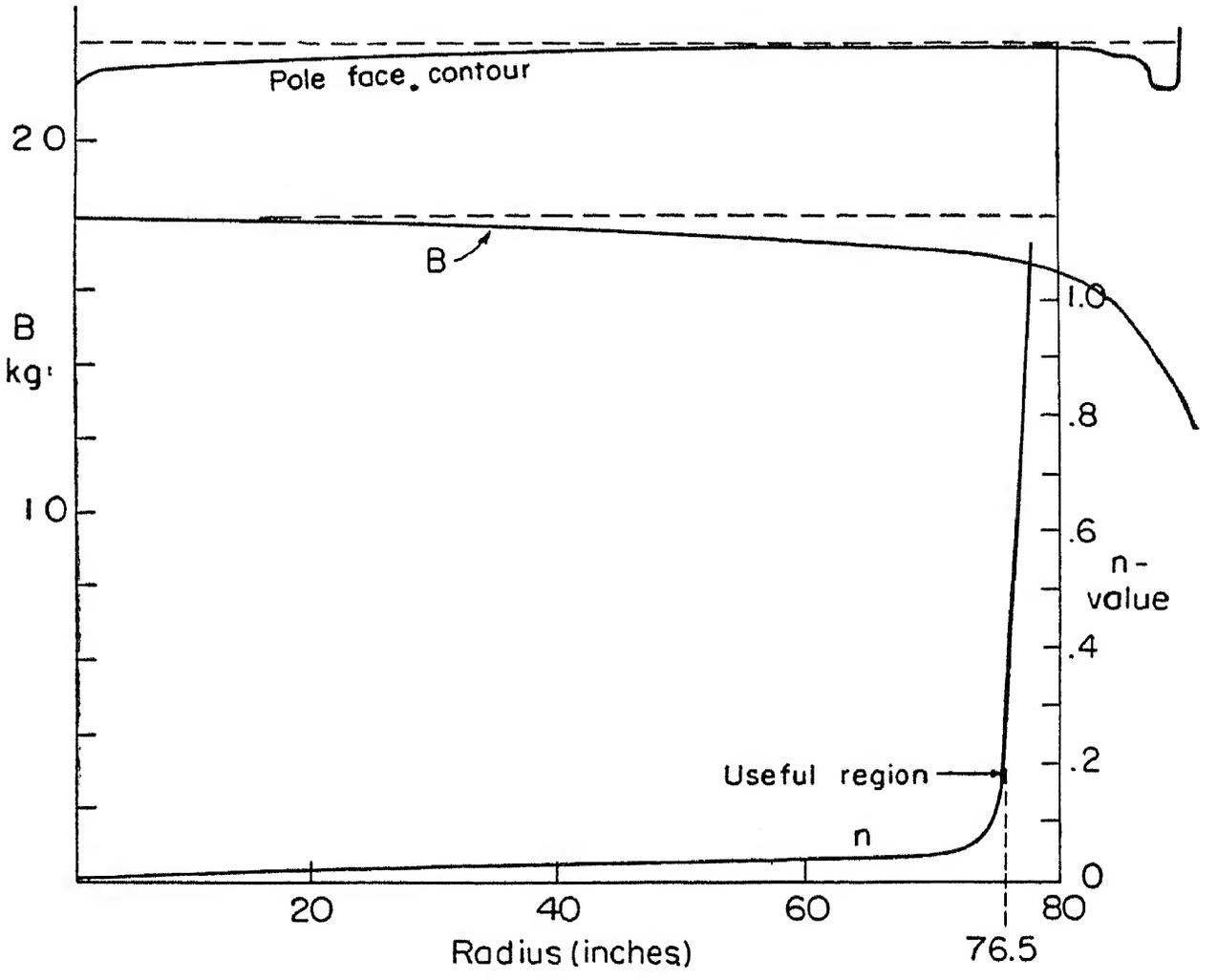

FIG. 4-5. Pole face contour of the Chicago magnet to provide the radially decreasing field needed for focusing, with a plot of flux density *vs.* radius at one value of excitation. The plot of n-value *vs.* radius illustrates the extent of the useful region of field.

ejecting an emergent beam of ions must start their deflections here.

Some ions may have small enough oscillation amplitudes to survive past the $n = 0.20$ resonance. If so, they may be lost by another harmonic resonance at $n = 0.25$ between the vertical oscillation frequency and the orbital frequency. If ions survive both, they may reach the limit of stability at $n = 1.0$, where the paths become opening spirals. In one cyclotron an oscillographic record of the radiation from the D's showed three peaks, one corresponding to the resonance at $n = 0.20$, one at $n = 0.25$, and one for $n = 1.0$.

4.4 Capture Efficiency

The intensity of the resonant ion beam depends on the number of ions captured in stable synchronous orbits at the start of acceleration. Ions are emitted from a gaseous discharge source at the center of the chamber, quite similar to the source used in standard cyclotrons. Ions are accelerated in bunches during the frequency sweeps, so there is only a limited time interval in which ions emitted from the source can be accepted into stable orbits. The source is usually pulsed to provide the maximum steady ion output during a time which overlaps this acceptance interval. Ions formed during the pulse are drawn toward and into the D by the applied rf potential. Capture efficiency can be defined as the ratio of ions accepted into stable orbits during the acceptance interval to the maximum number possible with continuous operation at constant frequency. The calculation of capture efficiency is one of the principal objects of theoretical studies, and the primary problem in design is that of maximizing capture efficiency, or the effective duty cycle.

Bohm and Foldy[16] have worked out the theory of ion bunching and of capture in phase-stable orbits. Their analysis shows the limiting phase angles of particles for capture relative to the rf phase, and the frequency difference between applied frequency and the resonant ion rotation frequency which will be accepted. They compute the instantaneous probability of capture of an ion and integrate over the phase angle and the time interval representing the frequency difference to obtain an overall or time-average capture efficiency.

Experimental measurements reported by Bohm and Foldy of beam intensity in the Berkeley 184-in. cyclotron as a function of the rate of frequency modulation and the applied rf voltage (which determines the equilibrium phase angle) verify the theoretical predictions. The functional relations are in excellent qualitative agreement, and even the total intensities are in reasonable agreement with the computed estimates of beam intensity. Other operational results and further checking with the theory are described by Henrich, Sewell, and Vale.[17] Still

further confirmation comes from the University of Chicago measurements and tests. These results are sufficient to show that the mechanism of ion bunching and capture is reasonably well understood.

4.5 Radiofrequency Oscillator

The variable frequency system for powering the D in a synchrocyclotron depends for its frequency variation on the mechanical modulation of the resonant D circuit by a rotating variable capacitor. The rf power to drive the circuit comes from a closely coupled, self-excited oscillator, which must have broad band characteristics to cover the wide frequency range. A range of frequency modulation of over 30 % is required for high-energy protons in the larger machines, and if both protons and deuterons are to be accelerated with the same rf system, the range extends over a factor of 2 or more. The numerical values of frequencies extend from about 30 Mc (low-energy proton resonance at a magnetic field of 20 kilogauss) to 10 Mc (deuterons of 300 Mev at 15 kilogauss). The quarter-wavelength of 30 Mc radiation is about 8 ft, and so it is less than the physical dimensions of the chamber and electrodes. Tuning such a large physical system over this wide frequency range brings in many technical and electrical problems.

Several methods of coupling the variable capacitor to the D circuit are discussed in the paper by Schmidt[18] which describes the system used for the model tests on the 37-in. magnet. The method used for the model, and the first system used for the 184-in. machine,[19] is shown in Fig. 4-6a. It is basically a half-wave resonant line, loaded with the D at one end and the variable capacitor at the far end of the D-stem and having a coupling loop to the oscillator located near the rf node.

A revised rf system for large synchrocyclotrons was designed by MacKenzie.[27] It allows tuning over a wider frequency range to cover both proton and deuteron resonance. In this system a stub line is added behind the capacitor, with a grounded node at the end of the stub line. This is equivalent to making

the D circuit a three-quarter wavelength resonant line, and it is called the three-quarter-wave circuit, illustrated in Fig. 4-6b. In tuning over this broad frequency range the circuit shifts gradually from a three-quarter wave resonance at high frequencies to a quarter-wave resonance at low frequencies.

For both systems described above the rotating capacitor is located externally to the cyclotron, in its own separate vacuum chamber. The primary problems are the technical ones of structural strength in rotation and electrical insulation of the rotor. Leads and brushes must be designed for low rf resistance. Maximum capacitance requires close spacing of the blades, and spark breakdown between blades is a limitation; smooth rounded corners, highly polished surfaces, and fast pumps which result in a good vacuum are essential.

Smaller cyclotrons can use a simpler arrangement of the rotating capacitor known as the quarter-wavelength circuit and illustrated in Fig. 4-6c. The capacitor is located at the back of the D, which is supported on two quarter-wave stub lines, where it effectively tunes the electrical length of the quarter-wave system. In this location the capacitor is within the cyclotron vacuum chamber and rotates in the magnetic fringing fields at the edge of the poles. The same basic design of multiple, parallel plates is employed. At Rochester the capacitor blades are made of ceramic and are silver plated to reduce eddy current heating due to rotation in the magnetic field.

In the Columbia University installation a modification of the quarter-wave cavity resonator is used, even though dimensions are so large that the D-stem stub lines reduce to zero length. The capacitor is located along the leading edge of the D in the strong magnetic field between poles, illustrated in Fig. 4-6d. Two rows of rotor blades are used for symmetry, one above and another below the D. Rotor diameter is small, to fit in the small space between the D surface and the pole face. The capacitor is used at maximum effectiveness when located at the open end of the quarter-wave resonator where voltage is a maximum, so its capacitance can be a minimum. This system

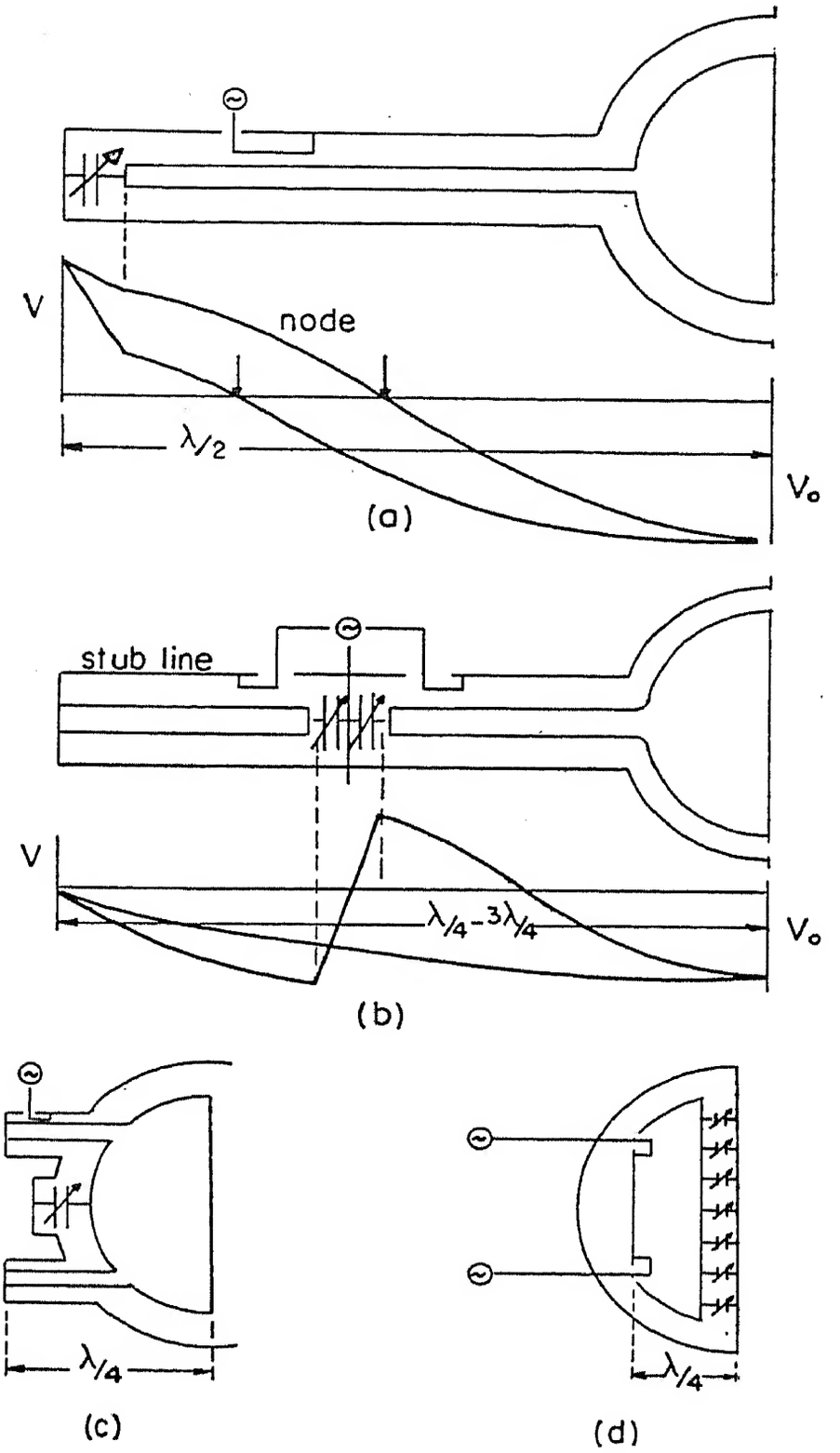

FIG. 4-6. Variable frequency rf systems for the synchrocyclotron. (a) Half-wave resonant D-line with variable capacitor at end of D-stem; (b) three-quarter wave system using variable capacitor and quarter-wave stub line; (c) quarter-wave D-stems with variable capacitor at back of the D; (d) quarter-wave D with variable capacitor on the diametral face of the D.

is essentially free from possible parasitic oscillations and is the only system which could in principle be extended to indefinitely large pole face diameters. Eddy current problems have been severe, and also the maintenance of the shaft bearings, but the development is now essentially completed and results in reasonably satisfactory operation.

4.6 Vacuum Chamber

The vacuum chamber is little more than a shell surrounding the pole face disks, and supports atmospheric pressure only on the side surfaces. A typical chamber is that for the Rochester machine, shown in the sketch of Fig. 4-7. The chamber walls are constructed of nonmagnetic stainless steel plates,

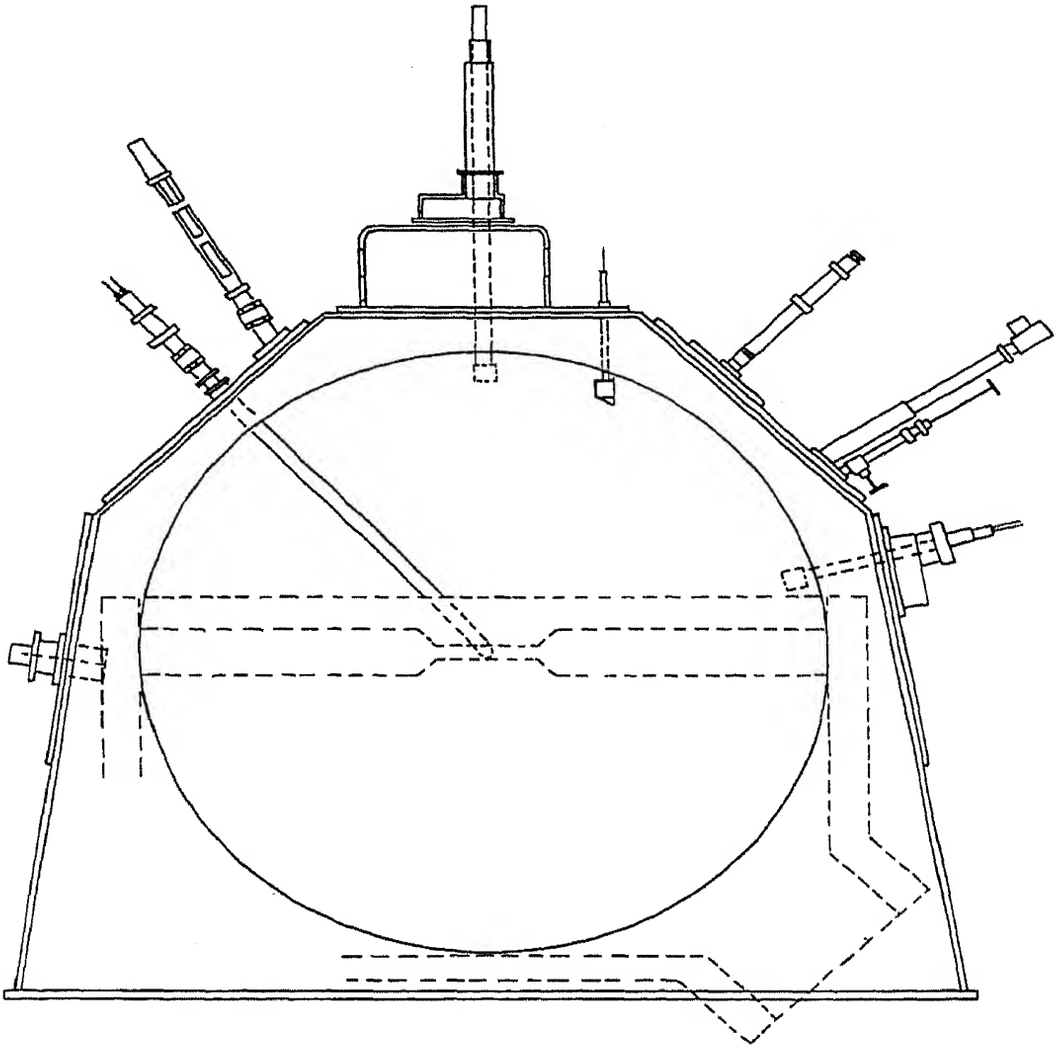

FIG. 4-7. Vacuum chamber for the Rochester synchrocyclotron.

welded to form the chamber shell, and including large side ports for inserting the D and for mounting pumps, ion source, probe targets, and other equipment.

Vacuum engineering has reached a high stage of development in synchrocyclotron laboratories, including many satisfactory types of vacuum seals, flexible joints, and other devices. The large ring seals between pole disks and chamber wall are made with packing rings to compress small rubber gaskets. High-speed pumps, attached through large manifolds and baffles, are required to maintain suitably low chamber pressure in such a large volume. Pressures of better than 1×10^{-5} mm Hg are required.

Electrical discharges between the D and ground have caused considerable trouble in most large chambers. The mechanism of the discharge is not clearly understood. It resembles the cumulative "blue-glow" discharge common in standard cyclotrons, but is incident at considerably lower voltages and lower pressures in the large volumes surrounding the D in synchrocyclotrons. It seems to involve electron oscillations and positive ion orbits in the large spaces available. It can be restricted by reducing the volume available for discharge by inserting copper sheet liners close to the D and D-stems. The most satisfactory method of suppressing this low-voltage discharge is to apply dc electrical bias to the D, or to other suitable electrodes, to sweep out the ions and electrons which originate the discharge. To accomplish this, most designers have provided that the D be insulated from ground, so that such a clearing field can be obtained by direct dc biasing of the D. Others use grids of wires, installed on the copper liners surrounding the D, which are maintained at suitable potentials to provide a clearing field.

4.7 Target Arrangements and Beam Properties

The simplest targets to use in the synchrocyclotron are probes inserted from the edge on the median plane, which are struck by the expanding ion beam. The radial location is a

measure of the ion beam energy. Charged particles produced in the target are deflected in the magnetic field; protons and positive mesons curl inward, and negative mesons curve outward. In the early days photographic emulsions suitably located (and shielded) were used to detect and observe tracks of the mesons. Fast neutrons, gamma rays, and neutral mesons travel tangentially away from the target and can traverse a port in a thick shielding wall behind which detection instruments are located.

Experimental arrangements in modern meson-producing synchrocyclotrons take full advantage of the magnetic field around the probe target. Mesons coming from the target are deflected and analyzed so that they emerge from the field in directions determined by meson energy. Shielding walls are located close to the target, with channels arranged to transmit well-defined energy groups. Both positive and negative mesons can be obtained in separate beams. For some energy groups the magnetic field has some focusing properties. It can be combined with external magnetic lenses to concentrate intensities on the channel. In this way meson beams have been ob-obtained from the Chicago machine having fluxes of 10^3 mesons/cm^2/sec.

The time-average beam intensity at the probe target is of the order of 1 microampere for most large machines. It consists of repeated bursts of pulses at the frequency of the applied rf, extended over a time of the order of one or more phase oscillations (1000 to 10,000 pulses), so the duration of the burst is about 0.1 msec. The bursts are repeated at the cyclic repetition rate of the rotating capacitor, between 60 and 300 rps.

The deflection of resonant ions to produce an emergent beam is complicated by the fact that the change in orbit radius per turn during acceleration is extremely small. The deflector septum and applied dc deflecting field successful with the standard cyclotron cannot be used. Furthermore, the beam blows up into vertical oscillations at the radius of the $n = 0.2$ point, so that it does not spray outward as in the cyclotron. However,

the properties of the orbits caused by the particle oscillations can be used to assist in ejection of a beam. Radial phase oscillations have amplitudes of several inches, and radial free oscillations occur of the same magnitude. These can be excited to larger amplitudes, sufficient to throw the beam into wide oscillations.

The most successful ejection system, developed at Berkeley, uses a pulsed electrostatic field to excite radial free oscillations. See Fig. 4-8. The deflector consists of four curved bars, spaced so the beam can expand out to the space between the bars on the median plane before pulsing. The dc pulse forces the ions inward, and after about one turn, they have swung out to their maximum radial amplitude, which is several

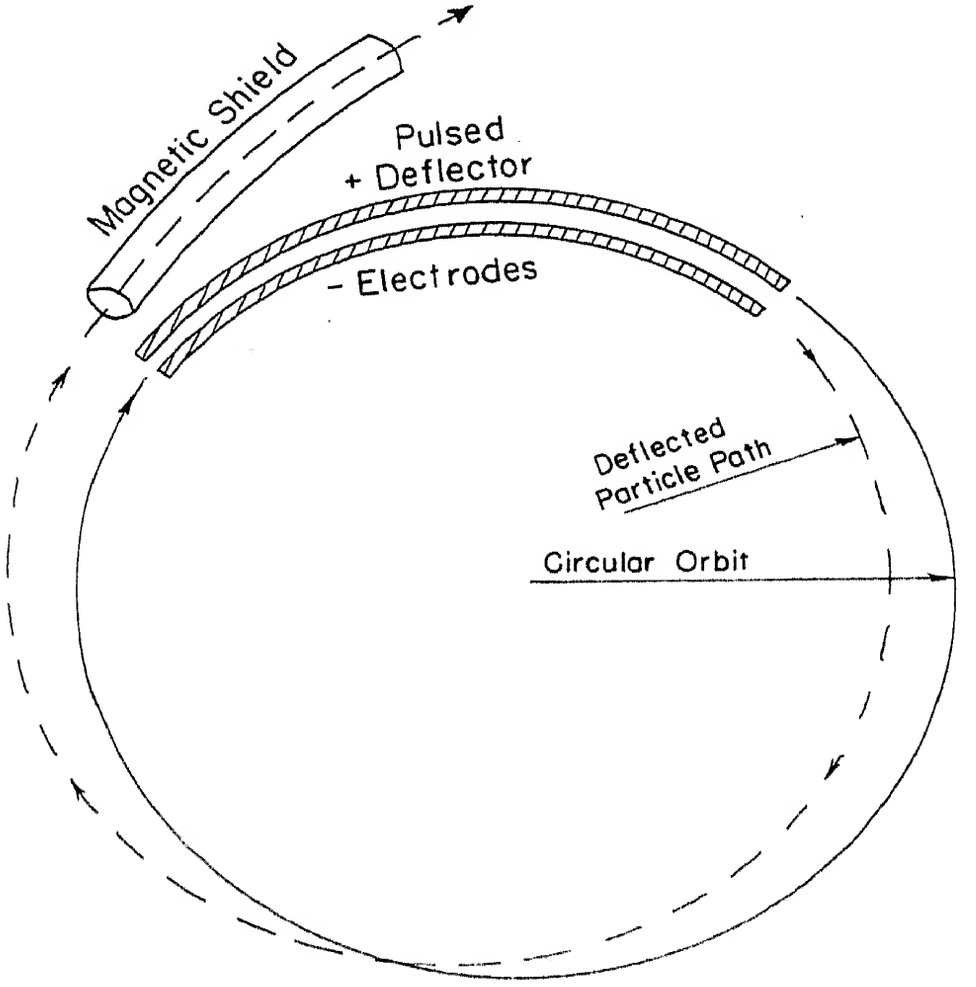

FIG. 4-8. Pulsed electrostatic deflector system for the Berkeley synchrocyclotron with the magnetic shield used to guide the emergent beam.

inches larger than the radius of the deflector bars. At this location the ions enter a magnetic shielded channel in which their paths are rapidly opening spirals, so they emerge from the chamber. The voltage pulse is on for a time approximately equal to the one revolution of the ions, about 0.1 microsecond. The magnitude of the field is the order of 75,000 volts/cm, requiring pulses of $\pm$100,000 volts on the two sets of electrodes. This is supplied by a very-high-voltage pulse transformer. The efficiency of the deflector is low, giving a useful ejected beam of the order of a few per cent of the circulating beam in the cyclotron. The advantage of having such an emergent proton beam outside the shielding walls is significant for some types of studies. The chief disadvantage is the short pulse length, which makes the emergent beam impractical for electronic counter experiments.

A simpler method of obtaining an emergent beam which has the advantage of a much longer duty cycle, but gives considerably smaller intensity, is the scattering target. Particles scattered by a thin probe target through small angles are set into free oscillations. Some of these will have the right direction and amplitude to enter a magnetic shielded channel for further deflection. Intensities are the order of a few per cent of the electrostatic pulsed deflector output, but they are better adapted to counter experiments since the output consists of a sequence of rf pulses spread out over several milliseconds.

CHAPTER 5

Linear Accelerators

5.1 Characteristics of Linear Acceleration

The linear accelerator uses an oscillating electric field applied to a linear, periodic array of electrodes, with a constant applied frequency which is in resonance with the motion of the particles. Particles are accelerated in a straight line, rather than in the circular orbits of magnetic accelerators. Electrode spacings are arranged so that particles arrive at each gap between electrodes in the same phase of the electric field and so experience an acceleration at each gap.

The chief advantage of the linear accelerator lies in the excellent collimation of the emergent beam, as compared with the spreading emergent beams from circular accelerators. The small size of the target spot and the high beam density improve and simplify many types of experiments, such as studies of small angle scattering and angular distributions. Shielding problems are simplified by the opportunity to use small channels in the shields, and background intensity due to scattered radiation is more easily controlled.

At a few Mev energy the chief disadvantage is the broad spread in energy of the beam, resulting from the variation in phase at which particles cross the gaps. Direct voltage machines such as the electrostatic generator produce much better energy uniformity. At higher energies linear accelerators become physically long, and a multiplicity of rf power sources is required to supply the extended electrode system. Increased costs of high-frequency power equipment and the difficulties of phase adjustment of many parallel units become the limitations.

Design problems differ for accelerators of electrons or of

protons, as they also do for circular accelerators. In the earliest designs, only rather heavy positive ions could be used, owing to the limitations of the available high-frequency power supplies. With the steady improvement of rf power sources during the past decade, it has become possible to build practical accelerators for protons and also for electrons. Proton accelerators use relatively low frequencies (50 to 200 Mc) because of the low proton velocities during most of the acceleration. Electrons attain the velocity of light at modest energies and can be accelerated in small structures which are resonant at microwave frequencies (3000 Mc). These structures are best described as waveguides, rather than arrays of electrodes, and particle acceleration can be described in terms of the wave properties of the field. In such a waveguide the electrodes are replaced by diaphragms which load the guide so that the phase velocity is made equal to the electron velocity. The applied rf electric fields set up standing or traveling waves in the loaded waveguide. A group of electrons riding this wave will pick up energy continuously, similar to the motion of a surfboard down the advancing front of a water wave.

Beam intensity can be significantly higher in an electron accelerator than in a proton accelerator. This is based on the fact that protons exert repulsive space-charge forces on each other, tending to diverge the beam, whereas these forces reduce to zero at the relativistic velocities of electrons so that an electron beam does not tend to diverge. Furthermore, the technical problems of producing a high-intensity electron beam (from hot cathodes) are much simpler than those for positive ion sources.

In addition to the technical advantages, designers have also hoped that linear accelerators might be less expensive than circular magnetic accelerators. This possibility is based on the (approximately) linear proportionality between cost and energy as length is extended. Circular accelerators, on the other hand, require magnets for which the cost increases roughly with T^3 (for relativistic particles). This difference in the cost equations

suggests that linear accelerators might become more economical at sufficiently high energies. However, the several sequential developments of magnetic accelerators, from the cyclotron with its solid core magnet, to the synchrotron with its much lighter ring magnet, to the alternating gradient synchrotron, which still further decreases magnet dimensions and cost, have retained the economic advantage of the magnetic accelerators up to the present.

The linear accelerator has not yet been extended into the Bev range. However, the need for high-energy electrons of several Bev energy is now becoming evident, and circular electron accelerators suffer from a limitation due to the rapid increase in the energy lost by radiation at these very high energies. So it seems possible that the linear accelerator may eventually prove to be a practical means of attaining really high electron energies.

5.2 Early Designs

The first linear accelerator, described by Wideröe[21] in 1929, was the forerunner of all resonance accelerators. It consisted of two cylindrical electrodes to which an alternating voltage was applied, with a frequency which allowed electrode potentials to be reversed during the time required for the heavy ions (K^+ and Na^+ ions) to traverse the first electrode, resulting in two accelerations and a final energy twice that obtained in a single gap.

Sloan[22,23] and others extended the development to ten or more electrodes but were limited by existing radiofrequency techniques to frequencies which restricted the application to relatively heavy ions (Li^+, Hg^{++}, etc.) and to quite low energies (1 to 2 Mev). The electrodes were connected alternately to two bus bars supplied by the rf power source. This elementary form of the linear accelerator is illustrated in Fig. 5-1. Since they could operate only at relatively low frequencies and with heavy ions of low energy, the usefulness of these early accelerators in nuclear research was insignificant.

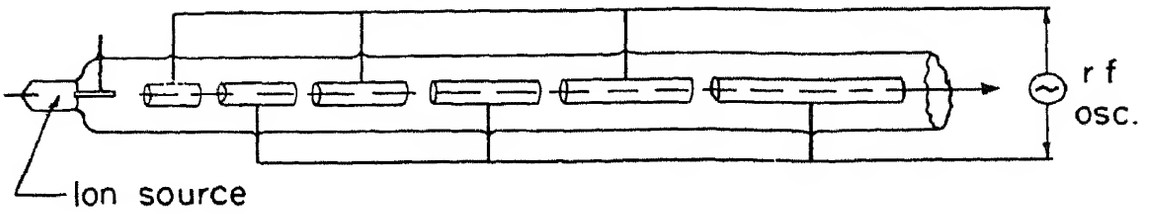

FIG. 5-1. Early linear accelerator. Spacings between cylindrical electrodes increase with increasing particle velocity.

The separation L between accelerating gaps is the distance traversed by the particles during one-half cycle of the applied electric field. So the length is given by:

$$L = \tfrac{1}{2}v/f \tag{5-1}$$

where v is particle velocity and f is the frequency. Each time a particle crosses a gap, it finds an accelerating field, so the energy increases by an increment $V_e e$, where V_e is the voltage across the gap at the instant the particle crosses.

At low energies, velocity increases as the square root of the energy, so successive gap separations must increase in a sequence proportional to the square roots of integers. For a particle to be in exact resonance and to obtain the same energy increment $V_e e$ on each traversal, the gap separation distance L_i for the ith electrode is given by:

$$L_i = \frac{1}{2f}\left(\frac{2e}{m} V_e\right)^{1/2} i^{1/2} \tag{5-2}$$

At relativistic energies particle velocity approaches the velocity of light, and gap spacings become constant:

$$L_i = \frac{c}{2f} = \lambda/2 \tag{5-3}$$

where λ is the wavelength of the applied radiofrequency on the electrode system. Electrodes would be spaced at half-wavelength intervals.

The energy increment comes from an oscillating field given by:

$$V_e = V \sin \phi_e \tag{5-4}$$

where V is the peak applied rf potential difference across the gap and ϕ_e is the phase at which the particle crosses the gap. Choice of the sine function is equivalent to defining zero phase as the instant when voltage is zero and increasing toward the polarity which provides acceleration.

For more generality we recognize that the accelerating potential may vary along the length of the accelerator. We can describe this by a relation:

$$V = V_f (z/z_f)^k \tag{5-5}$$

where V_f is the voltage across the final gap and z_f is the total length of the accelerator. The parameter k defines the type of variation with distance. If $k = 0$, voltage is constant on all gaps; if $k = \frac{1}{2}$, voltage increases with the velocity and with gap spacing, and so the average electric field along the axis is constant; if $k = 1$, voltage increases linearly with distance along the accelerator.

The early linear accelerators (before 1945) used constant voltage per gap ($k = 0$). The gaps between tubular electrodes were short, and the lengths of the electrodes increased with $i^{1/2}$ as given by Eq. 5-2, so that the positive ions spent most of their time in the field free regions inside the electrodes or "drift tubes." Relatively few electrodes were used (10 to 30) so the precision of spacing was not critical. Resonance was maintained by an experimental balance of the applied voltage V to the value required by the electrode spacing. The phase ϕ_e was close to 90°, so that only particles which crossed the gaps when the voltage was near maximum would remain in resonance.

5.3 Phase Stability

By 1945 two factors combined to provide a major change in the design of linear accelerators. The intensive development during World War II of ultra-high-frequency radar techniques, with an improved understanding of the properties of waveguides and the development of pulsed power sources, extended the available frequency range into the microwave region. At these high frequencies (up to 3000 Mc) linear accelerators became

practical for light positive ions and for electrons. At the same time the proposal of the principle of phase stability by McMillan[5] and Veksler[6] allowed the linear resonance principle to be modified to obtain synchronous stability during acceleration. These factors have resulted in a new class of phase-stable accelerators, both for protons and electrons, using very high peak power and pulsed with a short duty cycle.

Phase-stable synchronous acceleration can be obtained in the linear system of electrodes under certain conditions. Oscillations in the phase of crossing the gaps occur in a manner entirely similar to that applying to the synchrotron and described in Chaps. 2 and 3. One value of voltage across the gaps is correct for resonance with the periodic structure, the value V_e used in Eq. 5-4, associated with an equilibrium phase angle ϕ_e. In general the peak voltage across the gaps, V_m, will be greater than V_e, and in practice a value of twice the equilibrium value is common, which means that $\phi_e = 30°$.

To show the existence of phase stability consider a particle crossing the gap at another phase, illustrated by the point t_1 on the voltage-time graph of Fig. 5-2, when the voltage is higher than V_e. This particle will gain more than the correct amount of energy, will have a higher velocity, and so will take a shorter time to reach the next accelerating gap. The resultant phase shifts at the second, third, etc., gaps will eventually reduce the energy per acceleration until it reaches the equilibrium value. This process is illustrated by points t_2, t_3, etc., in Fig. 5-2. The accumulated excess energy will continue the phase shift so

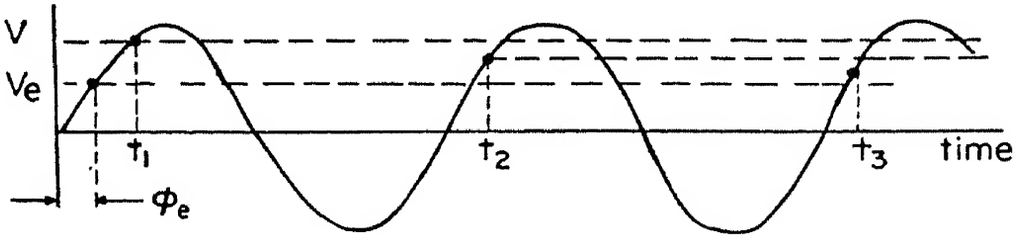

FIG. 5-2. Phase relations in linear acceleration. Phase oscillations are centered around an equilibrium phase φ_e and a voltage V_e on the rising side of the voltage wave.

the particle gets less than the equilibrium acceleration, and the situation is reversed. The resultant motion is a stable oscillation of phase about the equilibrium value.

The region of stability in phase focusing is centered about a phase ϕ_e when the voltage across the gap is increasing. The alternate position with decreasing voltage would lead to instability. This situation is just the reverse of that required for phase stability in the synchrotron.

A consequence of the stable phase being on the rising side of the voltage wave is that the particles experience lateral defocusing. This can be understood in terms of the change in the electric field in the gap during the time required for the particle to cross the gap. The shape of the electric field in a gap between cylindrical electrodes is illustrated in Fig. 5-3. Particles which are displaced from the geometrical axis experience convergent forces as they enter the gap and divergent forces as they leave. Since the magnitude of the electric field increases with time, near the stable phase position, the divergent forces predominate. The result is a radial or lateral defocusing of the beam. Special axial focusing devices are required to compensate for this effect. Furthermore, even though such axial focusing is provided, some of the particles will perform radial oscillations so that they traverse slightly longer paths than a particle on the axis, which means that they will acquire a phase shift relative to the axial particles.

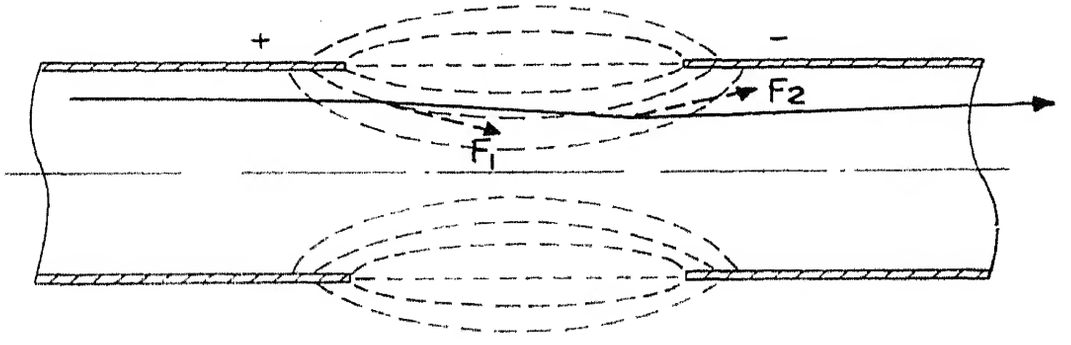

FIG. 5-3. Electric field between cylindrical electrodes showing convergent forces acting on nonaxial particles when entering the gap and divergent forces on leaving. In the linear accelerator the divergent forces are stronger owing to the increasing electric field while the particle is crossing the gap.

As particle velocity increases, the magnitude of the defocusing effect becomes smaller, and when particles reach the velocity of light, they are in neutral equilibrium. This can be understood by noting that when the velocity of the particle becomes equal to that of the traveling electric wave no phase difference can develop between particle and field while crossing a gap; the converging and diverging forces are now identical. So electrons are subject to defocusing forces only in the early stages of acceleration where their energy is below 1 or 2 Mev. Protons, however, will experience some defocusing over the entire acceleration.

5.4 The Linac

The prototype of the modern proton accelerator, known as a linac, was developed by Alvarez[24] and his associates at the University of California Radiation Laboratory, paralleling the development of the electron synchrotron in the same laboratory by McMillan. Construction was started in 1946, and a proton beam of 32-Mev energy was obtained in 1948. The machine has been in use since that date as a research tool.

In the linac tubular electrodes of increasing length are used as in earlier accelerators, but the resonant circuit used to provide a rf potential across the gaps is considerably modified to improve the electrical efficiency of the system. The electric circuit is made in the form of a hollow, cylindrical cavity with the electrodes mounted along the axis, having distributed inductance and capacitance, rather than the lumped constant circuit which was illustrated previously in Fig. 5-1.

A resonant cavity of this type has several modes of oscillation, with different electrical efficiencies, Q. Three possible modes are illustrated in Fig. 5-4, in which the gap spacings are respectively $\frac{1}{2}$, 1, and 2 wave lengths of the electric waves in the cavity, or in which the spacings are given by $\frac{1}{2}\beta\lambda$, $\beta\lambda$, and $2\beta\lambda$, where $\beta = v/c$ and λ is the wavelength. The first case, in which $L = \frac{1}{2}\beta\lambda = \frac{1}{2}v/f$, is identical with the mode used in the early accelerators. It can be noted that large circulating currents

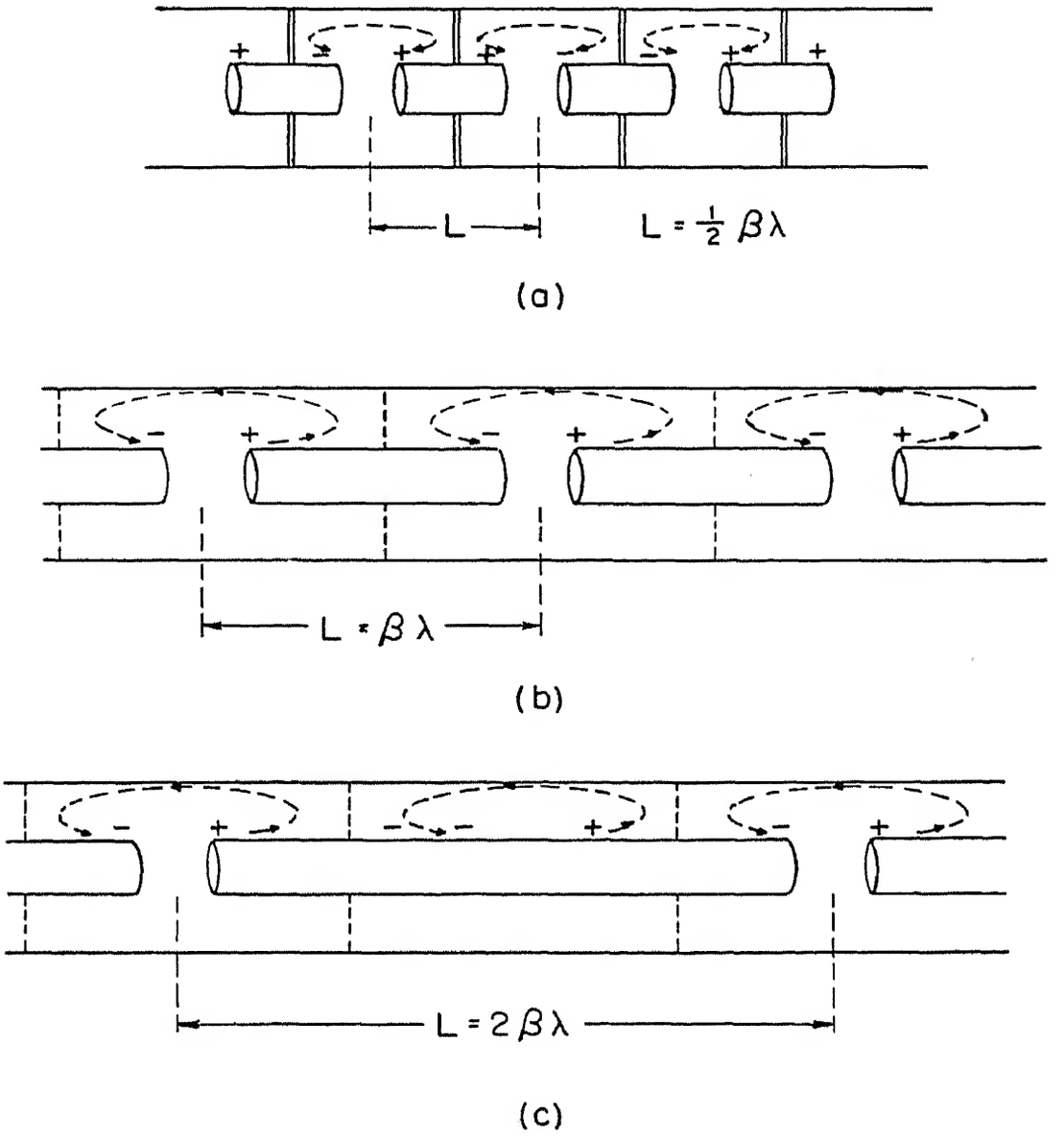

FIG. 5-4. Modes of oscillation of a resonant cavity formed of a tubular outer conductor and coaxial cylindrical drift tubes. (a) $L = \frac{1}{2}\beta\lambda$, large currents exist in the supporting diaphragms; (b) $L = \beta\lambda$, circulating currents are confined to the tubular surfaces; (c) $L = 2\beta\lambda$, alternate mode when longer drift tubes are desired.

must exist in the stems or diaphragms which support the electrodes, leading to large losses or a low Q. The $L = \beta\lambda$ mode requires circulating currents only along the electrodes and on the inner wall of the surrounding cavity and has a much higher Q. In principle each unit cell of the system, contained between the dotted lines at the location of the electrode stems or supports, is a system resonant at the impressed frequency. The spacing

between gap centers is one guide wavelength, and the polarities and phases are the same in each gap. The $2\beta\lambda$ mode is an alternative with much the same electrical properties except that the spacing is two guide wavelengths. It would become useful in the case where particle velocity is low and the distance of travel during one period of the radiofrequency would require an impractically short electrode length with the $\beta\lambda$ mode.

Electrode dimensions of the Berkeley linac were chosen to accommodate a beam diameter of 1 to 2 in., anticipating considerable spreading of the beam due to the defocusing forces and scattering due to the thin foil focusing devices planned to compensate for such defocusing. Drift tube electrodes with this internal aperture could not be shorter than about 4 in. because of the penetration of fields in the aperture. The injection energy was 4 Mev, the maximum possible with an electrostatic generator. These parameters determined the operating frequency, taken to be 200 Mc, and the linear dimensions of the electrodes. The gaps were made one-third of the electrode lengths, and the thirty drift tubes occupied a total length of about 40 ft.

The structure is a large resonant cavity 40 ft long and about 4 ft in diameter, with the array of drift tubes of increasing length mounted along the axis. This cavity resonates efficiently in the $\beta\lambda$ longitudinal standing wave mode, such that each electrode is in the center of a one-wavelength sub-unit of the cavity which is resonant at 200 Mc. The resonant frequency is maintained constant along the structure, in which gap spacing increases with proton velocity, by suitably decreasing the external diameter of the drift tubes which affects the capacitance in the unit cell. The accelerator is illustrated in Fig. 5-5.

Surplus radar tubes and power supplies were made available to the Radiation Laboratory by the U. S. Signal Corps. This equipment was chosen because it was adapted to the 200-Mc frequency. The rf power supply consists of thirty oscillator tubes coupled with small loops through the side of the 4-ft cavity at each sub-unit. The tight coupling of the resonant sub-

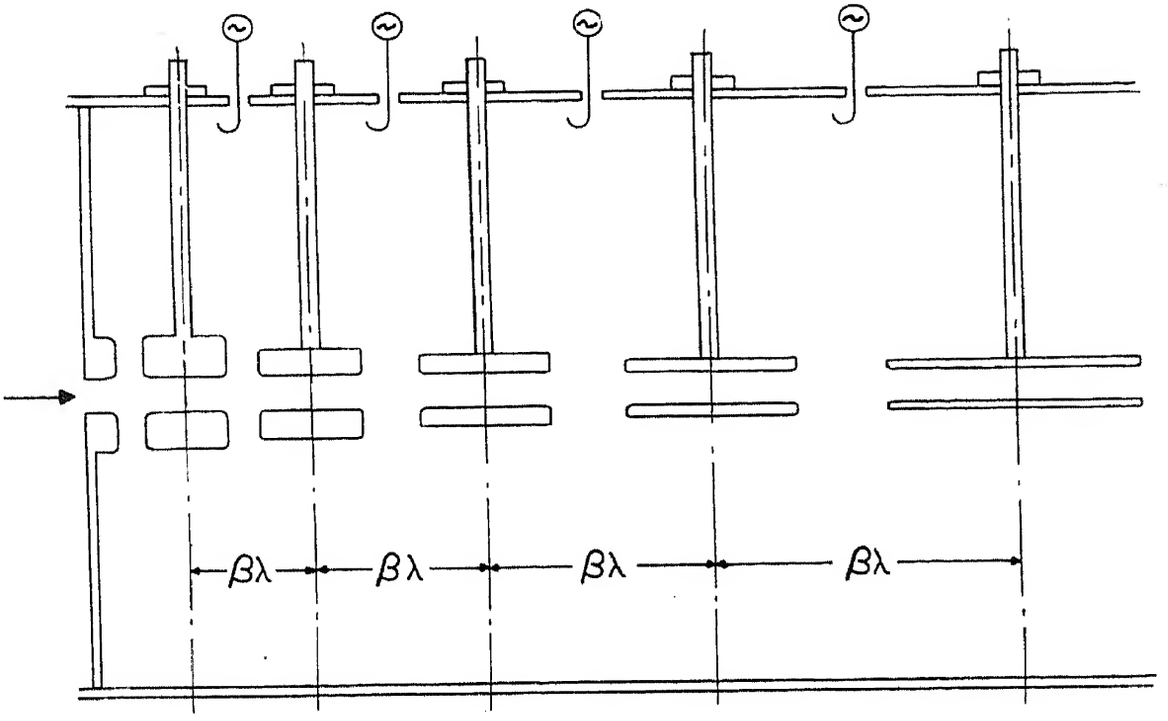

FIG. 5-5. Schematic of proton linac showing drift tubes of increasing length and decreasing diameter to maintain resonance at constant frequency.

cavities maintains a constant phase for the thirty oscillators. Tubes are excited in parallel from a master oscillator at 200-Mc frequency. Plate power for the tubes is obtained from a pulse forming network producing a dc pulse of 500 microseconds duration at a repetition frequency of 15 per second.

Protons are first accelerated to 4 Mev in a horizontal electrostatic generator, designed and built by C. Turner[25] following the experience of Herb at the University of Wisconsin. The ion source is pulsed for 500 microseconds at the repetition frequency, resulting in pulse intensities of about 1 ma of protons. On injection into the linac along the axis of the drift tubes the protons are accelerated by an additional 28 Mev in the thirty gaps, acquiring a final energy of 32 Mev, the designed maximum. Phase focusing in the linac results in the 500-microsecond pulse being modulated at the 200-Mc frequency. The average current of 32-Mev protons during the pulse is about 0.5 ma, and the duty cycle results in a time-average current of about 4×10^{-6} amp. This is comparable with the output of a synchrocyclotron.

The method originally proposed and used by Alvarez to control defocusing in the linac was to mount thin foils at the entrance of the drift tubes. The electric field between a cylinder and a plane is always converging when the field is accelerating, as illustrated in Fig. 5-6, which removes the defocusing effect. The foils were made of Be (low Z) to minimize the small angle Coulomb scattering in the foil and were extremely thin to keep energy losses small. However, the rf discharges in the cavity, which accompany outgassing and conditioning of the surfaces, burned or tore the foils, so the method had to be abandoned. An alternative scheme used grids of Be metal strips in similar locations. These grids were specially shaped to leave the maximum clear aperture along the axis and to have a high aperture-to-grid bar ratio. The grids successfully resisted the discharges, but beam intensity has reduced because the grids intercepted a significant fraction of the beam. Eventually all grids were removed except a few in the early drift tubes, so total beam intensity was not reduced below 50 %. However, this compromise resulted in an undesirable increase in the beam spot size.

One other linac is under construction, by Williams, at the

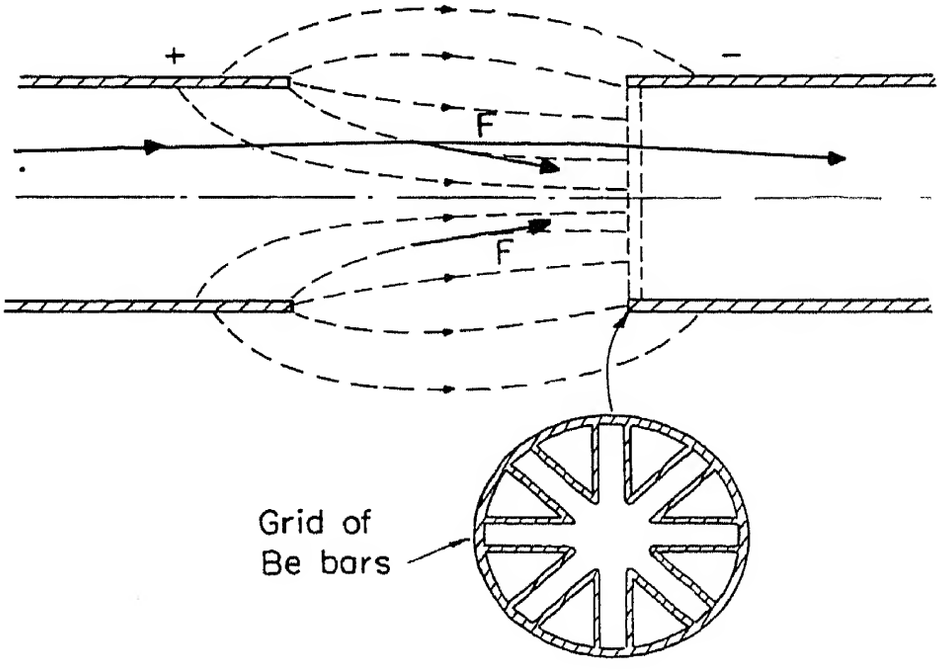

FIG. 5-6. Convergent forces on acceleration between a cylinder and a plane electrode or grid.

University of Minnesota. It is designed for 50- to 80-Mev protons and uses the same resonance principle and the same basic design as the Berkeley linac. The major difference is in the use of resnatron tubes as oscillators to provide the 200-Mc rf power. These tubes are planned to yield 4 megawatts rf power output in a 300-microsecond pulse, or 8.5 megawatts in a 40-microsecond pulse. Preliminary operation at 10 Mev using one resnatron was reported in February, 1954.

Developments at the Harwell AERE Laboratory in England have culminated in a program for construction of a 600-Mev proton linear accelerator designed for extremely high beam intensities. With average intensities of the order of milliamperes, rather than microamperes, the output of mesons could be expected to exceed by several orders of magnitude that obtained from synchrocyclotrons or other proton accelerators. The basic problem is the development of klystrons or other vacuum tubes to deliver the necessary high pulse power at 200 to 400 Mc.

5.5 The Focusing Problem

One of the most useful applications of the principle of alternating gradient focusing, described in Chap. 7, is the use of magnetic or electrostatic quadrupole lenses to compensate for the defocusing forces in the linear accelerator. The properties of the 4-pole magnetic lenses are discussed in Chap. 7, where it is shown that a pair of such units forms a convergent lens for particles diverging in either transverse coordinate. The advantage over the traditional solenoidal lens is in the smaller amount of iron or power required for a given focal length. For very high energy particles the solenoidal lens requires an exorbitant amount of power.

Several investigators have installed such 4-pole lenses to collimate and focus the emergent particle beams from accelerators. Cork and Zajec[25a] have applied it to the 20-Mev deuterons from the Berkeley cyclotron, with the result of decreasing beam spot size on the target and increasing beam density by a factor of 30. Similar results were obtained with

the 32-Mev beam from the linac. The output beams from Van de Graaff accelerators at Oak Ridge, M.I.T., and several other institutions have been focused with such lenses.

Blewett[26] has proposed the use of alternating gradient focusing in the electrode structures of linear accelerators to cancel out the divergence of the beam continuously along the path of the particles. In his proposal 4-pole electrostatic lenses would be mounted inside the drift tubes, with the hyperbolic axis along the centerline. Electrostatic potentials would be applied to the four hyperbolic electrodes sufficient to compensate for the divergence due to the electric fields between drift tubes. The increasing length of the drift tubes allows an increasing length of lens unit, which is close to that required by the increasing energy of the particles to maintain the compensation. Calculations of the lengths and field strengths required for a typical linac are given in Blewett's paper. Alternatively, magnetic lenses could be used between drift tubes, but this involves a more complicated geometric structure. The use of external magnetic lenses allows the lens design to be independent of drift tube length (except for practical considerations of the electrical leads). However, it requires that the accelerator tube be small enough to fit between the pole tips, and it may be necessary to use lumped circuits rather than waveguides.

A preliminary trial of the use of lenses inside the drift tubes has been reported by the Berkeley group, using the existing drift tubes of the 32-Mev linac. The beam density on the target was increased by a factor of 20, and the total beam intensity was doubled relative to the best performance with the focusing grids. Although this correcting system was not ideally designed and insulation difficulties developed, it shows the potential usefulness of alternating gradient focusing in the linac.

Future developments of linacs will probably incorporate the A.G. focusing technique, which offers an opportunity to eliminate the one serious flaw in previous accelerators. At Brookhaven and at Geneva (the CERN Laboratory) designs are in progress for linacs of about 50 Mev to be used as injectors

into the multi-Bev accelerators now contemplated in these laboratories.

5.6 Electron Linear Accelerators

The special characteristics of the electron accelerator are based on the fact that electrons approach the velocity of light at relatively low energies ($v = 0.98c$ at 2 Mev), and that with this constant velocity the spacings between accelerator gaps become equal. It is possible to build a resonant structure with much shorter spacings between electrodes, which takes on the characteristics of a microwave waveguide and allows the use of the techniques and power sources at 3000 Mc developed in the radar field. The availability of magnetrons and klystrons with extremely high peak power ratings on pulsed operation at this frequency has made it possible to design electron accelerators for much higher energies than those developed for protons.

Scientists and engineers in many laboratories recognized this opportunity. Development started in 1946 on preliminary, low-energy accelerators to test the principles and design concepts, at the Telecommunications Research Establishment (TRE) Laboratory in England, and at M.I.T., Stanford, Yale, Purdue, and other universities in the United States. The development centered on two major problems, the design of suitable waveguides for the accelerating system, and the phasing of multiple pulsed power sources such as magnetrons or klystrons. The British results are mostly in the form of internal reports in the TRE and AERE (Harwell) Laboratories; the leader in these studies was D. W. Fry.[27] The M.I.T. project under the direction of J. C. Slater has been reported in several publications.[28] The Stanford development started under the late W. W. Hansen and has been continued by Ginzton, Panofsky and others.[29]

The properties of a periodic array of uniformly spaced electrodes can best be described by considering the system to be a loaded waveguide, in which the phase velocity of the traveling wave is made equal to that of the electrons. The phase velocity of a wave in an open tubular waveguide is greater than the

velocity of light. In order to reduce it to the electron velocity c, the structure must be loaded with either lumped or distributed reactive elements. The usual method of loading is to insert iris diaphragms inside the tube, spaced periodically at some precise fraction of the desired guide wavelength. Such an iris-loaded tubular waveguide is illustrated in Fig. 5-7.

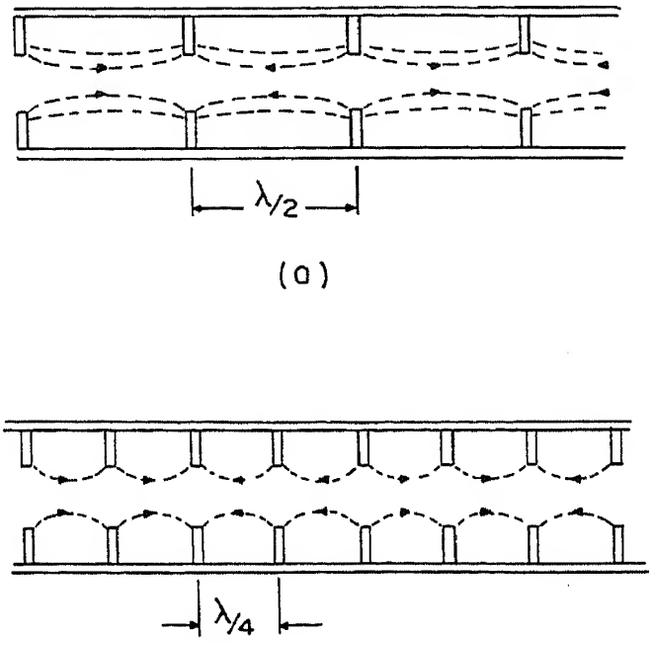

FIG. 5-7. Longitudinal cross section of circular wave guides for electron linear accelerators. (a) Iris-loaded wave guide for a standing wave accelerator; diaphragms are located at ½λ intervals, the π-mode. (b) Traveling wave waveguide. Diaphragms are located at ¼λ intervals, the $\pi/2$-mode.

The wave form propagated in such a periodic structure can be expressed as a Fourier series, in which only one of the components will have a velocity of propagation equal to the electron velocity. Other components will have different velocities and will act only as rapidly oscillating perturbing fields on the electrons, so their effects cancel out. The wave which is propagated with the largest amplitude is that for which the spacing between diaphragms is half of the guide wavelength. This is called the π-mode, illustrated by Fig. 5-7a. If the struc-

ture is terminated after a finite number of diaphragms, so that the waves are reflected from the ends, a standing wave is set up along the guide, consisting of two sinusoidal components which are out of phase by 180°. The guide acts like a resonant cavity for this frequency, with the diaphragms located at the nodes of the standing wave pattern.

Another way of using the loaded wave guide is to employ a nonreflecting termination and to obtain a traveling wave. This can be considered as consisting of a sine wave and a cosine wave with a phase difference of 90°. The two components can be excited separately by feeding power into at least two suitably spaced points. In order to maintain symmetry in the fields, the diaphragms must be spaced at 90° phase intervals. This is described as the $\pi/2$-mode, shown in Fig. 5-7b.

The relative advantages of the standing wave and traveling wave systems have been analyzed and discussed in detail by Slater,[28] who finds advantages for the standing wave type at relatively low energies, and by Ginzton, Hansen, and Kennedy[29] who conclude that the traveling wave type gives better power economy for the higher-energy accelerator at Stanford. A single, traveling wave results in higher electric fields, for a given power input, than a standing wave which has two out-of-phase components. On the other hand, the traveling wave can be maintained only in a guide operated in the $\pi/2$-mode, with diaphragms spaced at 90° phase points, so the resistive losses in the guide are larger than those in a standing wave tube which has half the number of diaphragms. Other comparisons involve details of diaphragm dimensions, methods of feeding power to the wave guide, and the power efficiency or Q of the cavity circuit.

The Stanford linear electron accelerator is the only one which has been developed to really high energies. It has operated at 600 Mev. The design is described in a technical report of the Stanford Microwave Laboratory.[30] The 3-in.-diameter, 3000-Mc waveguide is 220 ft long, a length capable of accelerating to 1 Bev when the final full power supply is

installed. It is planned to have 22 klystrons feeding the waveguide, each capable of maximum operation at 17 megawatts. In March of 1954 about fifteen were installed and operating at reduced power to give 200 megawatts peak pulse power over a pulse of 2 microseconds repeated at a rate of 60 per second. The maximum voltage gradient in the guide is 3,500,000 volts/ft, with an attenuation to one-third this value between klystron feed points. Phase focusing in the early stages of acceleration results in an energy spectrum with a width of 2%. The measured intensities at 600 Mev are about 10^{11} electrons per pulse, or a time average beam current of 1 microampere. Higher intensities could be obtained by increasing the repetition rate or the injection intensity, and at lower energies beam currents of up to 10 microamperes have been observed. The opportunity of attaining really high intensities, by increasing rf power and improving the duty cycle, constitutes one of the principal advantages of the electron linear accelerator over the several types of proton accelerators.

The primary problem and chief limitation of the Stanford machine is in the development and maintenance of the klystron power tubes. At present maintenance time and costs are excessive, making it difficult to operate at full power. With further development it can be hoped that this technical problem can be solved and the accelerator can be brought into operation at full energy. When this stage is reached, it will be possible to estimate the cost for extension to higher energies with more accuracy. Present estimates suggest that the cost of increasing the energy would be about $1000 per Mev.

CHAPTER 6

The Proton Synchrotron

The proton synchrotron is the most recently developed accelerator and produces the highest-energy particles obtained to date. It is also the largest and most expensive. The Brookhaven cosmotron came into test operation in June, 1952, at a record energy of 2.3 Bev protons and was raised to 3.0 Bev in early 1954. The name is symbolic of the fact that this energy overlaps the energy range of primary cosmic rays. A photograph of the Brookhaven cosmotron before shielding was installed is shown in the Frontispiece. The bevatron at the University of California Radiation Laboratory is nearing completion and is expected to attain a proton energy of 5 to 6 Bev. Preliminary operation at 4.9 Bev was announced in March, 1954. The cost of these machines, which is about two million dollars per billion volts, is high on the absolute scale, and has been subsidized by government funds. On a cost-per-volt basis, however, the proton synchrotron is the most economical of all accelerators, approaching a cost of 0.2 cent per volt.

For the first time particle energies are available greater than the rest mass of nucleons (0.938 Bev) or of any known heavy mesons. Meson formation processes and the properties of mesons can be studied under controlled laboratory conditions at energies extending into the cosmic ray region. Early results suggest that it may be possible to produce and study many of the "strange" particles of cosmic rays. Scientists anticipate an exciting time during the early years of research with these great accelerators.

The principle of phase-stable synchronous acceleration reaches its highest stage of development in the proton synchro-

tron. By combining the techniques used in earlier machines, their individual limitations have been side stepped, and a new range of energies has been made available.

The synchrocyclotron, which has been so successful as a proton accelerator in the 100- to 500-Mev range, requires a solid core magnet. Magnet weight and cost increase roughly with the cube of pole face diameter. Power costs also increase with the volume of the field between poles or with the cube of diameter if dimensions are scaled. If a synchrocyclotron were to be enlarged to produce protons of several Bev energy, the magnet would become exorbitant in weight and cost.

Magnetic electron accelerators such as the betatron or synchrotron have practical energy limits of the order of 0.5 and 2.0 Bev respectively due to the rapid onset of radiation losses experienced by the orbiting electrons, as discussed in Chap. 2. The limit of acceleration is reached when the radiation loss per turn becomes equal to the maximum practical accelerating voltage per turn. The radiation loss increases with the third power of the ratio of total energy to rest energy, (E/E_0).[3] Because of the larger proton rest energy, the equivalent limiting energy for protons would be $(1840)^3$ times larger than for electrons. At any energies considered to date the radiation loss by protons is negligible.

So the proton synchrotron uses a ring magnet to reduce magnet cost, accelerates protons to avoid the radiation loss limitation, and operates on the principle of synchronous acceleration at constant radius. This extension of the principle was appreciated by machine designers in several laboratories, and several groups independently calculated the basic requirements and dimensional parameters.

6.1 Historical Development

The first proposal of a proton accelerator using a ring magnet, in which both magnetic field and frequency of the accelerating electric field are varied, was made by Professor M. L. Oliphant, of the University of Birmingham, England, to

the British Directorate of Atomic Energy in 1943. Because of wartime security restrictions, the proposal was not published at that time. It is reported in a detailed design study by Oliphant, Gooden, and Hide[31] published in 1947, accompanied by a theoretical analysis of orbit stability by Gooden, Jensen, and Symonds.[32] An accelerator for protons of 1.0 Bev following these designs has been under construction at the University of Birmingham for some years. Professor Oliphant's return to his native Australia and the untimely death of Dr. Gooden, the chief scientist on the project, slowed progress toward completion of this machine, which was the first proton synchrotron to be started. Because of this early start, the basic magnet design was frozen and construction ordered before improved design concepts developed in the United States could be incorporated, and it lacks some of the advantageous features of the latter. However, construction is now complete, and preliminary operation at 0.9 Bev was reported in the summer of 1953.

Meanwhile, the principle of phase stability in synchronous accelerators was announced by McMillan[5] and Veksler[6] in 1945. This principle led to the development of the synchrocyclotron and of the electron synchrotron, at the University of California and in several other laboratories. Both papers describe two techniques for synchronous acceleration, involving the use of frequency modulation for heavy particles or of an increasing magnetic field for electrons. Both papers also include the possibility of acceleration of protons at constant radius by varying both frequency and magnetic field, but neither paper was primarily concerned with this more complicated application.

Design studies for proton synchrotrons in the United States started early in 1947 in two laboratories supported by the U. S. Atomic Energy Commission. Dr. W. M. Brobeck,[33] of the University of California Radiation Laboratory, made a preliminary report of a possible design for 10-Bev protons in 1948, which was primarily a study of the practicability of a pulsed power supply for the large ring magnet required. The name bevatron was given to this billion-electron-volt accelerator.

Meanwhile, preliminary designs of a similar accelerator were started at the Brookhaven National Laboratory under the direction of the writer, on leave from the Massachusetts Institute of Technology, as Chairman of the Accelerator Project. The stimulus to start this development came from Professor I. I. Rabi, of Columbia University. The early Brookhaven plans were reported in papers by Livingston[34] and others before the American Physical Society in 1948. As the design approached completion, a description was published by Livingston, Blewett, Green, and Haworth[35] in January, 1950. This machine was soon given the laboratory name of the cosmotron.

Both the Berkeley Radiation Laboratory and Brookhaven were encouraged in these design studies by the Atomic Energy Commission officials responsible for research and development of instruments. When preliminary designs and cost estimates became available in 1948, a decision was made by representatives of the two laboratories and the AEC for the construction of two machines, a 2.5- to 3.0-Bev cosmotron at Brookhaven and a 5.0- to 6.0-Bev bevatron at the University of California. In both laboratories teams of scientists and engineers were assembled to complete designs and proceed with construction. Many of the members of these teams have contributed importantly to the designs, and the results must be considered the products of the joint efforts of a large number of individuals.

The Brookhaven cosmotron was first operated in June, 1952, and was rapidly tuned up to the maximum energy possible with the available power supply of 2.3 Bev. A period of engineering consolidation and "bug-picking" brought it back into operation at the date of the dedication ceremonies on December 15, 1952. Operation at the maximum designed energy of 3.0 Bev was announced in early 1954. Months, and possibly years, of further improvement can be expected, following experience in the development of other accelerators. However, experimental use of the high-energy protons is already under way, and many scientists at Brookhaven and the surrounding universities are engaged in the development of detection devices and in

performing experiments with the radiations coming from the machine. An unusually complete description of the final operating machine occupies a full issue of the *Review of Scientific Instruments*.[36]

Professor Oliphant[37] announced plans in 1950 to build a proton synchrotron at the University of Canberra, Australia, to reach 2.0 Bev energy. The original plans were of special design, in which a synchrocyclotron of 200 Mev was to be used as a source of ions for an "air-cored" synchrotron around the periphery. Oliphant called it a cyclo-synchrotron. No information has been published beyond the preliminary report referenced above, but design and construction are reportedly under way on several of the components.

6.2 Principle of Operation

The principle of operation is basically the same as for the electron synchrotron. A fixed orbit radius is used, and a ring-shaped magnet produces a magnetic field across a doughnut-shaped vacuum chamber enclosing the orbit. The magnetic field increases with time as the protons gain energy to maintain constant orbit radius. Ions are injected into the orbit at low energy when the magnetic field is small. Energy is supplied by an accelerating electric field applied across a gap at one or more points in the orbit. But unlike electrons, which approach the velocity of light at relatively low energies ($v = 0.98c$ at 2 Mev) and so have an essentially constant frequency of rotation during acceleration, protons do not reach constant velocity until they have much higher energies ($v = 0.98c$ at 4 Bev), so their velocity and frequency of rotation increase during the entire acceleration interval. The applied electric field must synchronize with the ion rotation frequency. In the proton synchrotron the frequency must be modulated over a wide range (about 1 to 10), determined by the energy at injection and the maximum energy. This requirement of a variable frequency accelerating voltage introduces new and complicated technical problems in the design of the accelerating system and

of the high-frequency oscillator. Furthermore, there is no automatic stabilization at a fixed frequency and orbit radius as in the electron synchrotron, but, to maintain the constant orbit radius, the frequency must be programed or controlled at each instant to match the rotation frequency of the ions as they gain in energy.

The same type of phase focusing exists as in the electron synchrotron, which bunches the particles about an equilibrium phase of the accelerating electric field. If the applied frequency is correct, the protons maintain a constant average orbit radius. But an error in frequency will cause the bunch of particles to gain energy at a rate not compatible with the increasing magnetic field, and they will spiral inward or outward and be lost against the walls of the chamber. The schedule of frequency modulation required does not follow any simple law but depends on the time rate of increase of the magnetic field, which is itself a function of the constants of the power supply and the properties of the magnet iron. So new problems of frequency control are encountered, which are unique to the proton synchrotron.

Ions are injected into the orbit by an auxiliary accelerator that produces a short pulse of particles which are as well defined in energy and as closely collimated in direction as possible. Deviations in direction, energy, or timing of the pulse at injection result in oscillations of the particles about the ideal circular orbits defined by the particle energy and the magnetic field. The amplitudes of these free oscillations, specified by the conditions at injection, determine minimum dimensions for the vacuum chamber and of the useful region of magnetic field. Focusing forces to produce stability are supplied by a radial decrease in magnetic field, limited as for the electron synchrotron to the range in field index n of $0 < n < 1$. The average value of n around the orbit determines the frequency of the radial and vertical free oscillations. For the range of n-values used in practice ($0.5 < n < 0.8$) the frequencies are in the range $0.7\ f_o$ to $0.9\ f_o$ where f_o is the orbital frequency. These oscillations are strongly damped in the increasing magnetic field,

varying in amplitude with $B^{-1/2}$. So the dimensions of the envelope enclosing the ions are reduced to a final cross section of a few square centimeters.

Oscillations occur in the phase at which particles cross the accelerating gap, and corresponding oscillations in energy are superimposed on the steady increase of energy with time. The energy variation results in radial phase oscillations so that the instantaneous orbit for each particle expands and contracts, centered on an equilibrium orbit defined by the applied frequency. Equations for computing the frequency of such phase oscillations are given in Chap. 2. This frequency is of the order of 0.01 f_o at the start of acceleration and 0.0001 f_o at maximum energy. This means that the particles require about 100 turns at the start and 10,000 turns at high energy to complete a phase oscillation. Some phase damping occurs during acceleration, sufficient to decrease the azimuthal extent of the bunch of ions to about half the original spread. Meanwhile the increasing field reduces the radial phase amplitude to about one-twentieth of the initial value.

The magnet is powered with a pulse which gives a rise time to maximum field of about 1 sec, then is reduced to zero in an equal interval. Ions reach maximum energy at the peak of the magnet cycle, at which time they are directed against a target. Pulses are repeated as often as desired, limited by the ratings of the power supply.

6.3 Design Features

The cosmotron was the first proton synchrotron to be completed, and much more information concerning it is available than for the bevatron or other machines under construction. Accordingly, the description in this chapter of the dimensions and design parameters required for a proton synchrotron will refer to the cosmotron. The successful operation, with a minimum of difficulties in tuning it up to high intensity, warrants confidence in the effectiveness of the design.

The relativistic relation between particle kinetic energy

T, magnetic field B, and orbit radius R is given (Eq. 2-8) by:

$$T^2 + 2E_0T = c^2e^2B^2R^2 \tag{6-1}$$

When T and E_0 are expressed in Bev units and B is in webers per square meter (units of 10,000 gauss) the radius is given by:

$$R = \frac{[T(T + 2E_0)]^{1/2}}{0.3B} \text{ m} \tag{6-2}$$

The first parameter to be determined is the flux density B. Iron-cored magnets have a practical limit on flux density set by saturation of the iron at roughly 18 kilogauss (1.8 webers/m^2). Laminated magnets, such as are required for pulsed operation, have other physical limitations due to eddy currents, lamination insulation, and space for clamps, which set the practical limits still lower. In the cosmotron bundles of laminations are arranged radially around a circle, leaving wedge-shaped spaces between bundles at the orbit. The average field in the gap between poles has a maximum value of 14 kilogauss. At this average field some portions of the iron circuit have reached saturation. Alternate designs with closer packing of the iron might result in higher fields, but would involve a more complex structure. The designer's choice is based on minimizing cost for a given BR value.

Equation 6-2 can be used to calculate orbit radius for the desired particle energy T, once the general design features are established and the maximum value of B is known. The orbit radius was found to be 30 ft for 3.0-Bev protons at 14 kilogauss for the cosmotron.

As the design studies developed it became evident that there were several reasons for providing segments in the orbit free from magnetic field. A design of a synchrotron with straight sections between two semicircular halves of a ring magnet, called a race-track, had been proposed by Crane[14] and analyzed theoretically by Dennison and Berlin[15] for the University of Michigan electron synchrotron. In this analysis it was shown that two symmetrically placed short gaps in the

magnetic field would not cause defocusing nor set up excessive ion oscillations. The stability would be even better with four or more straight sections. Still higher-frequency angular perturbations in the field such as those caused by magnet laminations or bundles of laminations would have an insignificant effect on ion oscillations. So a design was chosen, at Brookhaven and also at Berkeley, in which the circular magnet was spaced into four quadrants joined by straight sections free of magnetic field.

A field-free region is essential to accommodate the type of induction accelerator used in the cosmotron, or the tuned cavity used in the bevatron. Another is required for injection of the beam of protons from the source. A third is used to house pickup electrodes to detect the location and the timing of the rotating ion bunch. The fourth section is assigned to insert targets in the internal beam or, eventually, for ejecting an emergent beam of high-energy protons. In the bevatron the straight sections are also used as manifolds for the vacuum pumps on the chamber.

The choice in the cosmotron was four 10-ft straight sections, between quadrants of 30-ft radius. This length is adequate to provide a field-free region for the induction accelerator. Figure 6-1 shows a plan view of the machine illustrating the 4-quadrant construction.

Ions are accelerated to 3.5 to 4.0 Mev in a horizontal Van de Graaff electrostatic generator for injection into the cosmotron orbit. This generator is produced commercially by the High Voltage Engineering Corporation of Cambridge, Massachusetts and it gives a well-focused beam of protons, pulsed to high intensity for a time interval of about 75 microseconds, timed to overlap the desired injection time interval when the magnetic field has the proper value. The ion source is the high-intensity PIG (Philips ion gauge) type developed at the University of California. It has a peak pulsed output of about 3 ma of ions, of which about one-third consists of hydrogen atomic ions, or protons. The accelerated beam is analyzed into

components by a magnetic field which deflects the protons by 25°. The mass-2 hydrogen molecular ions are deflected a smaller amount and fall on a pair of electrodes which are used to control the corona current to the generator terminal and so to regulate voltage.

The analyzed and focused beam of protons is injected into the cosmotron at one of the straight sections by electrostatic deflection between a pair of curved electrodes spaced ½ in. apart. The beam is deflected through an angle of 30° on an arc of 10-ft radius of curvature by the electric field, which requires a potential difference of about 30 kv. The inflector electrodes are mounted on guide rails with screw adjustments available from outside the vacuum chamber, so the vertical and radial positions can be set to any desired value. The most satisfactory position was found to be on the median plane at the extreme outside of the useful region of magnetic field, on an orbit radius of 372 in. corresponding to the location of $n = 1.0$ at injection time. Small deviations in proton energy or in the inflector field result in angular deviations at injection. Since mistiming of the pulse causes misalignment with the equilibrium orbit, these parameters are adjusted by the operator to give maximum beam intensity.

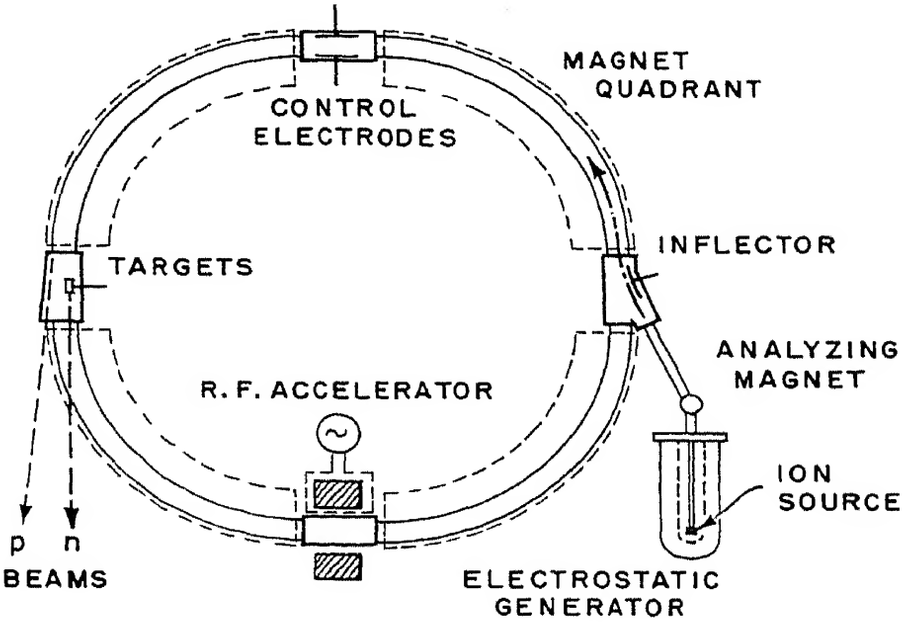

FIG. 6-1. Plan view of cosmotron magnet and assembly.

Particle oscillations at injection have amplitudes determined primarily by the angular divergence of the beam projected from the source, but may be increased farther by magnetic inhomogeneities or physical distortions of the orbit from symmetry. Vertical oscillation amplitudes may increase if the magnetic median plane, about which the oscillations are centered, deviates from the geometric center of the magnet gap. Initial radial amplitudes depend strongly on the time at which the beam is injected. There will be an instant at which the orbit radius for particles of injection energy will be identical with the radial location of the injector; if so, radial oscillations due to angular divergence will be centered about this circular orbit. At any later time the equilibrium orbit will be smaller, shrinking inward as magnetic field increases. The maximum allowable deviation in time occurs when the equilibrium orbit reaches the center of the chamber. Radial amplitude would then be equal to the full half-width of the chamber, and particles would just graze the inner wall. However, additional radial displacements occur as the particles develop phase oscillations, with an associated radial shift from the instantaneous orbit, so the time interval for acceptance is reduced somewhat below the above maximum.

Choice of chamber dimensions requires evaluation of total oscillation amplitudes, anticipating the effect of errors in beam energy and direction, including a suitable time interval for the injection pulse to provide adequate intensity and allowing a reasonable factor of safety. The decision of the designers of the cosmotron was to specify a magnet gap of 9½-in. height and 36-in. width, inside which a vacuum chamber could be located having a useful aperture of 6 in. by 30 in. This was estimated to allow a safety factor of about 3 in both dimensions. The justification of this choice is in the results. The observed beam was found to require less aperture than the chamber provides and defining slits which were installed temporarily to reduce the vertical dimension to 2 in. were still sufficient to allow a fraction of the beam to be accelerated.

The time of acceleration, during which the magnetic field

increases from about 300 to 14,000 gauss, is a basic parameter which influences many other design constants. A short rise time decreases the average power consumption in the magnet (primarily due to heat developed in the windings), but requires higher applied voltage on the inductive magnet coils and so increases the peak kva requirements of the generator. Scattering by residual gas in the chamber is reduced by a short rise time. The volts per turn required in the rf accelerating electric field depends directly on the rate of rise of the magnetic field. Cost of the rf accelerator unit increases with a high power of volts per turn, primarily because of the wide range of frequency modulation also required. The rise time chosen in the cosmotron design to balance these several factors is 1.0 sec, although an allowable range extends from 0.5 to 2.0 sec.

The repetition rate is limited by the average power rating of the magnet power supply, and by the cooling system used for the magnet coils. The chief advantage of high repetition rate is the increase in the time-average beam intensity available for experiments. In the cosmotron the magnet cycle consists of a 1-sec rise, a 1-sec fall, and a 3-sec rest, so pulses are repeated at 5-sec intervals. The high-energy protons are ejected or directed against a target at the peak of the cycle and are available during a burst of a few milliseconds duration, which can be stretched to about 50 msec if desired.

6.4 The Ring Magnet

The shape of the cosmotron magnet structure involves several unusual features. It is basically a C section with minimum size "window" for the windings. Choice of the C shape was influenced by the desire to provide ready access to the vacuum chamber around its entire outer periphery. Chamber assembly, maintenance, and vacuum testing are greatly simplified, and pumps can be located as frequently as desired along the length of the chamber. High-energy ions and neutrons emerge tangentially from the accelerator around the circumference, with only thin windows in the chamber wall for absorption

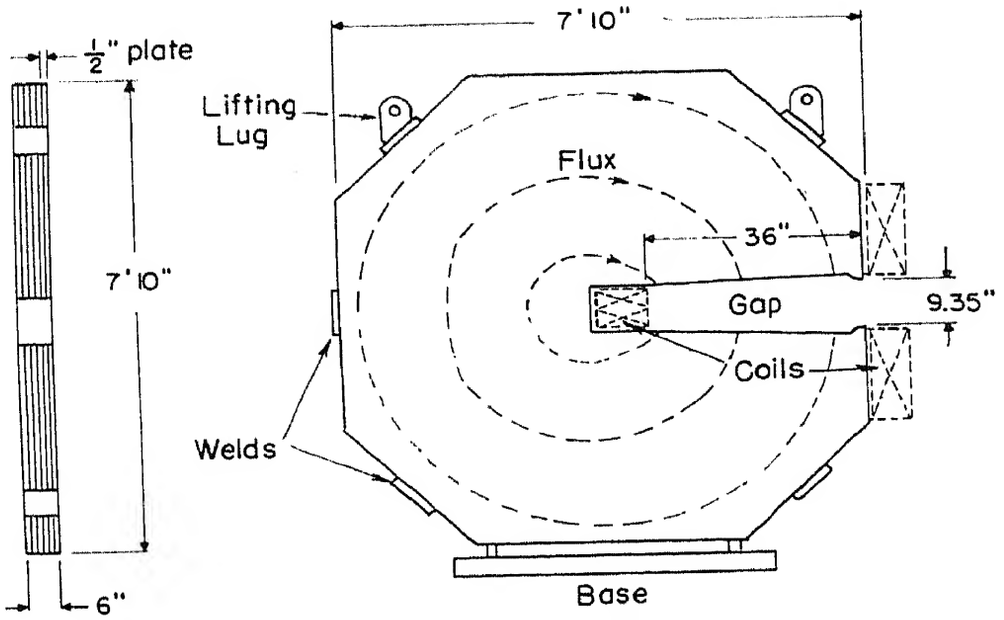

FIG. 6-2. Cross section of C-magnet and assembly of ½-in. plates into blocks.

and scattering of the radiations. The poleless C-shaped magnet circuit has minimum dimensions and weight, and requires only two accurately machined surfaces (the pole faces). The octagonal outer shape is a compromise achieved by cutting off the corners of square plates in manufacture. A cross-sectional view is shown in Fig. 6-2.

The magnet is constructed of ½-in. hot-rolled soft iron plate, with paper insulation between laminations to limit eddy currents. Calculations of the effect of eddy currents on field uniformity in the gap showed that ½-in. plate was satisfactory for the chosen rate of rise of field (averaging 14 kilogauss per second during the pulse). The laminations are stacked into bundles of twelve (about 6 in. thick), weighing about 6 tons each, for handling and machining. Each bundle is formed into a solid unit by straps welded across the outer edges of the plates. It should be noted that essentially no magnetic flux crosses these external welds, and, therefore, they do not increase eddy currents significantly. After assembly and welding of the individual bundles, the pole faces were machined to the precise dimensions determined by model tests to produce an n-value of 0.6 across the gap.

On delivery each of the 288 magnet units was put through an exhaustive magnetic test program, to determine the n-value, the location of the magnetic median plane, the remanent field, etc. A careful sorting and balancing procedure was used to assign a sequential order around the orbit, based on cancelling the extreme deviations and obtaining the most fine-grained distribution possible in the inhomogeneities. It is estimated that this procedure reduced the effect of the inhomogeneities on oscillation amplitudes by a factor of 3 below that which would have occurred with random stacking.

The excitation windings for the magnet are located as close to the magnet gap as possible. One coil is located in the slot of the C-magnet, and a divided return coil is placed above and below the gap around the outside of the iron. In principle a single slot winding would be sufficient to produce the desired field in the iron. However, such a single coil would produce large external fields in the air outside and inside the iron ring, which would increase the stored energy. The return windings serve the purpose of confining the magnetic field closely to the gap between poles and within the iron magnetic circuit.

Each quadrant is wound separately, with a total of 48 turns. The four quadrants are powered in series to obtain identical currents. The conductors are heavy copper bars, formed with an internal channel through which water is circulated for cooling. Each bar of quadrant length (about 50 ft) has water connections at each end. The water cooling for the 96 bars of each quadrant is supplied in parallel from water manifolds, through lengths of plastic hose to provide insulation. The water is pumped through a heat exchanger and a purifier system to maintain low electrical conductivity, with a flow sufficient to restrict temperature rise in the water to less than 10°F.

Dimensions of the conductors in the slot winding are made as small as practical, in order to fit within the narrow slot. The return windings located outside the magnet do not have as severe space limitations and are made 50% larger.

End connections joining the slot winding and the return

windings are also water-cooled, formed with silver-brazed right-angle joints at the corners. Heavy clamps are used to hold the conductors from shifting due to magnetic forces, and stiff springs between layers in the end connections allow takeup for expansion due to heating.

The power supply for the magnet provides a pulsed current rising approximately linearly with time for 1 sec, then dropping to zero as rapidly as possible. This cycle is repeated at 5-sec intervals. At 14 kilogauss in the magnet gap, the total stored energy in the magnet is 1.2×10^7 joules, while the heat dissipated per cycle is about one-fifth this amount. A method is required which will re-use the stored energy. The technique chosen is to use a motor-flywheel-generator-rectifier system, in which energy is stored in the flywheel to provide power during the pulse, and excess magnetic energy is returned to the flywheel between pulses. The ac generator and ignitron rectifier bank are rated for the peak kva load required for the pulse. This requires a nominal rating of 20,000 kva for the generator. The flywheel is designed to store about 10 times the energy required per pulse, so that its speed is reduced by 5% at the peak of the cycle. The motor will bring the speed back to the original value in the interval between power cycles, making up the energy dissipated in heat. It is rated for the average power demand. In operation, the bank of 24 ignitrons in a 12-phase circuit have their grids controlled to rectify the generator output and apply it to the magnet during the 1-sec acceleration interval. The ignitrons are then switched to inverter action to return the stored energy in the magnet (less heat losses) to the alternator-flywheel during the following second.

Choice of voltage output for the generator fixes the number of turns in the magnet winding. Manufacturers advised a rating of about 6000 volts for a generator of this rating, which will drop by 25% under full load. Number of turns can be derived from the relation:

$$V = N \frac{dI}{dt} + N^2 R_1 I \qquad (6\text{-}3)$$

where R_1 is the resistance of a 1-turn winding, and I is the current in this 1-turn. The total magnetic flux (including the stray field) and the rate of rise with time were determined from magnet model tests. Coil dimensions determine the resistance of the coil, and the ampere turns required were obtained from the model studies. The number of turns required for the cosmotron was found to be $N = 48$ turns.

The excitation to produce 14,000 gauss in the magnet gap was found to be given by $NI = 3.36 \times 10^5$ ampere turns. The peak current in the 48-turn coil is $I = 7000$ amp. Resistance of the coil proves to be $R = 0.14$ ohm, and the inductance varies during the cycle (due to the variation in permeability of iron) from 0.47 henry at the start, to a maximum of 0.80 henry at 1000 gauss, and to a final value of about 0.25 henry. The time constant of this inductive circuit is of the order of magnitude of 4 sec. However, the actual magnetic field rise is nolinear, starting at 16.5 kg/sec and falling to 9.8 kg/sec at 1 sec. The time cycle for voltage and current shown in Fig. 6-3 is computed

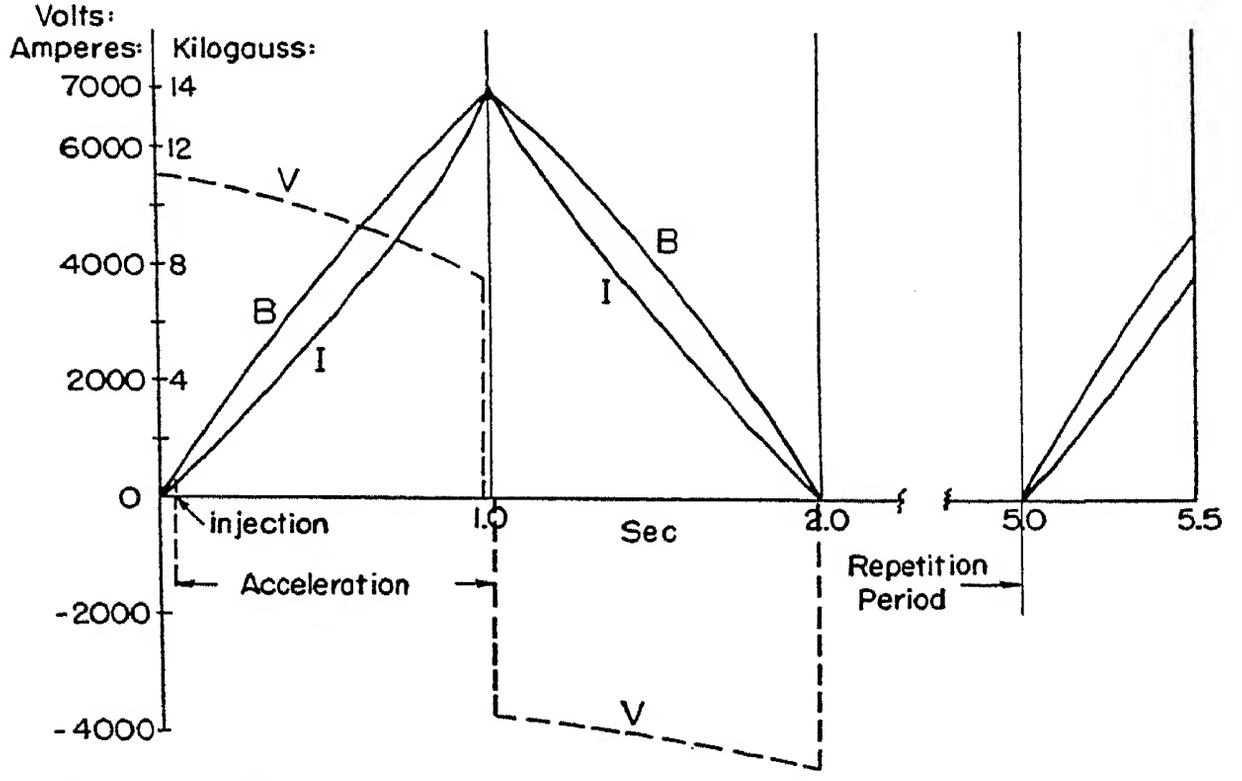

FIG. 6-3. Time cycle of magnet voltage and current and of the magnetic field at the orbit.

from the magnet properties. The rate of change of magnetic field dB/dt determines the necessary volts per turn for acceleration, which is shown in Fig. 6-4 as a function of time during the accelerating interval. Also shown in Fig. 6-4 is the frequency-time cycle obtained from the magnetic field.

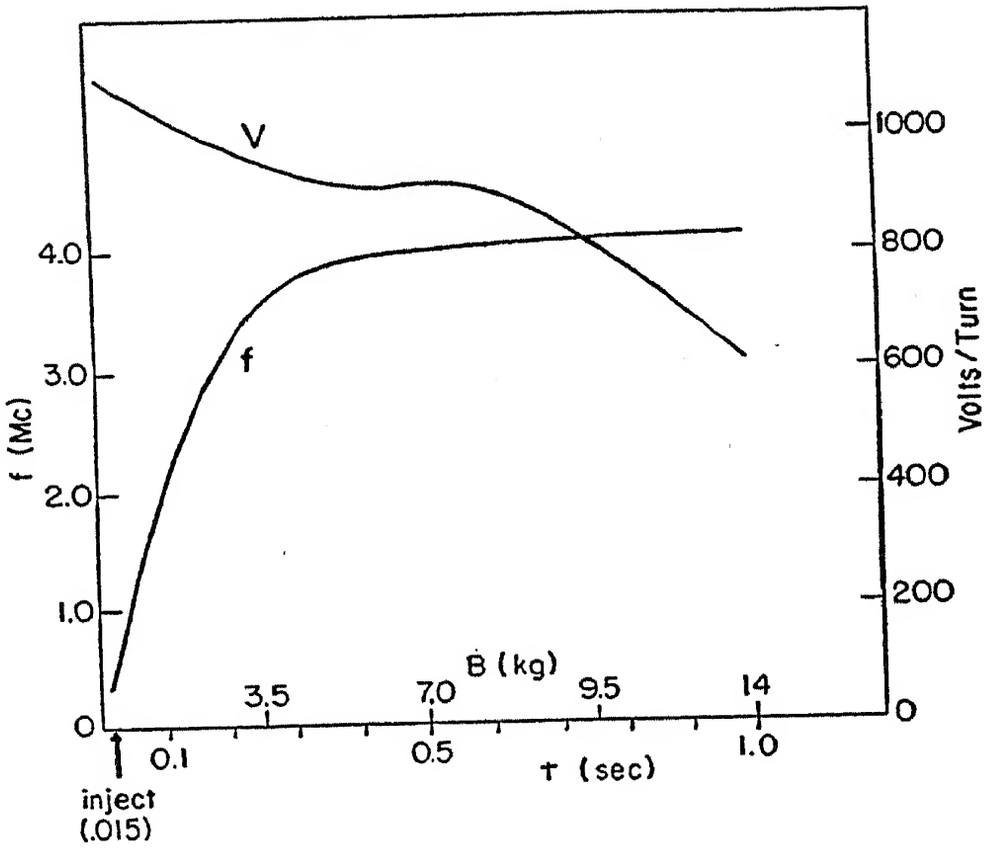

FIG. 6-4. Ion rotation frequency and accelerating voltage per turn required during acceleration.

6.5 Radiofrequency Accelerator

The average energy increment required to maintain resonance is about 1000 ev per turn. About twice this value is provided to allow phase oscillations to swing through their full range of stability. The accelerating potential is applied across a gap formed by a short insulating section. The requirements are, then, a rf voltage synchronized with the ion rotation frequency which starts at about 2400 volts peak at 0.35 Mc and extends to about 1400 volts peak at 4.20 Mc following the frequency and amplitude schedules shown in Fig. 6-4.

These accelerating potentials are modest as compared

with those used in cyclotrons or other resonance accelerators. But the wide range of frequency variation, by a factor of 1:12, and the requirement of following accurately a predetermined schedule, are unique features.

The accelerating system for the cosmotron is essentially a rf transformer. A ferromagnetic core surrounds the particle orbit at one of the straight sections. The core material is a ferrite chosen to have a useful magnetic permeability at frequencies up to the maximum of 4.2 Mc. Power is fed to a one-turn primary winding from a broad-band rf amplifier driven by an oscillator which is tuned over the frequency cycle. The particle orbits can be vizualized as one-turn secondary windings linking the transformer core. Each time a particle traverses the core, it experiences an electromotive force equivalent to that which would obtain in a one-turn secondary winding of the transformer.

Another description of the accelerating system is that it is an induction accelerator, depending on the time rate of change of flux linking the particle orbit, as in the betatron. During most of its path the proton is within a grounded metal vacuum chamber. Only while it is traversing the insulating gap at the location of the flux core can it experience the electromotive force. The time rate of change of flux within the magnetic core linking the orbit at the instant the particle is crossing the gap determines the electromotive force and so the energy acquired by the particle. In this sense the ferromagnetic core linking the orbit is equivalent to the flux core in a betatron. The distinction is that protons in a cosmotron experience individual accelerations, once each time they cross the gap, whereas in the betatron the induced electromotive force is maintained steadily around the entire orbit.

A third way of describing the properties of the rf accelerator is that it is equivalent to a cavity resonator heavily loaded with material of high magnetic permeability and high dielectric constant. The cavity is the copper shield around the core, and the potential is developed across the insulated gap in

the vacuum chamber. If it were air filled, this cavity would be resonant at too high a frequency because of its small dimensions. If loaded with low-loss, high-dielectric material, as for the quarter-wave resonators used with electron synchrotrons, the resonant frequency would be lower, but the impedance would also be low at resonance. But when loaded with ferromagnetic material, the resonant frequency is reduced to a value smaller than the orbital frequency. The cavity is broadly resonant and has sufficiently high impedance that it can be driven at frequencies far off its resonance.

The core material is a ferromagnetic ferrite, which is a semiconductor with conductivity about 10^{-7} that for metals, so eddy current limitations are extended to much higher frequencies. The relative magnetic permeability of this material is in the range between 500 and 100 over the frequency band used. It is available under trade names such as Ferroxcube (North American Philips Co.) and Ferramic (General Ceramics and Steatite Corp.). A variety of types are produced, with widely varying properties, and for many different applications. The electrical and magnetic properties of such ferrites are described by publications of the Philips Laboratories, and the particular application to the cosmotron is discussed by Blewett, Plotkin, and Blewitt of the Brookhaven staff in the published report.[36]

Several thousand pounds of ferrite were used to construct the core, arranged in many picture frame units separated and insulated to limit eddy currents and to prevent standing-wave modes in the cavity. Each frame was assembled from bars (or rods) with ground surfaces cemented together to minimize air gaps in the magnetic circuit.

The scheduled frequency cycle is derived from the magnetic cycle and depends on the performance of the full-scale magnet under operating conditions. The variable frequency signal is generated by an electronically tuned oscillator in which the tuning is accomplished by varying the saturation, and hence the inductance, of a small ferromagnetic core in the oscillator

circuit. This saturable inductance is a toroid having two windings, a dc winding threading the toroid to produce the saturating flux in the core and a rf winding threaded through a hole cut in the side of the toroid with a figure-eight winding in which the dc flux cancels out.

A diode network with twenty paralleling R-C circuits of different time constants, each controllable with dial-operated resistors, is used to produce a signal having the proper current versus time function. This output current is used to saturate the core. By tuning the time constants and amplitudes of these paralleling diode circuits, a time cycle can be produced which is within 0.1 % of the calculated frequency cycle over the full 1-sec interval. Furthermore, the controls can be used to trim the shape of the cycle at will.

The frequency cycle must be triggered to start at the proper time and on the proper frequency to match the resonant frequency of the ions at injection. The timing signal is obtained by an integrating coil in the magnetic field, which accumulates charge on a capacitor, and is used to trigger a biased thyratron, calibrated to initiate a pulse at the desired magnetic field.

The variable frequency signal is used to drive a broadband power amplifier, with three stages of voltage amplification and one power stage, in which two 50-kw power tubes are used in push-pull. This amplifier represents possibly the highest power system yet built for such a wide bandwidth, and many unusual problems were met and solved in the development.

6.6 Vacuum Chamber

The vacuum chamber is formed of four quadrants fitting between magnet pole faces, joined by four connecting straight sections. Each quadrant is a framework of nonmagnetic stainless steel laminations, with large thin sheets of Myvaseal plastic to form the vacuum wall. The structure is assembled on two 1-in. by 8-in. bars, bent to the curvature of the quadrant

which form the inner and outer faces of the chamber. Bridged across the 36-in. chamber width are several hundred flat steel bars $\frac{5}{8}$-in. thick and 2 in. wide, separated by gaps about $\frac{1}{32}$ in. wide, to form the top and bottom surfaces of the box. The 2-in. wide bars are laminations to limit eddy currents in the surface. Each bar is attached by an insulated pin at either end. The $\frac{1}{8}$-in. thick plastic sheet covering top and bottom surfaces is sealed against gaskets by clamp bars to provide the vacuum seal. The structure is economically designed to use the minimum steel section and results in an internal clearance between bars under vacuum of 6 in. Figure 6-5 is a sketch of the vacuum chamber showing its construction.

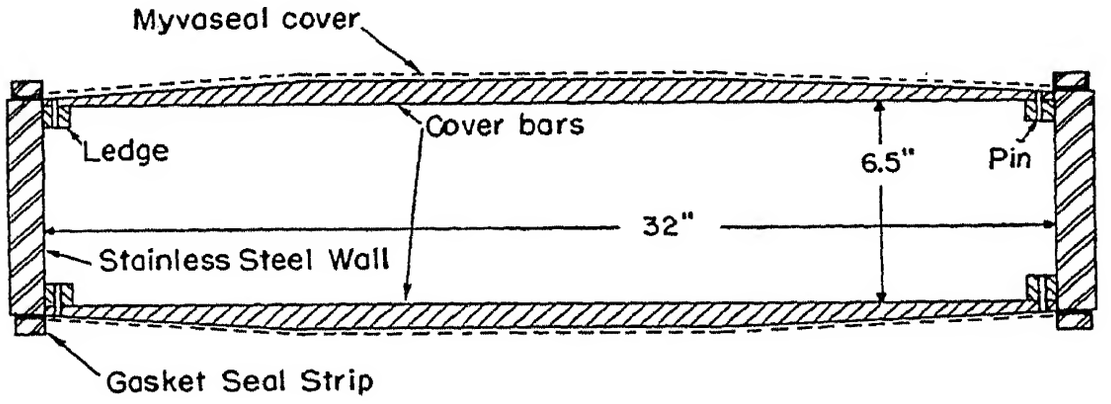

FIG. 6-5. Cross section of the cosmotron vacuum chamber.

The vacuum chamber boxes in the straight sections are joined to the ends of the quadrant chambers by large flexible nonmagnetic stainless steel bellows and have flap valves installed to allow sections of the chamber to be isolated for vacuum testing. Many large ports and cover plates allow for the insertion of electrodes, targets, or other devices. One straight section box is of small cross section, with an insulating gap in the steel wall, used with the rf accelerator. Another is specially shaped on the outer faces to install the inflection plates.

The pumping system consists of twelve identical high-vacuum pump stations, distributed around the chamber with three on each quadrant. Each station has a large manifold connecting to the chamber, a refrigerated baffle, a 20-in. silicone-

oil diffusion pump, a high-vacuum close-off valve, a booster pump, and all necessary valves and gauges. Four centrally located mechanical pumps supply the rough backing vacuum for the twelve diffusion pumps, with welded fore-vacuum lines distributed to the stations.

Pump station units are interchangeable, and several spare units are maintained for replacement. The close-off valves allow a pump unit to be replaced without losing vacuum in the main chamber. The valves are pneumatically operated and are controlled electronically by overload gauges so that a pump can be closed off automatically if a leak develops or vacuum is lost overnight. The cosmotron can operate satisfactorily with several pumps removed, if need be.

Vacuum plumbing is a major problem in all accelerators. In a chamber as large as the cosmotron, many safety devices and interlocks are required. All joints which have gasket seals are arranged with a double seal so helium can be circulated between gaskets to detect leaks (with a helium leak detector on the pump output line), or a rough vacuum pump can be installed to control a leak until a maintenance shutdown is desirable. Alarm type gauges are located at each pump station, and operate pilot lamps at the control panel so the operator can check the vacuum system at a glance.

Scattering by the residual gas in the vacuum chamber will result in some loss of ions from the beam. A theoretical study by Blachman and Courant[36] predicted that the loss in intensity during the early part of the cycle (maximum loss occurring at about 10 Mev) would be adequately small for a chamber pressure of 1×10^{-5} mm Hg. Measurements during early operation showed the loss to be negligible even at pressures of 2×10^{-5}. As a consequence of this tolerance to gas pressure, the vacuum problems in the cosmotron have been less troublesome than expected.

6.7 Target Arrangements and Shielding

Beam intensity in the cosmotron has exceeded expectations. With 1 ma of protons injected over an effective accept-

ance time interval of about 30 microseconds, the number of protons available for acceleration is about 2×10^{11} protons per pulse. The phase acceptance angle of π radians allows about half of these to be bunched into stable synchronous orbits, or 1×10^{11} protons per pulse. The high-energy beam intensity has risen steadily since the initial operation from about 5×10^{8} to a present value of 1×10^{10} protons per pulse. This means that 10% of the available ions are retained and accelerated at high energy. At the present top energy of 3.0 Bev this represents a time-average power in the beam of one watt.

The high-energy beam can be diverted radially to strike a target in several ways. If the rf oscillator is turned off before the magnetic field reaches its peak, the particle will spiral inward at the rate of about 0.002 in. per turn or per 0.25 microsecond; so the beam will move radially inward by 1 in. in about 0.12 millisecond. Or, a modulation of applied frequency can be used to shift the stable phase angle. This can increase the volts per turn, and the beam will spiral outward toward a target. Since the maximum rate of increase is about twice the average value, the beam can be moved outward at the same rate given above.

For some experiments it is desirable to slow down the rate of cleanup of the beam against a target as much as possible. This can be accomplished by a small change in the applied frequency. The longest output pulse obtained to date is about 50 msec, representing 200,000 revolutions. An electronic particle detector, such as a telescope of two or more scintillation crystals with photomultiplier tubes, can be made to have a time resolution of better than 0.25 microseconds, and therefore can resolve the individual pulses, if the coincidence counting and data storage systems can handle this rate.

In other experiments extremely short beam pulses are desirable, such as those utilizing time-of-flight techniques to observe very short lifetime processes. The shortest pulse possible by the method of contracting the beam against a target is about 0.1 msec.

Targets can be located permanently a few inches from

the inner chamber wall. A small fraction of the beam may be lost against such targets during injection. At high energy the beam can be contracted to strike the target. The grazing incidence associated with the small contraction per turn means that each target is essentially a thin target, since it cannot be aligned with sufficient precision to have the beam miss on one turn and be completely within the target on the next turn. Small angle scattering in a thin foil extending beyond the face of the target results in free oscillations which produce a diffuse spot of several inches diameter at the target on the next impact. In this sense a thick target becomes effectively so on the second turn, for a fraction of the beam.

A wire target has been used successfully without expanding or contracting the beam. This wire is mounted on a shaft above beam level which can be quickly rotated to turn the wire down into the center of the chamber. The beam is diffuse, about 2 in. across, and only a small fraction of the ions strike the wire in any one turn. When they do, the cross section for scattering is small, and the ions continue to be accelerated, ultimately striking the wire many times. In this way the small wire will eventually cleanup the entire beam. The efficiency is estimated as 10 %

Ram-in targets have been developed, which can be thrust into position well inside either the inner or outer wall of the chamber in a very short time, using pneumatic cylinders. The beam can then be contracted or expanded to hit the target.

Regardless of the type of target used, a large fraction of the beam is scattered by sufficiently large angles to be thrown out against the chamber walls during the following turn. The resulting spray of radiation flies off the orbit tangentially, forming a narrow band on the horizontal plane, where it impinges against the shield or the walls of the room. The target area shows the highest intensity, but about half the radiation appears to be distributed around the rest of the orbit.

The basic shield designed for the cosmotron is a stack of large concrete blocks of 8-ft radial thickness forming an arc of

about 120° around the machine centered on the target location and interposed between it and the control and observation areas. Four layers of blocks, each weighing 8 tons, form a shield 9 ft high, with the top layer overhanging the stack to form a sort of tunnel between the magnet and the shield. A layer of 6-in. bricks is located between the two central layers of blocks, on the horizontal plane of the beam. Channels can be formed between bricks to transmit beams of radiation through the shield where desired. The attenuation of concrete for this high-energy radiation is measured to be a factor of 10 for each 3.6 ft. The total attenuation factor for the 12-ft tangential thickness of the shield is about 4×10^{-4}.

Scattered radiation of much lower energy than the primary beam from the target comes from degradation and back scattering. Only a rough estimate of its intensity was possible in advance, and no shielding was designed specifically for this component. As a consequence of the high beam intensity obtained, the scattered radiation was somewhat excessive in the areas adjacent to the targets. Additional overhead shielding of 2-ft concrete beams spanning the target straight section has reduced the scattered intensity to acceptable levels.

Electronic detection systems have specialized in the use of crystal scintillation counters, arranged in telescopes, with coincidence pulses to detect the charged particle products of reactions. With these instruments π-meson interactions have been studied from 200-Mev to 1.5-Bev meson energy, and for both positive and negative π-mesons.

Fast neutrons emerge tangentially with energies up to the maximum proton energy. Also, many low-energy neutrons are observed, in the energy range around 0.5 Bev, probably the products of star formation.

Meson intensity is about 10 per square centimeter per pulse outside the 8-ft concrete shield, adequate to analyze into energy bands of about 100-Mev width for the study of meson processes as a function of energy. Both positive and negative mesons are available in the direct beams from a target (at a

minimum angle of 30° to the beam). Negative mesons at more forward angles are analyzed and deflected outward by the cosmotron magnetic field to provide a spectrum of energies. One of the impressive features of the cosmotron is the set of meson channels in the shield labeled "300 Mev," "500 Mev," "1.0 Bev," available for meson experiments.

CHAPTER 7

Alternating Gradient Focusing

7.1 The Stability Principle

The magnetic fields used to guide particles in existing accelerators are arranged to provide focusing forces by using a small radial decrease in field, as described in earlier chapters. The exponent defining the radial gradient is in the range $0 < n < 1$, and the resultant focusing in the vertical and radial coordinates is weak, as illustrated by free oscillation wavelengths which are in all cases longer than the circumferential length of the orbit. This is the maximum amount of magnetic focusing possible with fields in which the magnetic gradient is uniform in azimuth.

A new principle of alternating gradient (or strong) focusing was discovered in the summer of 1952 at the Brookhaven National Laboratory by Courant, Livingston, and Snyder.[38]

About six months after the original article was submitted to the *Physical Review* for publication, it was called to our attention that Mr. Nicholas Christofilos, an electrical engineer from Athens, had made a study of resonance accelerators which included the alternating gradient principle. His privately printed report "Focusing System for Ions and Electrons and Application in Magnetic Resonance Particle Accelerators" is dated 1950. It is clear that Mr. Christofilos deserves credit for the earliest enunciation of the principle. It is also true that the work reported in reference 38 was independent.

Strong focusing involves the use of very much larger radial gradients in the field, of which n is of the order of hundreds or thousands instead of less than unity. These strong gradient sectors are alternated so as to be directed radially inward and radi-

ally outward in succession around the orbit. Qualitatively, each is a magnetic lens which is converging in one transverse coordinate and diverging in the other. The continuous sequence of alternately positive and negative lenses, for both coordinates, results in convergence for both radial and vertical displacements. Particles perform oscillations about the equilibrium orbit of much higher frequency and much smaller amplitude than in a field of smaller, uniform n-value. The vacuum chamber can be much smaller, and the dimensions of the magnet to produce the field are reduced to about one-fifth or one-tenth. The volume and stored energy of the field are also reduced by large factors. So the cost per unit length of the magnet to provide the guide field and the cost of its power supply are greatly reduced. Magnets of much larger orbit radius, capable of accelerating particles to much higher energy, become economically feasible.

The discovery of alternating gradient focusing was precipitated by a proposal by Livingston that, in higher-energy machines of the cosmotron type, the C-shaped magnets should be placed around the particle orbit facing alternately inside and outside. By this means, effects of back leg saturation and fringing on the shape of the field in the magnet gap could be made to average out, with a resultant larger and more usable magnetic aperture. However, to correct extreme variations in fringing field and saturation effects, which involve positive n-values for the sectors facing outward, the inward-facing sectors would need to have negative values of n. Before such an arrangement could be utilized, it was necessary to determine the effects of alternately positive and negative n-values on orbit stability. A preliminary theoretical analysis by Courant led to the (then) surprising result that the stability of free oscillations was much improved by such alternating gradients. Furthermore, Snyder soon pointed out that this was an example of a more general principle—that of the dynamic stability derived from rapidly alternating forces in many mechanical, optical, and electrical systems.

An understanding of this general stability principle can be obtained by considering first some of the simpler mechanical and optical applications. For example, an inverted pendulum is obviously unstable under static forces. It will fall over to one side with an infinitesimal displacement from the vertical. However, if the base of the pendulum is oscillated rapidly up and down through a short stroke, the pendulum becomes stable in the vertical position for several bands of oscillation frequencies above a minimum or threshold frequency. A theoretical analysis of the motion of such an inverted pendulum is given by Jaeger.[39] The result is given in the form of the Mathieu equation as:

$$\frac{d^2\theta}{dt^2} \pm \left[\left(\frac{g}{l}\right)^2 \pm \frac{a\omega^2}{l} \cos \omega t\right] \theta = 0 \qquad (7\text{-}1)$$

where g/l is the ratio of the acceleration of gravity to the length, a/l is the ratio of oscillation amplitude to length, ω is the angular frequency and θ is the angular displacement. The plus and minus signs represent the upward and downward direction of motion of the oscillating base. Solutions to the Mathieu functions show bands of stability in ω separated by narrow unstable regions.

Another mechanical system which is frequently used as a model to illustrate the stability principle is the alternating trough. It is clear that a ball will roll along a concave-upward trough, and that any deviations in direction will be corrected. It is equally clear that a ball will roll off the side of an inverted or convex trough. In the intermediate case of a flat plane the result depends solely on the precision of aiming. The alternating trough is formed of successive, equal-length sections of concave and convex trough, with the centerlines of all sections at the same level and forming a straight line, and with smoothly molded transition sections between. For a given geometry (radius of curvature of the trough, length of sections and separations) there will be a range of velocities within which a ball rolling along the trough will perform stable oscillations with a

limited maximum amplitude. The stability range can be demonstrated by rolling the ball from different heights down an inclined plane to give it a start at one end. The oscillations are periodic but not harmonic. The shape of the trajectory is a complicated curve which repeats itself periodically, the wave form depending on the phase of the motion relative to the trough periodicity. Even rather wide deviations in the angle of injection of the ball at the start result in paths which stay within the trough, for the correct velocity. The paths are quite similar to the orbits of a particle in an alternating gradient accelerator, if they were to be unrolled into a straight line.

This same type of stability is illustrated in lens optics. Consider the well-known equation for computing the overall focal length F of two thin lenses of individual focal lengths, f_1 and f_2, which are separated by a distance t:

$$\frac{1}{F} = \frac{1}{f_1} + \frac{1}{f_2} - \frac{t}{f_1 f_2} \tag{7-2}$$

If we take focal lengths of equal magnitude, but with one converging and one diverging, we have $f_2 = -f_1$, and we find:

$$F = |f|^2/t \tag{7-2a}$$

The combined focal length is positive (converging) for such a pair of lenses. A similar result is obtained if the lenses are thick when the spacing between them is suitably defined as the distance between principal planes. It can be shown, furthermore, that a continuous sequence of positive and negative lenses of equal focal length will be converging, since it is the equivalent of a sequence of convergent pairs. This sequence will be convergent if the separation between focal planes of successive lenses d is in the range $-2F < d < 2F$. A modification of this principle is used in the design of periscopes.

Still more information can be obtained from the optical analogy. With a sequence of alternately positive and negative optical lenses the rays traverse the converging units at the greatest distance from the axis. This is often phrased in optics

by the statement that the positive lens is the aperture stop. The angular deviation of a ray in traversing a lens is proportional to the distance from the axis. So the deviation in the convergent components will exceed that in the divergent ones. This argument leads to the general conclusion that an alternating sequence will be convergent for spacings in which the ray being considered does not cross the axis.

7.2 The A-G Magnetic Lens

We now return to the problem of magnetic focusing. A single region of inhomogeneous magnetic field which produces convergence of an ion beam in one plane will cause divergence in the plane at right angles. In other words, a field which has a field gradient, dB_y/dz in one plane has a gradient, dB_z/dy in the same plane which is directed normal to the first. The direction of this associated gradient is such as to produce a focusing effect opposite in sense to that of the first field.

For our purpose, and in order to analyze the effects most simply, it is helpful to assume that the two transverse gradients are equal in magnitude: $dB_y/dz = dB_z/dy = k$. This situation exists in a field for which the components are given by $B_x = 0$ (particle direction along the x-axis), $B_y = kz$, and $B_z = ky$. Such a field can be obtained by shaping the pole faces as rectangular hyperbolas, illustrated in Fig. 7-1; the four symmetrical poles are arranged to be alternately N and S poles. To the extent that the pole faces remain magnetic equipotentials, the field gradients are of equal magnitude and are uniform throughout the entire volume between poles. The field is zero along the x-axis in such a 4-pole magnet and has opposite directions on either side of the center point. It is clear that, in one transverse coordinate, deviant particles will be focused about the x-axis. Straightforward application of the vector rule for direction of the force on a moving charged particle in this field will show that particles will be defocused in the other transverse coordinate.

A single, short section of field between poles of a 4-pole

magnet of length l will act as a convergent lens in one plane, with a focal length f measured from a principal plane located at a distance x_p inside the physical boundary of the field. The lens will be divergent in the other transverse plane, with the same focal length (but negative) measured from an equivalent principal plane. To maintain the optical analogy, it is useful to express these distances in terms of the magnetic properties of the field and the properties of the beam of particles.

The equations of motion in the transverse coordinates are given by:

$$\frac{d^2y}{dx^2} + \frac{1}{BR}\frac{dB_z}{dy}\,y = 0 \quad \text{or} \quad \frac{d^2y}{dx^2} + Ky = 0 \qquad (7\text{-}3a)$$

$$\frac{d^2z}{dx^2} - \frac{1}{BR}\frac{dB_y}{dz}\,z = 0 \quad \text{or} \quad \frac{d^2z}{dx^2} - Kz = 0 \qquad (7\text{-}3b)$$

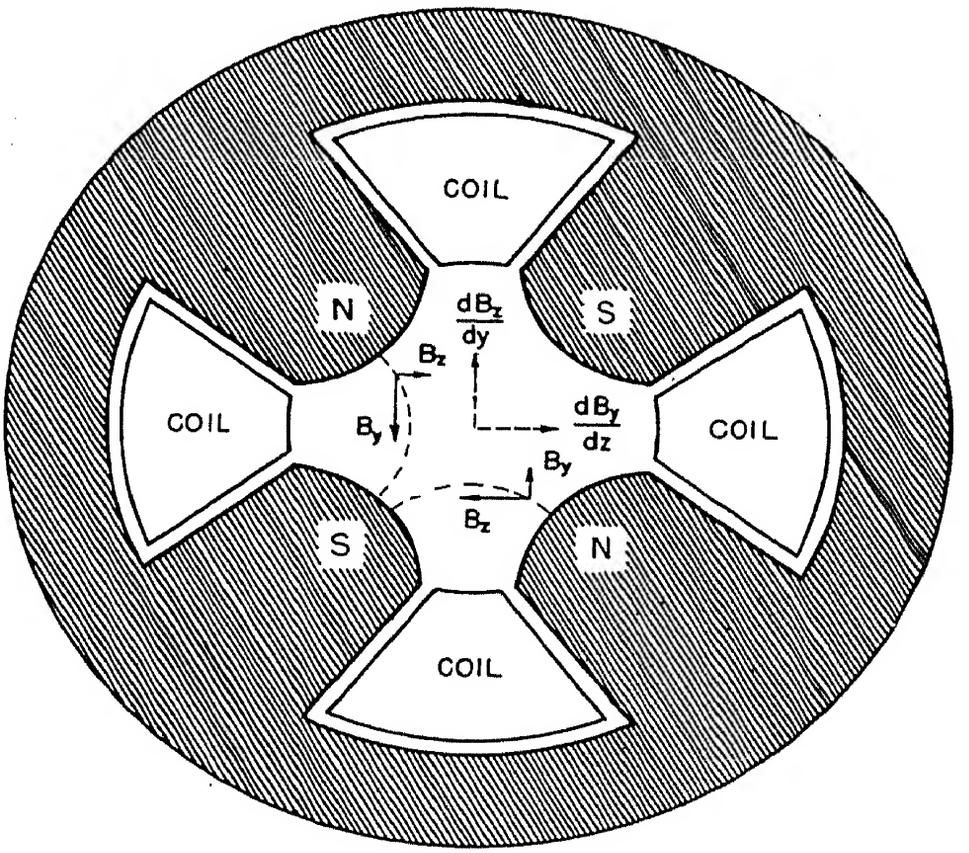

FIG. 7-1. Four-pole magnet providing uniform magnetic gradients in both transverse coordinates. The pole faces are shaped to a rectangular hyperbola.

The constant, $K = (1/BR)(dB_z/dy)$, can be expressed in words as the field gradient divided by the momentum per unit charge, since $mv/e = BR$ for a particle moving in a circular orbit in a magnetic field. These equations can be solved for the trajectory of the particles to give the focal constants of the lens described above as:

$$x_p = \frac{1 - \cos K^{1/2} l}{K^{1/2} \sin K^{1/2} l} \tag{7-4}$$

$$f = \frac{1}{K^{1/2} \sin K^{1/2} l} \tag{7-5}$$

To continue the analysis, a compound lens which is convergent in both transverse planes can be formed of two units in sequence, with the second rotated 90° relative to the first. We use K_1 and K_2 for the lens constants and l_1 and l_2 for the lengths of the two units, with a physical spacing d between them. Inserting the values above in Eq. 7-2, we find the overall focal length of the pair of units to be given by:

$$\frac{1}{F} = K_1^{1/2} \sin K_1^{1/2} l_1 \cos K_2^{1/2} l_2 + K_2^{1/2} \sin K_2^{1/2} l_2 \cos K_1^{1/2} l_1 - d K_1^{1/2} K_2^{1/2} \sin K_1^{1/2} l_1 \sin K_2^{1/2} l_2 \tag{7-6}$$

For a simple example we choose two identical lens units, with $K_2 = -K_1 = K$ and $l_2 = l_1 = l$. In this case the equation for focal length reduces to:

$$\frac{1}{F} = K^{1/2} (\sin K^{1/2} l \cosh K^{1/2} l - \sinh K^{1/2} l \cos K^{1/2} l + d K^{1/2} \sin K^{1/2} l \sinh K^{1/2} l) \tag{7-7}$$

The condition that the lens system be convergent is that the argument $K^{1/2} l$ be positive and not greater than some value approaching π, depending on the magnitude of the separation distance d. Thus, the lens can be designed for any desired focal length by suitable choice of $K^{1/2} l$ and d. In this simple case

where K's and l's are equal, the focal lengths are equal for displacements in both the xy and xz planes, as becomes evident when $-K$ is substituted for K in Eq. 7-7. However, the locations of the principal planes will differ, depending on whether the initial action is converging or diverging. This leads to an astigmatic image in the simple case assumed. The astigmatism can be corrected, and the two focal planes superimposed, by slight modification of the parameters, such as making $l_2 < l_1$ or by operating with a K_2 slightly smaller in magnitude than K_1, which can be obtained by decreasing the flux density and hence the field gradient in the second unit. The double focusing of the compensating lenses is illustrated in Fig. 7-2, showing alternatively divergent and convergent forces in the two sections.

A lens to serve the above purpose can be built of two 4-pole magnets units with hyperbolic pole faces. The spacing between units can be reduced to that necessary to accommodate the magnet windings. The effective aperture of such a lens is a circle of diameter $D = \sqrt{2}a$, where a is the spacing between centers of the hyperbolic poles.

A simpler relation for computing focal lengths can be obtained from Eq. 7-7 by expanding in terms of the arguments and

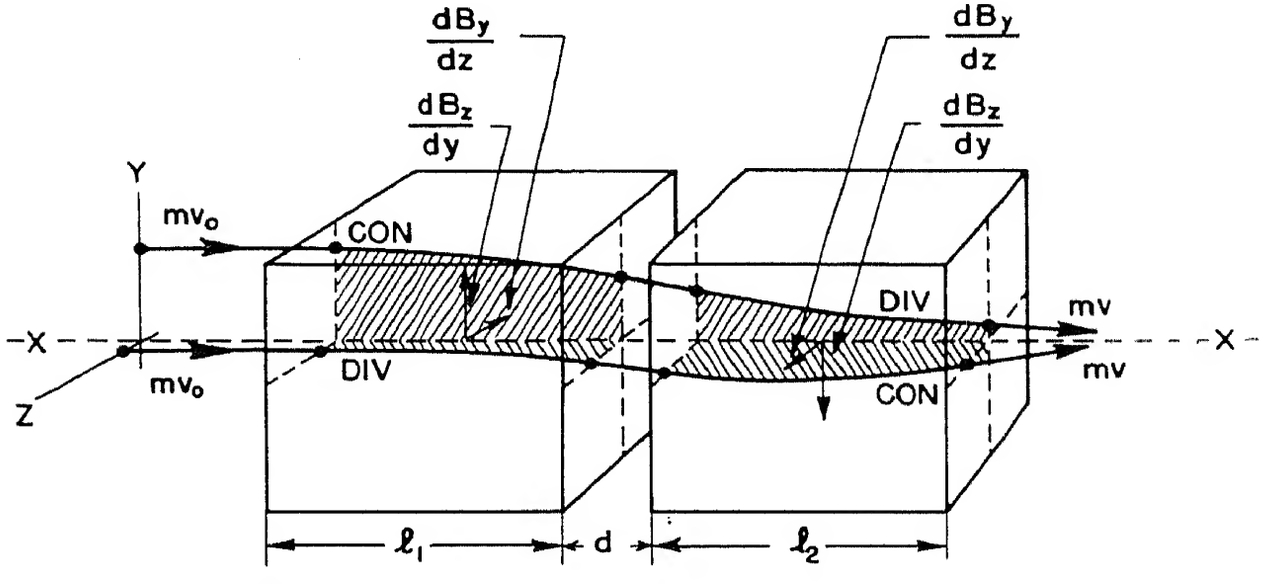

FIG. 7-2. Double focusing by a pair of matched magnetic lenses, in which the sense of the magnetic gradients is reversed.

using only the first significant terms:

$$\frac{1}{F} = K^2 l^2[(2/3)l + d] \tag{7-8}$$

As a numerical example, let us design a lens to focus protons of 4-Mev energy, which have a momentum BR of about 10^5 gauss-inches, with a magnet in which the aperture a is 2 in. and the maximum field across this 2-in. gap is 10 kilogauss. The field gradient $dB/dy = dB/dz = 10^4$ gauss/inch. So the constant $K = 0.1$. If we choose $K^{1/2}l = \pi/4$ and a spacing d of 2 in., the length of each magnet unit l is 2.5 in., the total length is 7 in., and the focal length computed from Eq. 7-8 is 4.4 in. Choice of a smaller value of $K^{1/2}l$ will lead to shorter magnets and longer focal lengths. The focal spot can be made anastigmatic by varying the exciting current in one of the units relative to the other. Longer focal lengths can be obtained by reducing the current in both windings. The astigmatic property of the lens can be utilized in special cases such as focusing the emergent beam from a cyclotron, which usually is narrow in the vertical direction and broad radially, and is itself astigmatic, to obtain a point focus.

Electric fields can also be used to produce the alternating gradients, as was pointed out by Blewett[26] in a companion paper. Uniform and equal electric field gradients can be produced between four electrodes which are sections of a rectangular hyperbola, in which the electrodes are connected alternately to potentials of V and $-V$. The electric field between electrodes has the same pattern as the magnetic field in the 4-pole magnet, and the forces on a moving charged particle lead to convergence in a plane at 45° to the hyperbolic axes and divergence in the perpendicular plane. Let the gradients be given by $dE_z/dy = dE_y/dz$, and let the velocity of the particle (in the x-direction) be v. The properties of the lens will be given by substituting $(1/v)\, dE/dy$ for dB/dy and $(1/v)\, dE/dz$ for dB/dz in the magnetic lens formulas. The momentum per unit charge (BR in

the magnetic case) is given in terms of the kinetic energy T and rest energy E_0, as:

$$mv/e = T(T + 2E_0)^{1/2}/ce \tag{7-9}$$

A handy rule-of-thumb in the mks system of units is that the numerical magnitude of electric field gradient must be 300 times larger than that of the magnetic field gradient to produce the same focal properties.

Some of the most useful applications of the alternating gradient focusing principle are in the use of such two-unit lenses to focus beams of particles in the laboratory. A simple demonstration can be arranged with a cathode ray tube by mounting two sets of 4-pole coils on the neck of the tube (with or without iron cores) and adjusting currents and coil orientations to produce a point focus on the screen.

7.3 The A-G Synchrotron

A sequence of alternately converging and diverging magnetic lenses of equal strength, properly spaced around an orbit, can be arranged to provide strong restoring forces for displacements in position or angle within the orbit. This strong focusing leads to free oscillations of higher frequency, shorter wavelength, and smaller amplitude than for a synchrotron with uniform field gradient. Synchrotron oscillation amplitudes for a given momentum displacement are also reduced, which allows the use of much smaller size vacuum chambers and of smaller and cheaper magnets to produce the guide field.

The magnitude of the focusing forces is directly related to the magnitude of the field index, $n = (-r/B)(dB/dr)$ which can be made very large if alternating gradients are used to produce stability. Let the circular orbit consist of N sectors of equal length with different values of field index, n_1 (positive) and n_2 (negative) in alternate sectors. The equations of vertical and radial oscillations (See Eqs. 2-18, 2-20 in Chap. 2) are

then:

$$\frac{d^2z}{d\theta^2} + n_1 z = 0; \quad \frac{d^2r}{d\theta^2} + (1 - n_1)r = 0 \quad \text{(odd sectors)} \tag{7-10a}$$

$$\frac{d^2z}{d\theta^2} + n_2 z = 0; \quad \frac{d^2r}{d\theta^2} + (1 - n_2)r = 0 \quad \text{(even sectors)} \tag{7-10b}$$

Solutions can be obtained by the use of recursion formulas, and are of the form:

$$Z_k = Ae^{i2\pi\mu_z k} \quad \text{and} \quad R_k = Be^{i2\pi\mu_r k} \tag{7-11}$$

where the coefficient μ_z is given by:

$$\cos 2\pi\mu_z = \cos \frac{2\pi {n_1}^{1/2}}{N} \cos \frac{2\pi {n_2}^{1/2}}{N} - \frac{n_1 + n_2}{2(n_1 n_2)^{1/2}} \sin \frac{2\pi {n_1}^{1/2}}{N} \sin \frac{2\pi {n_2}^{1/2}}{N} \tag{7-12}$$

The coefficient μ_r is given by the same expression, with n_1 and n_2 replaced by $(1 - n_1)$ and $(1 - n_2)$ respectively. If the motion is to be stable for both radial and vertical displacements, the limits are established by the conditions:

$$-1 < \cos 2\pi\mu_z < 1, \quad -1 < \cos 2\pi\mu_r < 1 \tag{7-13}$$

These limits have been plotted in Fig. 7-3 for very large values of the n's and of N, and the coordinates are given in terms of n_1/N^2 and n_2/N^2. The range of stable values of n is widest when N is large and when $n_2 = -n_1$, and the center of the region of stability ($\cos 2\pi\mu = 0$) occurs for:

$$|n| = N^2/16 \tag{7-14}$$

The early results[38] described above led to the hope that a broad region of stability would be available, and that the precision in magnet construction required for uniform gradient synchrotrons might be side stepped by use of this principle of strong focusing. However, further and more detailed con-

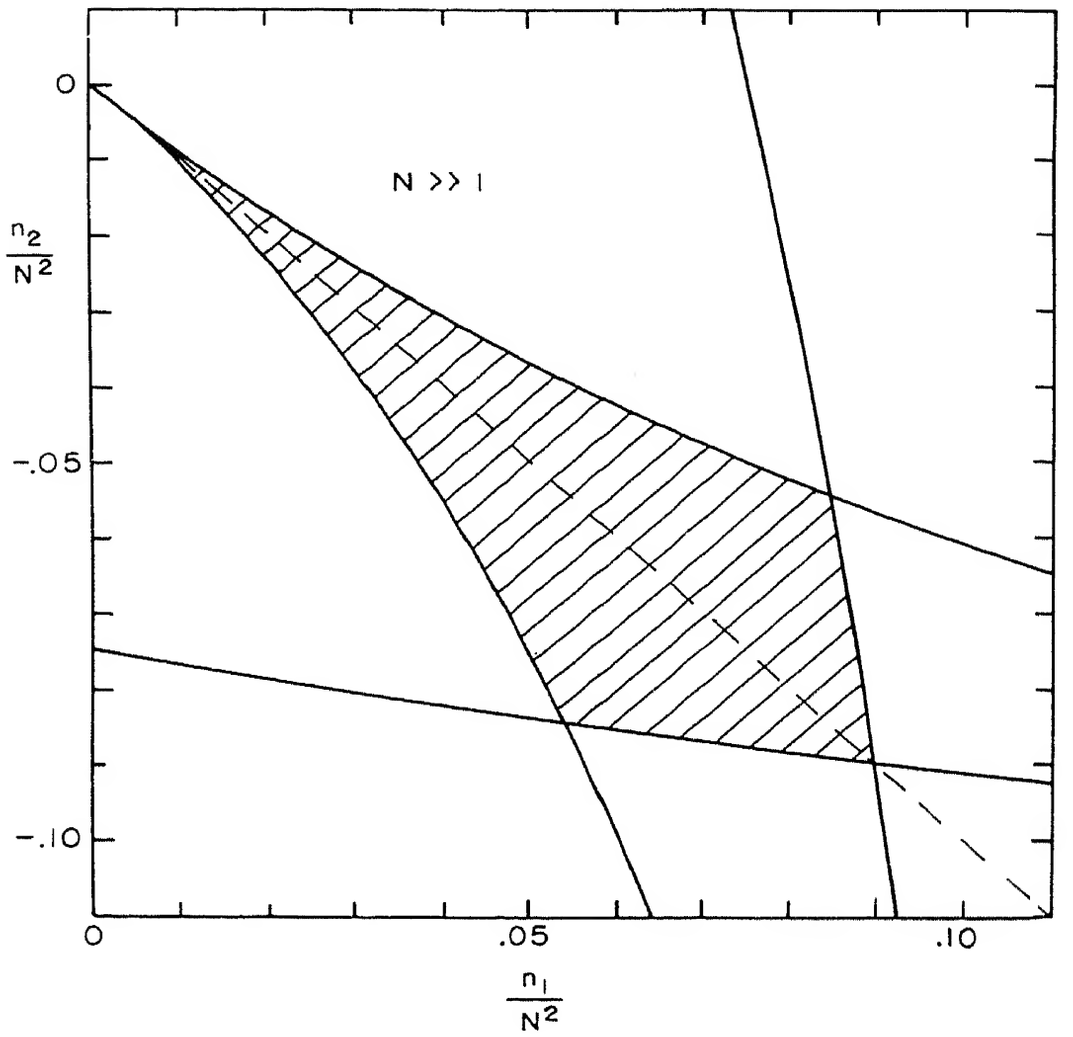

FIG. 7-3. Stability diagram for an ideal alternating gradient accelerator. Coordinates are in terms of n/N^2 where n is the n-value and N is the number of focusing units around the orbit.

siderations have modified this hope. J. D. Lawson and F. K. Goward at the Atomic Energy Research Establishment at Harwell, England, who were investigating the possibility of using this focusing principle for the CERN (Western European Laboratory) high-energy accelerator, pointed out the problem of resonance buildup of oscillation amplitudes possible if the frequency of betatron oscillations is an exact multiple of the frequency of revolution. If so, the betatron oscillations would repeat in phase in successive revolutions. Any azimuthal inhomogeneity, such as would result from slight misalignment of a magnet sector or a distortion of the magnetic field, would excite oscillations of linearly increasing magnitude. Calcula-

tions show that an error of 0.01 in. could lead to loss of the beam in less than ten revolutions, if the frequencies were in resonance, for the machine described in the early publication.

The number of possible resonances within the stability range depends on the number of betatron wavelengths around the orbit. This, in turn, depends on the n-value and the number of sectors N. For the large values of n and N originally conceived, the frequency of betatron oscillation was about 50 times the orbital frequency, so there would be 50 betatron wavelengths per revolution. In order to stay safely between resonances it would be necessary to maintain the n-value constant to within $\pm 0.5\,\%$. Furthermore, unstable stop-bands exist around half-integral values of the number of betatron wavelengths, which lowers the precision requirement to below $\pm 0.25\,\%$. Such considerations have resulted in reducing the values of n and N which can be used in the alternating gradient synchrotron.

When the stability diagram is drawn for finite values of n and N, with the resonances and stop bands inserted, we find a small but adequate "diamond" representing the allowed variations. This is illustrated in Fig. 7-4, taken from the Cambridge Design Study,[40] based on an n-value of about 310 with $N = 48$ double sectors, which results in there being about 7 betatron wavelengths per turn around the orbit. The allowed variation in n-value to stay within the stability diamond is about $\pm 3\,\%$, a value which can be attained in practice if suitable compensating lenses and windings are used. Such a proposed design is based on the concept of maintaining uniform magnetic gradients and n-values in the alternating sectors. The design studies described below use this principle of uniform gradient across the aperture. Theoretical treatments involve only linear terms for such a field.

Other theoretical studies are in progress analyzing the nonlinear effects to see whether a field that is deliberately shaped to have a gradient which varies across the aperture would result in stable orbits. Preliminary results suggest that under certain

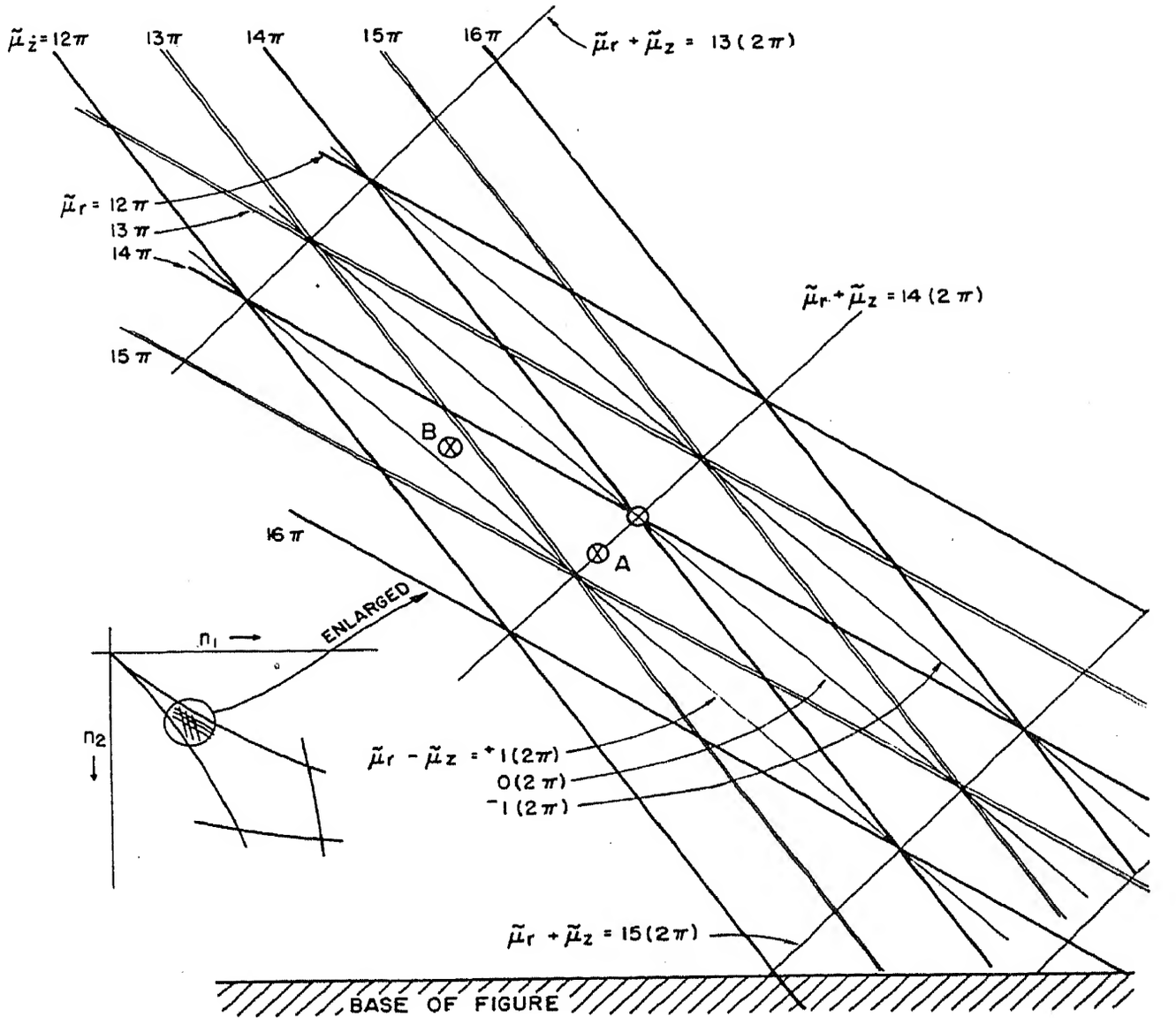

FIG. 7-4. Stability diagram for a practical alternating gradient synchrotron including the effects of errors and inhomogeneities. Orbital resonances and stop bands are indicated by the diagonal lines for a particular case.

conditions such nonconstant gradients might be helpful in reducing the buildup of oscillation amplitudes due to resonances of the type described above. If these results prove valid, pole faces could be shaped differently, and the limitations on the stable region described above might be lifted.

Synchronous stability is maintained in the alternating gradient machine. The modification is that the relation between particle energy and the circumference of the equilibrium orbit is changed. If the momentum of a particle differs from

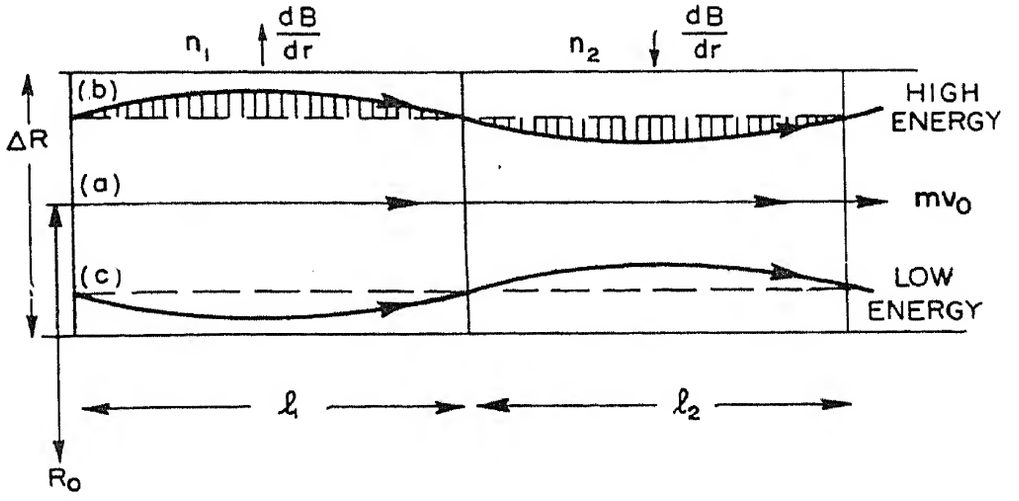

FIG. 7-5. Orbits for particles deviating from equilibrium energy.

its value at the central circular orbit, the new equilibrium orbit is no longer a circle, but is a periodic alternation of harmonic and hyperbolic functions superimposed on a circle of different equilibrium radius. The orbits for higher-energy and lower-energy particles than those at the central orbit are illustrated in Fig. 7-5, in which the curvature of the central orbit is neglected so that it appears as a straight line. The dotted lines through the displaced orbits represent their mean radial positions. If the gradients in the two sectors are equal and opposite, the average field along these dotted lines is the same as that of the central orbit. However, the average field along the actual displaced orbit for the upper curve (energy excess) is higher than that of the dotted line in both sectors, and smaller in both sectors for the lower orbit. The circumferential path length for the higher-energy particle is also longer than that of a true circle. Accordingly, the spread in mean orbit radius associated with a spread in momentum is smaller for the alternating gradient fields.

The compaction of orbits described above can be represented by the relation between the fractional change in orbit circumference and the fractional deviation in momentum:

$$\frac{\Delta L}{L} = \alpha \frac{\Delta p}{p} \tag{7-15}$$

For our special case, with $n_1 = -n_2 = |n|$, the factor α is:

$$\alpha = \frac{1}{n}\frac{2N}{\pi n^{1/2}}\frac{1}{\coth\dfrac{\pi n^{1/2}}{N} - \dfrac{\cot \pi n^{1/2}}{N}} \tag{7-16}$$

At the center of the stability range, where $n = N^2/16$, this expression reduces to: $\alpha = 4.85/|n|$; $\alpha = 0.01$, for example, for $n = 485$. For the conventional synchrotron, on the other hand, $\alpha = (1 - n)^{-1} \sim 2.5$.

Synchronous stability is governed by the change of the period of revolution with momentum. This change can be expressed in terms of the change in orbit circumference ΔL and the change in velocity Δv, as:

$$\frac{\Delta t}{t} = \frac{\Delta L}{L} - \frac{\Delta v}{v} = \left(\alpha - \frac{E^2}{E_0{}^2}\right)\frac{\Delta p}{p} \tag{7-17}$$

In the standard synchrotron, with small and uniform n, the quantity in brackets is always positive, since the relative increase in radius is greater than the relative increase in velocity. However, with large gradients the quantity α is small and the bracket is negative for values of E less than:

$$E_c = E_0/\alpha^{1/2} \tag{7-18}$$

For $E < E_c$ the change in velocity exceeds the change in orbit radius, and the particles have stable phase oscillations on the rising side of the voltage wave, as for the synchronous linear accelerator. For $E > E_c$ the normal type of synchrotron stability exists on the falling side of the voltage wave.

At the phase transition energy E_c the period of revolution is independent of radius and of energy, and synchronous stability disappears. This is the condition for cyclotron resonance. At this point the frequency of synchronous oscillation drops sharply to zero. In order to avoid loss of the beam at this phase transition, the phase of the applied radiofrequency accelerating voltage must be shifted so the equilibrium phase angle for the particles moves from the rising to the falling side of the voltage

wave, a phase jump of about 120°. Electronic devices to provide such a phase jump are practical, and most designers believe that the beam will traverse the phase transition without serious loss.

Phase oscillation frequency is given by:

$$\Omega_s = \omega_0 \frac{E_0}{E_c} \left[\frac{eV \cos \Psi_0}{2\pi E_c} h \left(1 - \alpha \frac{E_c}{E_0} \right)^2 \right]^{1/2} \qquad (7\text{-}19)$$

where ω_0 in this case is the relativistic maximum particle orbital angular frequency, V is the peak rf voltage, ψ_0 is the stable phase angle (usually chosen as about 30°) and h is the harmonic order of the applied rf frequency relative to orbital frequency. The value of this phase oscillation frequency varies from about $0.01f_0$ at the start to $0.0003f_0$ at maximum energy, varying somewhat with the individual parameters of a particular machine.

Phase amplitude depends on the stable phase angle. If this angle is very small, with the average acceleration small compared with the peak applied voltage, the stable range is nearly 2π radians. If the applied voltage is twice the average value required for acceleration, the stable phase angle is 30°. At 30° the acceptance is about 1.1π radians, so slightly over half of a uniformly distributed ring of ions in the orbit will be captured and set into phase oscillations. Phase amplitude is damped during acceleration, by a total factor of about 4, so the applied voltage excess can be decreased (stable phase angle increased) during the later portions of the acceleration cycle.

7.4 Design Studies for Multi-Bev Accelerators

The reduction in magnet cross section and power requirements possible by use of the strong-focusing principle makes it economically feasible to build much higher-energy accelerators in the same cost range as the cosmotron and bevatron. Present estimates suggest that machines with 5 times the energy of the existing proton synchrotrons can be built for about the same

cost. Further developments may make it possible to reach the 50- to 100-Bev range eventually.

Design studies in progress cover a wide energy range. The electron synchrotron at Cornell University is being rebuilt with smaller magnets and larger radius to produce 1- to 2-Bev electrons. Alternative sets of pole tips are planned for a uniform gradient machine similar to the cosmotron but with much reduced apertures, and alternating gradient pole tips to test the new principle. The Saclay Laboratory of the French Atomic Energy Commission is planning a 1.5-Bev proton A-G accelerator to test the principles and as a model for higher-energy machines.

A design group from the staffs of Harvard University and Massachusetts Institute of Technology in Cambridge, Massachusetts, has completed the preliminary design[40] for a 10- to 15-Bev proton accelerator. This energy is 5 times higher than the cosmotron maximum and would be in a scientifically interesting range. More recently this group has prepared a design study for a 5-Bev electron synchrotron. Another design group at Princeton University is investigating alternative principles of magnet design to produce focusing and of techniques for radio-frequency acceleration, also in the 10- to 15-Bev energy range.

The European Council for Nuclear Research (CERN) is making plans for an alternating gradient proton synchrotron of about 25 Bev, to be located in the new laboratory to be built near Geneva. In the preliminary phase of design, groups were active in Bergen, Copenhagen, Paris, the Harwell AERE Laboratory in England, and in several other European scientific centers. Dr. Odd Dahl, of Norway was the director of this design study. As of October, 1953, the staff began to assemble in Geneva, at the Institute of Physics of the University of Geneva, to prepare designs for the new laboratory. This effort represents a most promising opportunity for international scientific cooperation, and the results will be awaited with interest.

At the Brookhaven National Laboratory, where the principle of alternating gradient focusing was initiated, an intensive,

long-range program of design has been started. A new division, the Accelerator Development Division, which utilizes the experience of many of the cosmotron designers, has been formed under the supervision of Dr. L. J. Haworth, Director of the Brookhaven National Laboratory. The final energy goal has been chosen to be in the range of 25 to 35 Bev. The United States Atomic Energy Commission has recognized the importance of the high-energy particle field by subsidizing the design studies at Brookhaven, and also those at Cambridge and Princeton.

A strong interest in an alternating gradient accelerator has also developed in the midwestern United States, among representatives of the Universities of Chicago, Illinois, Michigan, Wisconsin, Minnesota, Iowa, Iowa State, Indiana, and the Argonne National Laboratory. Design and organizational planning is in the early stages, with an indication that the desired energy will be in the 20-Bev region.

This wide interest and high level of activity in design suggest that a new category of accelerators of much higher energy than achieved to date is to be expected.

The several design studies have already resulted in a few attempts to anticipate the engineering problems of construction and to predict dimensions and other basic parameters. The most detailed of these design studies is by the Cambridge group for a 15-Bev accelerator.[40] More general studies at Brookhaven have been used to estimate construction costs for machines of 1-, 20-, 30-, 50-, and 100-Bev energy. Tentative parameters have also been computed by the CERN group for 25 and 30 Bev. None of these has yet been finalized by detailed computations or engineering design, and many changes can be anticipated before construction begins. However, certain common features and general conclusions are becoming evident. These can be illustrated by the listing of tentative design parameters for a 5-Bev electron accelerator prepared by the Cambridge group and a similar list for a 30-Bev machine prepared at Brookhaven. These are given in Table 7-1.

Table 7-1. Design parameters for alternating-gradient accelerators.

	5 Bev electrons	30 Bev protons	Units
Orbit radius	68.3	260.	ft
Maximum field	8.0	13.0	kilogauss
Number of magnet unit cells	24.	60.	
Number of straight sections	48.	120.	
Magnet sector length	8.7	13.3	ft
Straight section length	4.2	5.0	ft
Circumference of magnet circle	662.	2190.	ft
Radius of magnet circle	99.	350.	ft
Magnet gap, central orbit	2.0	3.5	in
n_0-value, central orbit	103.	484.	
No. oscillations wavelengths/turn	5.2	8.75	
Injection energy	20.	50.	Mev
Injection magnetic field	32.	133.	gauss
Injection frequency of ions	1.6	0.14	Mc
Maximum frequency of ions	1.6	0.45	Mc
Radiofrequency harmonic order	64.	24.	
Applied rf frequency, injection	102.	3.4	Mc
Applied rf frequency, maximum	102.	10.8	Mc
Magnet rise time	1/120	1.0	sec
Volts/turn for acceleration	2,640.	81.	kv
Pulse repetition period	1/30	3.3	sec

7.5 Principles of Design

Many new concepts and unusual features are involved in the design of these alternating gradient machines. The large orbits, with the small cross section magnets, will be best housed in a doughnut-shaped building rather than in the traditional large room or vault. The shielding problem for the extremely high-energy and penetrating radiation in the horizontal plane can be answered by having this building in the form of an underground trench or tunnel. Adequate shielding over the trench will absorb the lower energy scattered radiations. Since it will no longer be possible, or desirable, for the operator's control console to overlook the machine, it can be located at any convenient central place, with provisions for full remote control.

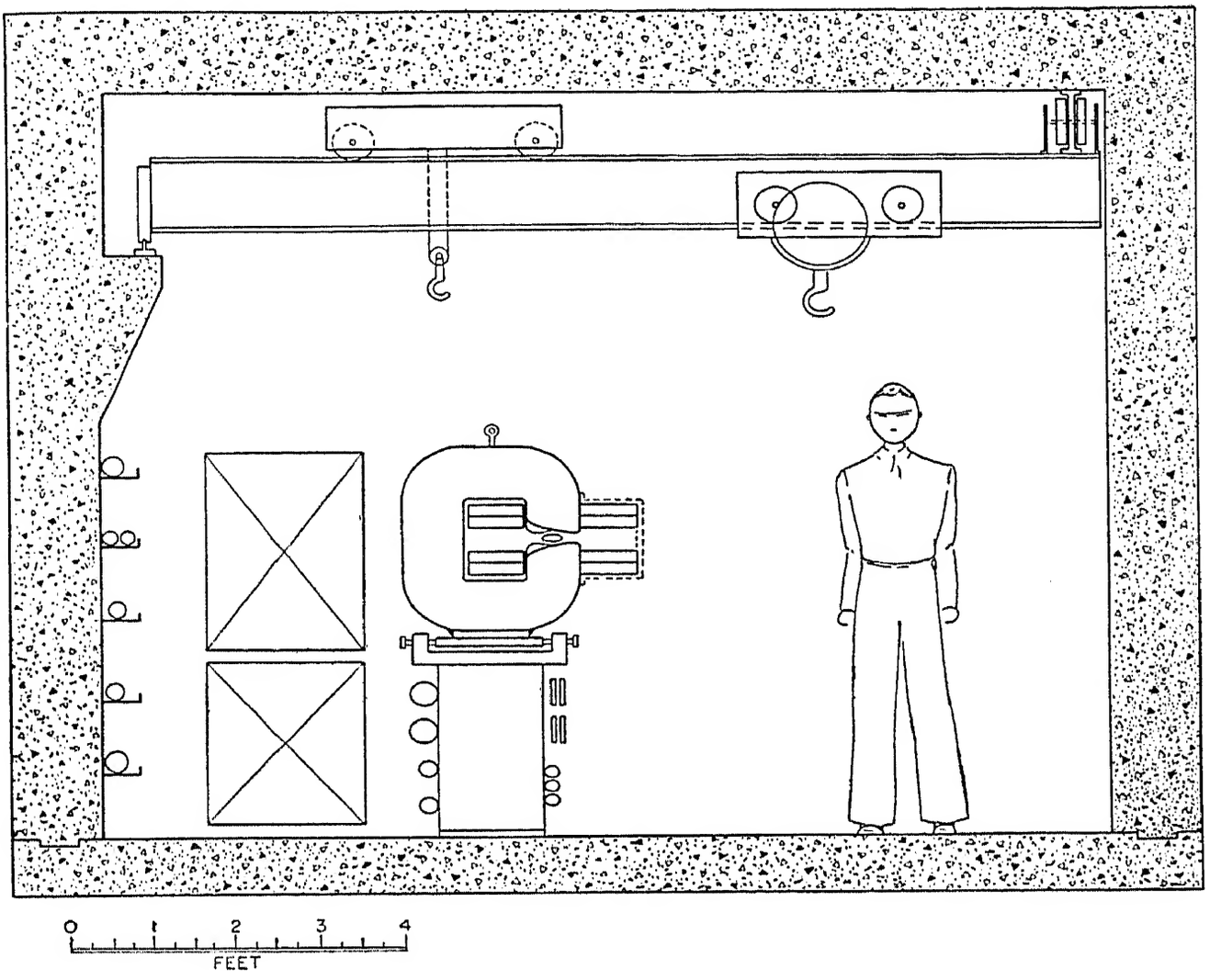

FIG. 7-6. Tunnel building for an alternating gradient synchrotron (proposed design).

A sketch of such a tunnel building is illustrated in Fig. 7-6, taken from the Cambridge Design Study.

The many duplicate magnet units, each of relatively small size, allow the use of efficient machine jigs and assembly line techniques in manufacture. The small size of most components, relative to other large accelerators, reduces the handling problem. Engineering development of a single prototype unit, with commercial production of the many duplicate units required, should result in a high quality of performance. The problems of maintenance and repair are simplified by the concept of replaceable units. Scheduled sequential servicing of the components, such as vacuum pump systems, is practical, to

reduce time lost for maintenance. In many ways this type of accelerator although large and expensive because of the large orbit radius, will be simpler to design, test and operate than the earlier machines using larger single components.

Magnet design is developing toward a simple C circuit with short, tapered poles, a return leg on one side only (to allow access for installing the chamber and egress for particle beams from a target), and copper coils of large cross section closely spaced about the gap. It can be illustrated by the sketch in Fig. 7-7 taken from the Cambridge Design Study. Pole tips are shaped closely to a rectangular hyperbola to give a uniform gradient over the aperture enclosed by the vacuum chamber, alternated right-to-left in successive lens units around the orbit.

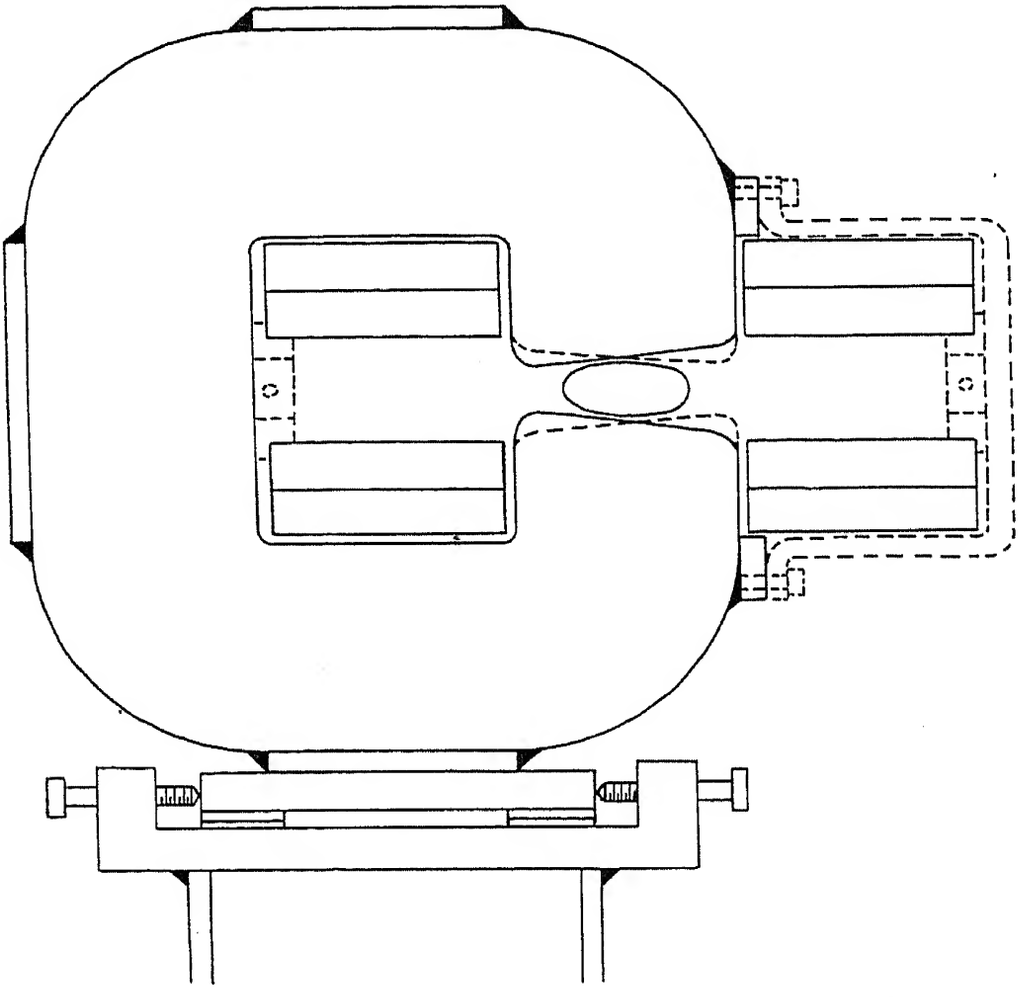

FIG. 7-7. Sketch of magnet cross section for an alternating gradient synchrotron, showing the small vacuum chamber.

The hyperbola constant and the location of the hyperbolic axis are computed to give the designed n_0-value. Since this n_0-value is somewhat smaller than those originally proposed, in order to obtain wider spacings between resonances, the hyperbolic pole faces are flatter, and the variation in gap length across the gap is smaller. A valuable consequence of this trend in design is that saturation of the pole tips, starting first on the short-gap side, is less pronounced, and corrections will be simpler. The required precision in shaping the pole faces is of the order of 0.5 %, and the uniformity between sectors is of the same order. A careful stacking and sorting procedure for the many plates of iron (to limit eddy currents) will be necessary to average out magnetic inhomogeneities. To achieve this precision each sector of the magnet could be assembled and welded into a structural unit before machining.

The number of magnet sectors and the arrangement of straight sections involves a numerical analysis which is the basis of the design. These numbers, combined with the n_0-value, determine the number of betatron oscillations around the orbit. In order to avoid orbital resonance, this number of betatron wavelengths should be nonintegral, and non-half-integral. (Note the choice of 5.2 and 8.75 in the table of parameters above.) The number of straight sections must be adequate to contain all necessary rf accelerating units, correcting magnetic lenses, the injector, targets and pickup electrodes. However, it should not be excessive and add length to the orbit unnecessarily.

The length of each magnet sector should not exceed that for which practical and economical means of assembly and machining are available. Straight section length must be adequate to install the necessary devices, particularly the rf accelerating units, but not so long as to increase the amplitudes of the betatron oscillations significantly. This increase in amplitude is a minimum if straight sections are located in the centers of the magnetic focusing lenses, rather than between lenses. A simple explanation of this last statement comes from the op-

mensions. The magnetic field time cycle also influences the magnet power requirements. A suitable balance is required to minimize total costs. Present designs for proton synchrotrons use magnet rise times of the order of 1 sec and cycle repetition rates of 10 to 20 per minute, based on magnet power and rf power considerations. Volts per turn, V, are given by the relation:

$$V = Cr_0 dB/dt \tag{7-20}$$

where C is the total orbit circumference including straight sections, r_0 is the central particle orbit radius within a sector, and dB/dt is the rate of rise of magnetic field. Table 7-1 shows the values obtained for the 30-Bev design.

The principle of radiofrequency acceleration which offers the most promise is that of induction acceleration using ferrite cores surrounding the orbit similar to the system used in the cosmotron. Many identical rf units are planned, equally spaced around the orbit, operating on a suitable harmonic of the orbital frequency so the units can all be driven in phase. Total rf power requirements to obtain a given value of V are inversely proportional to the number of rf units. This large number of drive points is also useful in reducing the amplitude of synchrotron oscillations.

Two methods are available for driving the ferrite-loaded cavities. The untuned cavity, such as is used in the cosmotron, must be driven by a wide-band amplifier over the frequency range, and so should be nonresonant. The chief problem is the low impedance of such a system, and the large currents required for excitation, especially at the low frequency end of the cycle. The other method is to tune the cavity to resonance over the frequency range by controlling the permeability of the ferrite core by means of a dc bias which partially saturates the core. A tuned cavity has a higher impedance, can be driven by a closely coupled oscillator and has a high Q which multiplies the impressed voltage. Choice of the method and the rf techniques used depend on the frequency range, the voltage required and

other constants of the circuit, and forms an interesting problem in radiofrequency engineering design.

Power rating and cost of the rf supply are steeply rising functions of the size and energy of the A-G proton synchrotron. This component may well be the economically limiting factor in extending energies toward the 100-Bev range

The practical limit for A-G electron synchrotrons is the rapidly increasing cost of the rf system to supply radiation losses. The limit for standard synchrotrons using a single rf accelerating gap at about 2 Bev can be raised to as much as 10 Bev by using many phased rf units in the straight sections, to provide the much higher voltage per turn required. In the Cambridge design presented in Table 7-1 the requirement is over 2.5 million volts per turn; it is achieved by using many (8 or 16) high-Q, resonant cavities operating at a high harmonic of the orbital frequency. At the designed energy of 5-Bev the cost of the rf system is not excessive, but this component will represent an increasing fraction of total cost as energy is increased.

Other components of the machine become much simpler than for earlier accelerators. The vacuum chamber, for example, can be a thin-walled tube of oval cross section, with transverse dimensions of only a few inches. Such a chamber is illustrated in Fig. 7-7, taken from the Cambridge study. The volume of the system is small so relatively small pumps can be used, and vacuum sealing problems are greatly simplified. The thin-walled vacuum chamber also allows radiations from a target to emerge with minimum absorption.

7.6 Conclusion

The foregoing description of plans and designs is a first attempt to write a new chapter—the latest—in the story of accelerator development. This story is an exciting one for the nuclear scientist and the accelerator designer. Accelerator development has paced the meteoric expansion of the field of nuclear physics during the last 25 years. At times the progress

of a successful new theory would spur the development of higher-energy accelerators. At other times the experimental results obtained from a recently completed accelerator of record-breaking energy would stimulate new theoretical progress. This teamwork of experimental and theoretical science has resulted in an exponential increase in particle energy with time.

Each class of accelerator has, in turn, gone through a phase of rapid expansion, from the early small machines built to test the principle and explore the problems of construction, to a maximum practical size, limited by some technical or economic barrier. Thus the electrostatic generator moved rapidly up to the 4-Mev limit set by electrical breakdown. The cyclotron blossomed from a laboratory curiosity to the powerful 60-in. size in less than ten years, limited only by the relativistic increase in mass of the accelerated ions. The synchrocyclotron seems now to have reached an economic limit due to the gigantic size and the rapid increase in cost of the solid cored magnet for still higher energies.

Just as one class of accelerator approached its practical energy limit, and progress seemed stalled, a new machine would be discovered raising the energy limits and starting a new chain of development. So we observe each type of accelerator holding the energy record for a time, only to be surpassed by the next. The sequence runs roughly through the Cockcroft-Walton voltage multiplier, the electrostatic generator, the cyclotron, the betatron, the synchrocyclotron and synchrotron, the proton synchrotron, and now the alternating gradient synchrotron.

This increase in energy of accelerators is illustrated in Fig. 7-8, in which points are plotted showing the development of each of the several classes of accelerators. The dates and energies are taken from the first published reports of reaching a new energy record in each case, often representing a delay of some months after the actual event. A logarithmic scale is used to compress the tremendous range in energy. On this plot it is possible to sketch an envelope curve representing the continuing rise in energy with time. The most significant feature

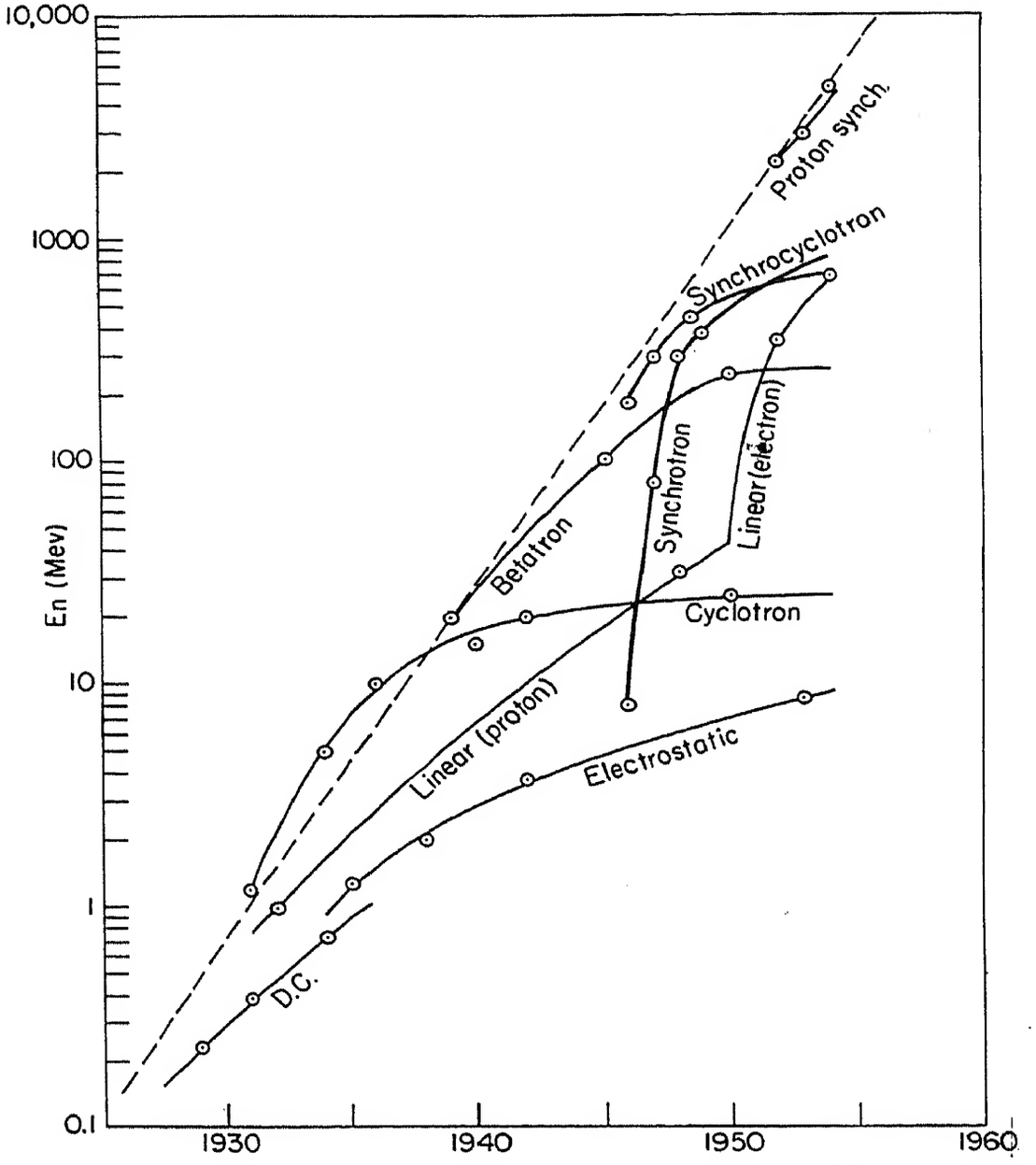

FIG. 7-8. Exponential rise in energy attained with accelerators during the past 25 years.

of the plot is the approximately linear slope of this envelope, which means that energy has in fact increased exponentially with time. The rate of rise is such that the energy has increased by a factor of 10 every six years, from a start at 100 kv in 1929 to 3 billion volts in 1952.

It is interesting to extrapolate this curve into the future, to predict the energy of accelerators after another six years. We have reason to hope that either the Brookhaven or the CERN A-G proton synchrotrons will have reached 25 Bev by that

time. Further extrapolation of this exponentially rising curve would predict truly gigantic accelerators which would exceed any possible budgets, even those of government laboratories. So we will postpone such speculation until the present machines can demonstrate their value to science.

Those of us in the accelerator field are frequently asked, "When will this development of higher-and-higher-energy accelerators stop?" Yet it must be recognized that it is not the urge to higher voltage which inspires this growth, but the pressure of the continuously expanding horizons of science. As long as there are unsolved problems in Nature which might be answered by higher-energy particles, and as long as the scientific urge to know the answers continues, there will be a steady and persistent demand to develop the tools and instruments required.

REFERENCES

1. R. E. Marshak, *Meson Physics*, McGraw-Hill, New York, 1952; B. Rossi, *High Energy Particles*, Prentice-Hall, New York, 1952.
2. W. B. Fowler, R. P. Shutt, A. M. Thorndike, and W. L. Whittemore, *Phys. Rev.*, **93**, 861 (1954).
3. D. W. Kerst and R. Serber, *Phys. Rev.*, **60**, 53 (1941).
4. J. P. Blewett, *Phys. Rev.*, **69**,, 87 (1946); J. Schwinger, *Phys. Rev.*, **75**, 1912 (1949).
5. E. M. McMillan, *Phys. Rev.*, **68**, 143 (1945).
6. V. Veksler, *J. Phys. U.S.S.R.*, **9**, 153 (1945).
7. R. Q. Twiss and N. H. Frank, *Rev. Sci. Instr.*, **20**, 1 (1949).
8. F. K. Goward and D. E. Barnes, *Nature*, **158**, 413 (1946).
9. F. R. Elder, *et al.*, *J. Appl. Phys.*, **18**, 810 (1947).
10. D. M. Dennison and T. Berlin, *Phys. Rev.*, **70**, 58 (1946).
11. D. Bohm and L. Foldy, *Phys. Rev.*, **70**, 249 (1946).
12. N. H. Frank, *Phys. Rev.*, **70**, 177 (1946).
13. J. Lawson, *Gen. Elec. Research Lab. Quart. Rept.*, Sept. 6, 1948.
14. H. R. Crane, *Phys. Rev.*, **69**, 542 (1946).
15. D. M. Dennison and T. Berlin, *Phys. Rev.*, **70**, 764 (1946).
16. D. Bohm and L. Foldy, *Phys. Rev.*, **72**, 649 (1947).
17. L. R. Henrich, D. C. Sewell, and J. Vale, *Rev. Sci. Instr.*, **20**, 887 (1949).
18. F. H. Schmidt, *Rev. Sci. Instr.*, **17**, 301 (1946).
19. K. R. MacKenzie, F. H. Schmidt, J. R. Woodyard, and L. F. Wouters, *Rev. Sci. Instr.*, **20**, 126 (1949).
20. K. R. MacKenzie, *Rev. Sci. Instr.*, **22**, 302 (1951).
21. R. Wideröe, *Arch. Electrotech.*, **21**, 387 (1929).
22. E. O. Lawrence and D. H. Sloan, *Phys. Rev.*, **38**, 2021 (1931).
23. D. H. Sloan and W. M. Coates, *Phys. Rev.*, **46**, 539 (1934).
24. L. W. Alvarez, *Phys. Rev.*, **70**, 799a (1946).
25. C. Turner, B. Cork, J. Ballam, and H. Gordon, *Phys. Rev.*, **73**, 534a (1948).

25a. B. Cork and E. Zajec, *Phys. Rev.*, **92**, 853a (1953).

26. J. P. Blewett, *Phys. Rev.*, **88**, 1197 (1952).
27. D. W. Fry, R. B. R-S.-Harvie, L. B. Mullett, and W. Walkinshaw, *Nature*, **160**, 351 (1947).

28. J. C. Slater, *Revs. Mod. Phys.*, **20**, 473 (1948).
29. E. L. Ginzton, W. W. Hansen, and W. R. Kennedy, *Rev. Sci. Instr.*, **19**, 89 (1948).
30. *Microwave Laboratory Report #185*, Stanford Univ., Palo Alto, Calif.
31. M. L. Oliphant, F. S. Gooden, and G. S. Hide, *Proc. Phys. Soc. London*, **59**, 666 (1947).
32. J. S. Gooden, H. H. Jensen and J. L. Symonds, *Proc. Phys. Soc. London*, **59**, 677 (1947).
33. W. M. Brobeck, *Rev. Sci. Instr.*, **19**, 545 (1948).
34. M. S. Livingston, *Phys. Rev.*, **73**, 1258a (1948).
35. M. S. Livingston, J. P. Blewett, K. Green, and L. J. Haworth, *Rev. Sci. Instr.*, **21**, 7 (1949).
36. Cosmotron Staff, *Rev. Sci. Instr.*, **24**, 723-870 (1953).
37. M. L. Oliphant, *Nature*, **165**, 466 (1950).
38. E. Courant, M. S. Livingston, and H. Snyder, *Phys. Rev.*, **88**, 1190 (1952).
39. J. C. Jaeger, *Introduction to Applied Mathematics*, Oxford, 1951, p. 355.
40. *Laboratory for Nuclear Science Tech. Rept. No. 60*, Massachusetts Institute of Technology, June 30, 1953.

INDEX